



Kent Academic Repository

Fung, Shelly Ann (2021) *Exploring the diversity of mitochondrion related organelles in Cryptosporidium species*. Master of Research (MRes) thesis, University of Kent,.

Downloaded from

<https://kar.kent.ac.uk/86754/> The University of Kent's Academic Repository KAR

The version of record is available from

<https://doi.org/10.22024/UniKent/01.02.86754>

This document version

UNSPECIFIED

DOI for this version

Licence for this version

CC BY-NC-SA (Attribution-NonCommercial-ShareAlike)

Additional information

Versions of research works

Versions of Record

If this version is the version of record, it is the same as the published version available on the publisher's web site. Cite as the published version.

Author Accepted Manuscripts

If this document is identified as the Author Accepted Manuscript it is the version after peer review but before type setting, copy editing or publisher branding. Cite as Surname, Initial. (Year) 'Title of article'. To be published in *Title of Journal*, Volume and issue numbers [peer-reviewed accepted version]. Available at: DOI or URL (Accessed: date).

Enquiries

If you have questions about this document contact ResearchSupport@kent.ac.uk. Please include the URL of the record in KAR. If you believe that your, or a third party's rights have been compromised through this document please see our [Take Down policy](https://www.kent.ac.uk/guides/kar-the-kent-academic-repository#policies) (available from <https://www.kent.ac.uk/guides/kar-the-kent-academic-repository#policies>).

Exploring the diversity of mitochondrion related organelles in *Cryptosporidium* species

**Research Masters submitted by Shelly Ann Fung
2019**

**Supervisor
Anastasios Tsaousis**

**University of
Kent**

**School of Biosciences, Stacey
Building,
University of Kent,
Canterbury, Kent,
CT2 7NJ**

Table of Contents

Declaration	Error! Bookmark not defined.
Acknowledgement	5
List of figures	6
List of tables	7
Supplementary Tables	7
Abbreviations	8
Abstract	11
1. Introduction	14
1.1 General background	14
1.2 Infection and Transmission	14
1.3 Species specificity	15
1.4 Epidemiology	20
1.5 Life cycle of <i>Cryptosporidium</i>	22
1.5.1 Excystation	22
1.5.2 Merogony	25
1.5.3 Gametogony and Fertilisation	25
1.5.4 Sporogony and Oocyst wall formation	26
1.6 Mitochondrial Functions	27
1.6.1 Protein Import Machinery	27
1.6.2 TCA	29
1.6.3 Oxidative Phosphorylation	30
1.6.3.1 Complex I NADH: ubiquinone oxidoreductase	30
1.6.3.2 Complex II: Succinate Dehydrogenase	30
1.6.3.3 Complex III: Cytochrome c Oxidoreductase	31
1.6.3.4 Complex IV : Cytochrome c Oxidase	32
1.6.3.5 Complex V : ATP Synthase	32
1.6.4 Fe-S Cluster Assembly	34
1.7 Mitochondrial Diversity	35
1.7.1 Aerobic mitochondria (Class I)	36
1.7.2 Anaerobic mitochondria (Class II)	37
1.7.3 Hydrogen-producing mitochondria (Class III)	37
1.7.4 Hydrogenosomes (Class IV)	37
1.7.5 Mitosomes (Class V)	38
1.8 Diversity of <i>Cryptosporidium</i> mitosomes	38

1.9 Hypothesis	40
2. Materials and Methods	42
2.1 Bioinformatics analyses- Gene IDs and protein sequences	42
2.2 Analysis of genome structure	45
3. Results	47
3.1 Genome for <i>Cryptosporidium</i>	47
3.2 Protein Import Machinery.....	51
3.3 The Citric Acid Cycle	57
3.4 The Electron Transport Chain	62
3.5 Fe-S Cluster.....	66
3.6 Glycolysis and Gluconeogenesis	71
3.7 Overview of mitochondrial pathways	77
4. Discussion.....	86
5. Conclusion and further research	91
6. Supplementary information	94
References	101

Declaration

I declare that this is my own work, except where I have acknowledged references and citations.

I took reasonable care to ensure that the work submitted is original and to the best of my knowledge does not breach any copyright laws.

Acknowledgement

Deuteronomy 31:6- Be strong and of good courage, do not fear nor be afraid of them; for the Lord your God, He is the One who goes with you. He will not leave you nor forsake you.

I would like to thank my Heavenly Father for helping me throughout this Masters. I thank Him for His Holy Spirit, who brought me comfort and wisdom in times when I felt like giving up.

To my supervisor Dr Anastasios Tsaousis, for his encouragement in helping me make this research a success, his constant push and discipline in ensuring that work was submitted.

I would like to thank my parents, Anika and Terry and the rest of my family for all their support throughout my two years of completing my Master's degree.

To my sweetest banana loaf, Samuel Cole for his constant encouragement, scriptures and prayers throughout this degree. For proof-reading my work and adding comments to ensure that the work was of an excellent standard.

To my twin, Abigail King for her love, prayers and facetime calls, keeping me motivated to keep on going and to push through.

To the finest bebs, Martha, Chidera and Norma for their daily messages and praying with me throughout this course.

To Ify, Tomi, Verina, Ayo, China, Keren, James, David, Jake, OGGM, C.O.G.I.C and NLC, for always sending me scriptures to keep me focused and motivated and proofreading.

To Rebecca, Chantel, my lovely housemates for their prayers , late nights of studying and also for their laughter.

To Tina, for her conversations and input in helping me remain encouraged, for studying with me and walking with me to campus on days when I didn't want to.

To my lab and university colleagues, Emma, Eleana, Alex, Niken and Eithar for keeping me on track when I couldn't carry on with the work anymore.

To my neighbour, Esther Toto for allowing me to use her internet to complete my thesis.

To Lin Riches, a darling angel for her compassion with dealing with sensitive information and offering great advice and being an amazing human being.

List of figures

Figure 1: Phylogenetic tree.....	17
Figure 2: Life cycle of <i>Cryptosporidium</i>	24
Figure 3: Sporozoite of <i>Cryptosporidium</i>	26
Figure 4: Overview of protein import.....	28
Figure 5: Overview of TCA and ETC.....	33
Figure 6: Overview of Fe-S Cluster Assembly.....	34
Figure 7: Classes of mitochondrion including the MROs.....	35
Figure 8: Flow chart of basic overview of the methods.....	46
Figure 9: Results: Mitochondrial protein import pathways	53-56
Figure 10: Results: TCA cycle for <i>Cryptosporidium</i> and <i>Plasmodium</i>	59-62
Figure 11: Results: The ETC content for <i>Cryptosporidium</i> and <i>Plasmodium</i>	64-66
Figure 12: Results: Fe-S cluster assembly in <i>Cryptosporidium</i> and <i>Plasmodium</i>	68-71
Figure 13: Results: Glycolysis/Gluconeogenesis in.....	73-76
Figure 14: Results: Overview of mitochondrial pathways/proteins	78-84

List of tables

Table 1: The 30 known species of <i>Cryptosporidium</i>	18
Table 2: The outbreaks of <i>Cryptosporidium</i>	21
Table 3: The websites that used to generate the protein sequences.....	42
Table 4: The overall pathway IDs used in KEGG	43
Table 5: General features of the <i>Cryptosporidium</i> genome.	48
Table 6: The number of predicted proteins present in the <i>Cryptosporidium</i> species.	49
Table 7: Specific proteins present within <i>Cryptosporidium</i> and <i>Plasmodium</i> species.	50
Table 8: Proteins present in the protein import machinery of <i>Cryptosporidium</i>	51-52
Table 9: Proteins present in the TCA cycle of <i>Cryptosporidium</i> and <i>P.falciparum</i>	57
Table 10: Complexes of the ETC present in <i>Cryptosporidium</i> and <i>Plasmodium</i>	63
Table 11: Proteins in Fe-S cluster assembly.....	67
Table 12: Proteins involved in Glycolysis and Gluconeogenesis.	72
Supplementary Table S 1: Identified proteins in ETC.....	94-96
Supplementary Table S 2: Predicted proteins identified in Fe-S cluster	97
Supplementary Table S 3: Predicted carrier proteins.	98
Supplementary Table S 4: Protein coding genes in the Ubiquinone synthesis.	98
Supplementary Table S 5: Protein coding genes in the pyruvate metabolism.	99

Abbreviations

ABCB6	ATP Binding Cassette Subfamily B Member 6
ABCB7	ATP Binding Cassette Subfamily B Member 7
Acetyl-CoA	Acetyl-coenzyme A
AIDS	Acquired immune deficiency syndrome
ANT	Adenine nucleotide translocator
AOX	Alternative oxidase
ADP	Adenosine diphosphate
ATP	Adenosine triphosphate
β -oxidation	Beta-oxidation
BLAST	Basic Local Alignment Search Tool
Co-A	Coenzyme A
CO ₂	Carbon dioxide
CPR	NADPH-cytochrome P450 reductase
<i>CryptoDB</i>	<i>Cryptosporidium</i> database
DNA	Deoxyribonucleic acid
EC number	Enzyme commission number
ETC	Electron transport chain
FADH ₂	Flavin adenine dinucleotide
Fe-S	Iron sulfur cluster assembly
FDX1	Ferredoxin
FDXR	Ferredoxin reductase
FDX1L	Ferredoxin 2
FXN	Frataxin
GDP	Guanosine-5'-diphosphate
GTP	Guanosine-5'-triphosphate
GLRX5	Glutaredoxin 5

Hsp70	Heat shock protein 70
Imp1	Inner membrane peptidase
IscA1	Iron sulfur cluster assembly 1
IscA2	Iron sulfur cluster assembly 2
IscS	Cysteine desulfurase
IscU	Iron-sulfur cluster assembly
Jac1	J-type co-chaperone
KEGG	Kyoto Encyclopaedia of Genes and Genomes
MFRN	mitoferrin
MIP	Major intrinsic protein
MPP	Mitochondrial processing peptidase
MQO	Malate-quinone oxidoreductase
MROs	Mitochondrion-related organelles
mtDNA	mitochondrial DNA
NCBI	National Center for Biotechnology Information
NADH/ NAD ⁺	Nicotinamide adenine dinucleotide (reduced)
OXA1	Oxidase assembly protein
PAM	Presequence translocase-associated motor
PDH	Pyruvate dehydrogenase
PEP	Phosphoenolpyruvate
PFO	Pyruvate: ferredoxin oxidoreductase
Pi	Phosphate
<i>PlasmoDB</i>	<i>Plasmodium</i> database
PNO	Pyruvate: NADP + oxidoreductase
PV	parasitophorous vacuole

QH ₂	Ubiquinol
Q	Ubiquinone/Coenzyme Q
SAM	Sorting and assembly
TCA	Tricarboxylic acid
TIM	Translocase of the inner membrane
TMHMM	Transmembrane Helices; Hidden Markov Model
TOM	Translocase of the outer membrane
Ub	Ubiquinone synthesis
μm	micrometre

Keywords: *Cryptosporidium*, protein import machinery, conserved, mitosomes, mitochondrial pathways.

Abstract

Cryptosporidium is an apicomplexan parasite that causes widespread diarrhoeal disease in both humans and animals. It is a parasite that is responsible for large waterborne outbreaks of Cryptosporidiosis. Humans are thought to acquire the parasite by the ingestion of oocysts, which are shed in the stool of infected animals or humans. Research has been done on this parasite, however up till now there has not been a treatment against this.

Cryptosporidium have lost their mitochondrial genome and therefore various mitochondrial pathways have been conserved in some of these species. Using bioinformatics analysis, we summarized the differences and similarities in the metabolic pathways in the mitosomes of six *Cryptosporidium* species (*C. parvum*, *C. hominis*, *C. tyzzeri*, *C. ubiquitum*, *C. andersoni* and *C. muris*). As only *C. parvum* and *C. hominis* pathways have been mapped on KEGG Pathway Database, amino acid sequences were extracted for proteins involved in glycolysis/gluconeogenesis (map00010), TCA cycle (map00020), protein import machinery (map03060), pentose phosphate pathway (map00030), pyruvate metabolism (map00620) and oxidative phosphorylation (map00190). Amino acid sequences for the protein coding genes were run in BlastP on *CryptoDB* using the set parameters. The gene results were analyzed and used to produce diagrams to show the metabolic pathways in the mitosomes of the *Cryptosporidium* species.

In this study we show that the essential TCA cycle enzymes were present in the gastric species *C. andersoni* and *C. muris*, whereas *C. parvum*, *C. hominis*, *C. tyzzeri* and *C. ubiquitum* only retain the membrane bound malate-quinone oxidoreductase (MQO) and pyruvate synthase. All species investigated showed a highly reduced protein import

machinery in comparison to *P.falciparum*, and conserved glycolysis/gluconeogenesis proteins and Fe-S (iron-sulfur) cluster assembly, suggesting that these two pathways are the main ways in which the parasite acquires energy.

Our results from the *CryptoDB* Blast search for the Protein Import Machinery and other pathways investigated contained some putative protein coding genes which needs to be experimentally validated. The Tim 9-10 which is responsible for transporting hydrophobic proteins to the inner mitochondrial membrane was annotated as uncharacterized in three protein coding genes: *C.hominis* (GY17_00000465), *C.parvum* (cgd6_4450) and *C.tyzzeri* (CTYZ_00001648). Further studies such as PCR analysis as well as Western blotting can be used to characterize the protein present and molecular structural analysis carried out to find out the shape and immunofluorescent assays as well as neutralization assays used to assess the function of the protein. The results from this study can be helpful to direct further research in understanding the functions of the mitosomes of these species and could be pivotal in developing new therapeutic drugs that are used to target various pathways in *Cryptosporidium* species.

Chapter 1

Introduction

1. Introduction

1.1 General background: *Cryptosporidium*

Cryptosporidium is a waterborne parasite of considerable importance. It belongs to apicomplexans, which includes notorious parasites such as *Plasmodium* and *Toxoplasma*. *Cryptosporidium* is responsible for the widespread diarrhoeal diseases, Cryptosporidiosis, that affects the gastrointestinal tract and respiratory tracts of humans and other vertebrate species. Transmission is by the faecal oral route and can be from animal to animal, animal to human or via direct contact. In immunocompetent individuals, infection with *Cryptosporidium* causes mild to acute self-limiting diarrhoea, whereas in infants and immunocompromised individuals such as those with AIDS, infection can be life threatening. *Cryptosporidium* can exist in the environment as hardy oocysts for prolonged periods of time. There are around 30 different species of *Cryptosporidium* that have been recognized in humans and livestock and they differ in host specificity. *C.parvum* and *C.hominis* are intestinal species and they are the most common causes of human Cryptosporidiosis.

1.2 Infection and Transmission

Cryptosporidium affects all individuals, however it is more severe in children under the age of two and immunocompromised individuals (Jaggi et al., 1994). It can lead to persistent diarrhoea that can cause malnutrition in children (Jaggi et al., 1994) and those who are HIV carriers (Gentile et al., 1991) (Hong, Wong and Gutierrez, 2007). *Cryptosporidium* infection can be asymptomatic, however the most common symptoms of infection with *Cryptosporidium* includes watery diarrhoea (Jokipii, Pohjola and Jokipii, 1983), abdominal pain, nausea, anorexia, tiredness, vomiting and fever (Bouzid et al., 2013). In immunocompetent people, Cryptosporidiosis is self-limiting and can last for up to 20 days.

Whereas, in immunocompromised individuals, the disease prolongs for long periods of time and can cause devastating effects. *Cryptosporidium* infection can spread through the gastrointestinal tract and extra-intestinal sites, however the main site of infection is the small intestine (Chalmers and Davies, 2010).

Cryptosporidium infection can be spread between humans and animals and can either be zoonotic (animals to humans) or anthroponotic (humans to animals). Individuals such as pet owners and veterinarians are commonly affected by zoonotic infections of *Cryptosporidium* as they are constantly in direct contact with animals (Preiser, Preiser and Madeo, 2003). On the other hand, anthroponotic infections occur as a result of direct human contact with contaminated materials such as dirty nappies, poor food hygiene in homes or nurseries (Ashbolt et al., 2003) (Hunt et al., 1984). In addition, infection can spread through ingestion of water or food that has been contaminated (Sischo et al., 2000).

1.3 Species specificity

Cryptosporidium species are distinguished by their host specificity and site of infection. There are around 30 different species of *Cryptosporidium* that have been described (Ryan, Fayer and Xiao, 2014) (Cacciò et al., 2005). **Table 1** shows the different *Cryptosporidium* species, major and minor host as well as the authors of the species. *C.parvum* is a zoonotic parasite that mainly infects the ileum of humans and livestock. *C.parvum* infects the intestine mainly in young calves and are detrimental to the cattle industry.

C.parvum oocysts are 5 x 7 µm (Hijawi et al. 2001) and they are responsible for most of the waterborne outbreaks of diarrhoeal disease in the human population (O'Donoghue, 1995). As *C.parvum* infects almost everything (humans and cattle in the gastrointestinal tract), it is very important due to the disease it causes. Comparatively, *C.andersoni*, the gastric

species, produces large oocysts, 7.4 x 5.6 µm and infects the abomasum of cattle (Lindsay et al., 2000). *C.hominis* and *C.parvum* are the species that cause infection mostly in humans (Ryan, Fayer and Xiao, 2014) and other species that have been reported to cause infection in humans include: *C.meleagridis*, *C.cuniculus* (Chalmers et al., 2009), *C.ubiquitum* (Fayer, Santín and Macarisin, 2010), and *C.felis*, *C.canis* (Jenkins et al., 2010).

In developed countries zoonotic infections are more common, whereas in developing countries anthroponotic infections with *Cryptosporidium* are mostly reported (Xiao et al., 2010). In European countries *C.hominis* and *C.parvum* are thought to be the major causes of human *Cryptosporidium* infections (Ryan, Fayer and Xiao, 2014). *C.felis* and *C.canis* cause major infections in developing countries, whilst *C.ubiquitum* has been recorded in industrialized regions. In the United Kingdom, zoonotic transmission of *Cryptosporidium* is the major route of infection in humans. Authorities reduced access to countryside areas due to the recent outbreak of foot and mouth disease. This ensured that humans were not in contact with farm or wild animals and their faeces (Hunter et al., 2003).

The phylogenetic tree taken from Tsaousis, Anastasios D and Keithly, Janet S. (2019)

(figure 1) shows how closely related the species chosen for this investigation are.

C.hominis and *C.parvum* the main agents for infections in humans are closely related on the phylogenetic tree, whereas *C.andersoni* and *C.muris* are thought to have diverged from the same arm of the tree. *C.tyzzeri* was also closer to *C.parvum* and *C.ubiquitum* the least common to all the other species, therefore these species chosen to give a boarder range of how the species have evolved over time.

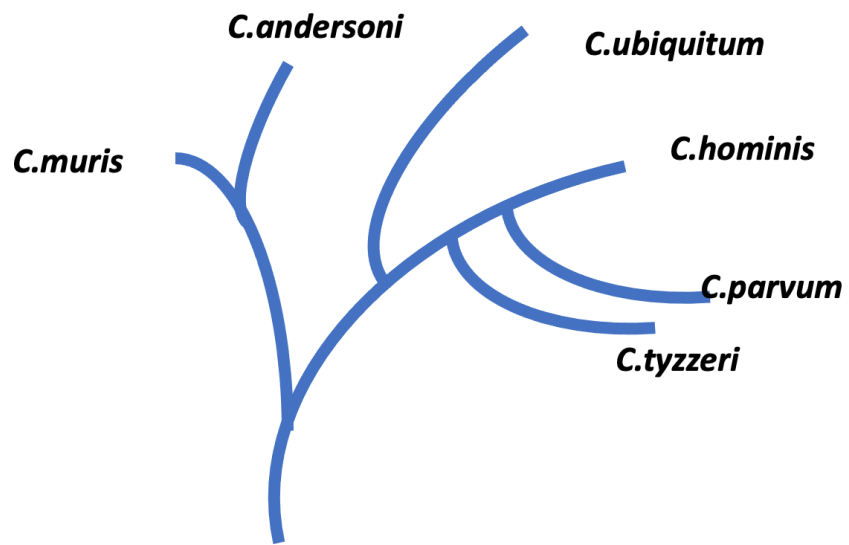


Figure 1 : Schematic diagram showing the phylogenetic tree for six *Cryptosporidium* species. *C.muris* and *C.andersoni* the gastric species are closely related, whereas the intestinal species *C.hominis* and *C.parvum* are closely related.

Table 1: The 30 known species of *Cryptosporidium*, with the corresponding host and information on infection sites. The authors of each species are listed below in the table.

Seven gastric species have been confirmed and twenty confirmed intestinal species.

C.parvum is the most widely studied *Cryptosporidium* species.

Species	Major host	Minor host	Confirmed primary location	Author
<i>C.muris</i>	rodents	humans	Gastric	Tyzzer, 1907 ,1910
<i>C.andersoni</i>	cattle	sheep	Gastric	Lindsay et al., 2000
<i>C.parvum</i>	Cattle, humans	deer , mice, pigs	Intestinal	Tyzzer, 1912
<i>C.hominis</i>	Humans	sheep	Intestinal	Morgan-Ryan et al.,2002
<i>C.tyzzeri</i>	Rodents		Intestinal	Ren et al., 2012
<i>C.ubiquitum</i>	Rodents		Intestinal	Fayer et al.,2010
<i>C.wrairi</i>	Guinea pigs		Intestinal	Vetterling et al.,1971
<i>C.felis</i>	cats	Humans, cattle	Intestinal	Iseki,1979
<i>C.meleagridis</i>	Turkeys, humans	parrots	Intestinal	Slavin,1955
<i>C.galli</i>	Chicken, finches		Gastric	Ryan et al.,2003
<i>C.serpentis</i>	Snakes, lizards		Gastric	Levine, 1980
<i>C.molnari</i>	Fish		Gastric	Alvarez-Pellitero and Sitjà-Bobadilla, 2002
<i>C.canis</i>	Dogs	humans	Intestinal	Fayer et al., 2001
<i>C.baileyi</i>	Chicken, turkeys	quails	Intestinal	Current, Upton and Haynes 1986)
<i>C. scophthalmi</i>	Fish		Intestinal	Alvarez-Pellitero et al., 2004
<i>C.varanii</i>	Lizards		Gastric	Levine, 1980
<i>C.fragile</i>	Toads		Gastric	Jirku et al., 2008
<i>C.suis</i>	Pigs		Intestinal	Ryan et al., 2004
<i>C.bovis</i>	Cattle	Sheep	Unknown	Fayer, Santín and Xiao, 2005
<i>C.fayeri</i>	Marsupials		Intestinal	Ryan, Power and Xiao, 2008
<i>C.ryanae</i>	Cattle		Unknown	Fayer, Santín and Trout, 2008
<i>C.xiaoi</i>	Sheep and goats		Unknown	Fayer, Santín and Macarisin, 2010
<i>C.scrofarum</i>	Pig		Intestinal	Kváč et al., 2013
<i>C.erinacei</i>	Horses, hedgehogs		Intestinal	Kváč et al. 2014
<i>C.macropodum</i>	Marsupials		Intestinal	Power and Ryan, 2008
<i>C.cuniculus</i>	Rabbit		Intestinal	Robinson et al., 2010
<i>C.pestis</i>	Cattle		intestinal	Šlapeta, 2006
<i>C.viatorum</i>	Humans		intestinal	Elwin et al., 2012
<i>C.ducismarci</i>	Tortoise		intestinal	Traversa, 2010
<i>C.agni</i>	Sheep		intestinal	Barker and Carbonell, 1974

Variation in species infecting humans can also be caused by seasonal factors and age of the host. *C.parvum* infections are predominantly seen in spring (Wielinga et al., 2008), (Zintl et al., 2008),(Budu-Amoako et al., 2012) and commonly infect adults (Wielinga et al., 2008). Whereas, *C.hominis* infections are more noticeable in autumn (Wielinga et al., 2008),(Zintl et al., 2008) , (Budu-Amoako et al., 2012) and are frequently in children (Wielinga et al., 2008).

1.4 Epidemiology

The first reported human case of Cryptosporidiosis was in 1972, of which there were two cases (Fayer, Morgan and Upton, 2000). Over the next six years, 11 cases were reported and now there have been reports on six continents (over 90 countries) except for Antarctica (Fayer, Morgan and Upton, 2000), (O'Donoghue, 1995), (Ryan, Fayer and Xiao, 2014). The majority of these outbreaks have been due to contaminated drinking water (*C.parvum*) or from human faecal matter (*C.hominis*) (Pedraza-Diaz et al., 2001). **Table 2** outlines various outbreaks in different countries, source, type and *Cryptosporidium* species that has caused this outbreak. Most of these outbreaks were as a result of waterborne infections with *C.parvum*, mostly in children.

The largest outbreak of waterborne disease caused by *C.hominis* occurred in the USA in Milwaukee in 1993. This was due to failure in treating the water effectively and millions of people were exposed to *Cryptosporidium*, leading to over 403,000 related cases (Mac Kenzie et al., 1994). Children living in countryside areas are more likely to be infected with *C.parvum* and other zoonotic species (Tumwine et al.,2003), as they are in close proximity to animals. Whereas, those children living in town and city areas are more likely to be infected with *C.hominis* (Llorente et al.,2007), (Essid et al.,2008). In 2013, there were 22,000 children affected by *Cryptosporidium* in Africa and Asia, which was one of the top four pathogens that cause diarrhoea in children (Ryan, Fayer and Xiao, 2014).

Table 2: The outbreaks of *Cryptosporidium* with the location, number of individuals that have been affected, type of infection, patient type, source and the species responsible.

Majority of the outbreaks were caused by *C.parvum*, hence why it is so widely investigated.

Country and year of outbreak	Number of cases	Patient type	Type	Source	Species	Reference
England and Scotland 2012	More than 300	Females	Foodborne	Fresh pre-cut salad leaves	<i>C.parvum</i>	McKerr et al.,2015
Sweden-Stockholm, 2002	80-1000	School children	Waterborne	Public swimming pool	<i>C.parvum genotype II</i>	Insulander et al.,2005
USA-Milwaukee, 1993	403,000 54 deaths reported	All but mostly females	Waterborne	Contamination of drinking water	Unknown	MacKenzie et al.,1994
Spain-Gipuzkoa, 2011	26	Children under two years	Other	Day care facility	Unknown	Artieda et al., 2012

A sewage leakage in the water well in San Antonio, Texas was the first documented outbreak of cryptosporidiosis (D'Antonio, 1985). There have been outbreaks caused by *C.parvum* in North America linked to direct contact with animals or contaminated food such as the Maine, USA apple cider outbreak in 1993 (Millard, 1994), and the Minnesota Zoo outbreak in 1997. These outbreaks were caused mostly by contaminated water or food and *C.parvum* seemed to be the parasite that caused this.

1.5 Life cycle of *Cryptosporidium*

The life cycle of *Cryptosporidium* species is a complex cycle that involves many different stages (**figure 2**). The life cycle of *Cryptosporidium* can be categorised in six different stages (Current and Garcia, 1991) excystation, merogony, gametogony, fertilization, oocyst wall formation and sporogony. The oocysts stage is of primary importance as this is needed for the survival and infectivity of the parasite. Oocysts can survive in the environment for several months under varying conditions such as increased temperature, pH and length of time (Reinoso, Becares and Smith, 2008) (Jenkins et al., 1997). They are hard spore like structures that have a diameter of 4-6 μm (Fayer, Morgan and Upton, 2000). The sporulated thick/ thin walled oocyst contains four sporozoites that are ingested or cause autoinfection respectively. There seems to be two auto-infective stages in *Cryptosporidium*: Type I meronts and the thin-walled oocysts.

1.5.1 Excystation

After the host ingests the oocysts and it arrives at the small intestine, the four sporozoites contained in the oocyst, undergo excystation and attach to the apical membrane of the epithelial cells in the small intestine (Borowski, Clode and Thompson, 2008).

Cryptosporidium oocysts are tough and durable structures, that are resistant to certain chemicals such as chlorine. Based on a study carried out by Jenkins Et Al (2020) *C.parvum* oocyst has been shown to be comprised of four layers. The outer surface layer of the oocyst is made of glycocalyx that has various proteins that aid in binding to the surface of epithelial cells, a central layer that contains lipids, a protein layer and an inner layer that has glycoprotein (A. Kuznar and Elimelech, 2020).

The outer layer of the oocyst is degraded by hydrochloric acid in the stomach. This encourages bile salts and digestive enzymes that trigger the release of sporozoites from a small suture in the oocysts wall (Reduker et al. 1985). Released sporozoites have to overcome a mucus barrier before attaching to the epithelial cells (Borowski, Clode and Thompson, 2008). The precise mechanism as to how *Cryptosporidium* overcomes this mucus barrier is unclear, however it is suggested that sporozoites have macromolecules on their surface such as Gal/GalNac-specific lectin (p30) binds to specific receptors on the epithelial cells (Bhat, Joe, Pereira Perrin and Ward, 2020) (Kuznar and Elimelech, 2005). The released sporozoites glide to the next intestinal cell so that they can develop into trophozoites. The sporozoites are spindle shaped and are roughly 4 x 0.6 µm in size (Leitch and He, 2012) and contains dense granules, single rhoptry, micronemes which are responsible for the attachment to host cell and gliding motility (Sunnotel et al., 2006) (**figure 3**).

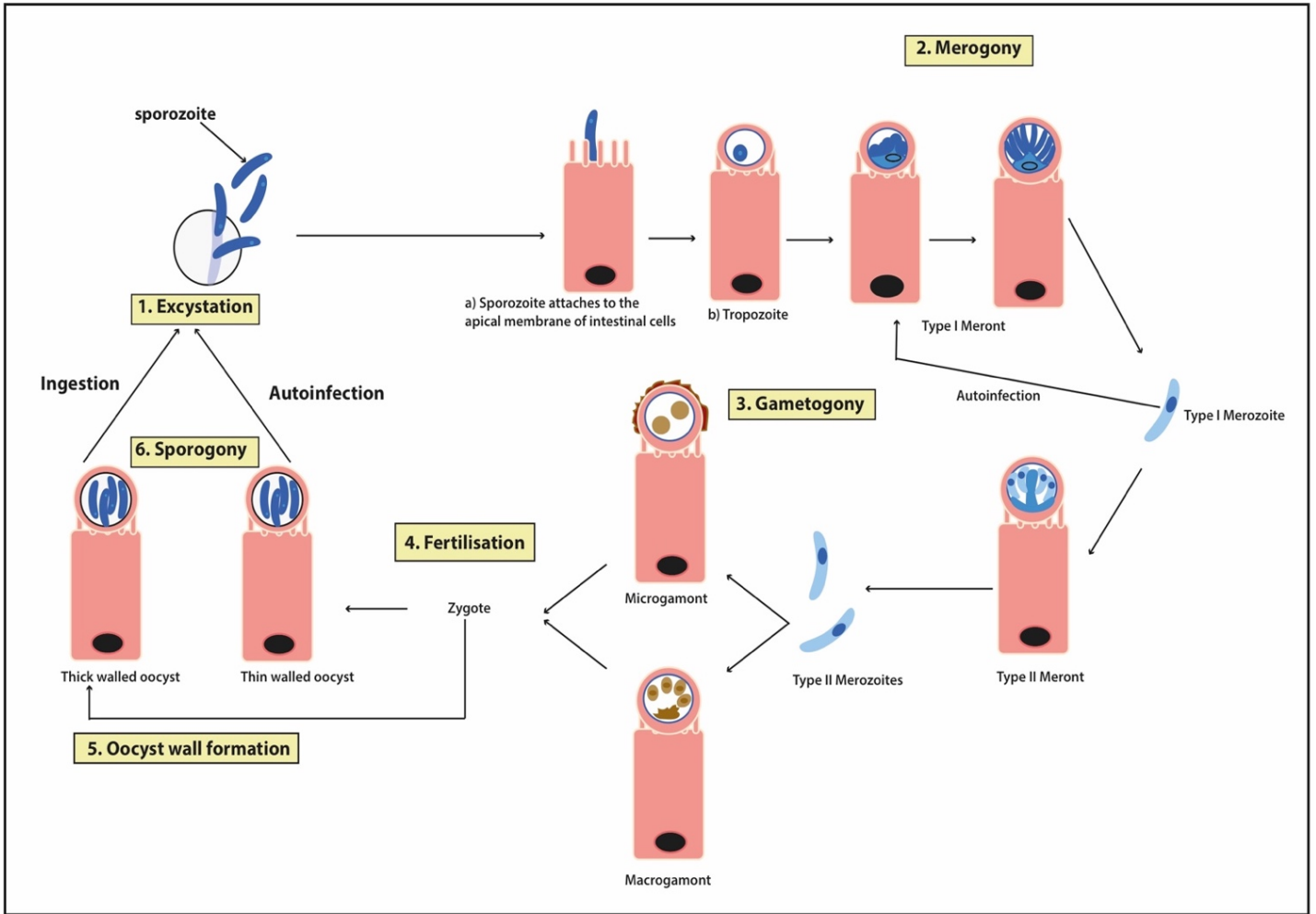


Figure 2: Schematic representation of the life cycle of *Cryptosporidium* parasite. Sporozoites excyst from oocyst and a) attach to the host cell developing into a (b) trophozoites . A parasitophorous vacuoles is formed around the trophozoite where they undergo asexual division (merogony) to form merozoites. Type 1 merozoites enter adjacent host cells to form type I meronts or type II meronts. Type II meronts enter host cells to form the sexual stages (gametogony) forming microgamonts and macrogamonts. Majority of the zygote formed develops into a thick wall oocyst that is environmentally resistant and the rest develop into a thin-walled oocyst that can cause autoinfection in the host, thus bypassing the repeated oral exposure to the thick walled oocysts.

1.5.2 Merogony

Upon attachment micronemes release molecules that trigger structural changes in the host cell. The attached sporozoite is then enveloped by the membrane of the microvilli of the epithelial cell, forming an extracellular parasitophorous vacuole (PV) (Chalmers and Davies, 2010). This vacuole protects the sporozoites from the harsh gut environments and allows the sporozoite to mature into a trophozoite which reproduces asexually by fission to produce meronts with contain merozoites. Two types of meronts are formed : type I and type II meronts (Current and Reese, 1986) . Type I meronts form eight merozoites (type I merozoites) that are released from the parasitophorous vacuole when they mature. Type I merozoites can also invade neighbouring host epithelial cells through a gliding motility, presumably using the actin-myosin cytoskeleton of the host cell (this mechanism is not clear) and form type II meronts that contain four merozoites (type II merozoites) (Thompson et al., 2005) (Leitch and He, 2012)

1.5.3 Gametogony and Fertilisation

The sexual phase of the life cycle of *Cryptosporidium* begins when type II merozoites are released and invade the host cell. Type II merozoites become either microgamete (formed from cellular fission), containing 14-16 non-flagellated microgametocytes or macrogamete (formed from enlarged type II merozoites). Microgametocytes rupture from the microgamete and fuse with the macrogametocytes to form a zygote (Leitch and He, 2012). The mature merozoite , which resembles a sporozoite, has a double membrane cuticle that contains the following organelles: endoplasmic reticulum with attached ribosomes, Golgi membrane, rhoptries and micronemes (Leitch and He, 2012).

1.5.4 Sporogony and Oocyst wall formation

The zygote develops into an oocysts and undergoes sporogony. The oocyst can differentiate into either a thick or thin walled oocyst that contains four sporozoites each (Leitch and He, 2012). Both differentiated oocysts are separated from the host epithelial cell as soon as sporulation and differentiation is completed. Thick walled oocysts (80%) are released into the lumen of the gastro-intestinal tract and are excreted from the host in faeces. Once in the environment these infective oocysts can cause infection in a new host when ingested, thus starting the cycle again (Fayer and Xiao, 2007). In addition, autoinfection occurs through the thin walled oocyst (20%), which excysts once they are separated from the epithelium and the cycle starts again (Leitch and He, 2012).

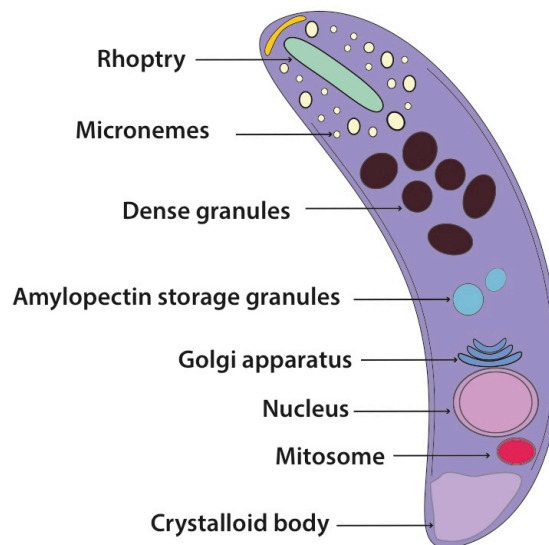


Figure 3: Schematic diagram showing the internal structures inside the sporozoite of *Cryptosporidium* (Keithly et al., 2005). The micronemes and rhoptry for entry into the host cells are found at the anterior end of the cell whilst the nucleus and the crystalloid body are at the posterior end. The double membrane bound organelle (mitosomes) is between the nucleus and crystalloid body.

1.6 Mitochondrial Functions

Mitochondrion, a double membrane-bound organelle is an important organelle in eukaryotes as it produces ATP which is needed to drive cellular needs of the cell. The mitochondrion contains its own genome (mtDNA-mitochondrial DNA), however proteins are encoded in the nucleus and transported into the organelle (Gross and Bhattacharya 2009). The typical mitochondrion contains a large number of proteins (more than 1000) that are involved in a wide variety of biochemical processes which includes: amino acid synthesis, urea synthesis, pyruvate metabolism, iron-sulfur biosynthesis, quinone metabolism, oxidative phosphorylation, steroid metabolism and fatty acid catabolism (Stairs et al., 2014) (Calvo and Mootha, 2010)

1.6.1 Protein Import Machinery

There are five complexes that are involved in protein import into the mitochondrion (Wiedemann and Pfanner, 2017) as shown in **figure 4**. The translocase of the outer membrane (TOM) complex is the site of recognizing cleavable and non-cleavable proteins for import into the inner membrane and outer membrane (Wiedemann and Pfanner, 2017). The TOM complex consists of three receptor proteins, TOM40, TOM22, TOM20 and the small TOM subunits 5,6,7. As the proteins are being translocated across the outer membrane, small chaperone membrane proteins, Tim, aid in the delivery of these proteins to their specific destination, either in the translocase of the inner membrane (TIM23/22), matrix or outer membrane SAM complex (Wiedemann and Pfanner, 2017). These Tim chaperones are normally found in pairs (Gentle et al. 2007), however research by (Alcock et al., 2011) confirmed the presence of a single TimS in *C.parvum* which has the capacity to form a homohexameric species. These pre-sequence carrying pre-proteins are handed

over to the TIM23/17/22 complex of the inner membrane via these small Tims. TIM23 subunits all have exposed domains in the intermembrane space and include the subunits: TIM50, TIM23 and TIM21. TIM 21 interacts with TIM17 determining the destination of the protein and TIM50 regulates the opening and closing of the channel (Brix et al., 1999). The chaperone protein Hsp70 is bound to PAM (Presequence translocase-Associated Motor) complex proteins and TIM44. Hsp70 helps to release proteins into the matrix, where MPP (mitochondrial processing peptidase) cleaves the N-terminal presequence (Neupert and Herrmann, 2007)

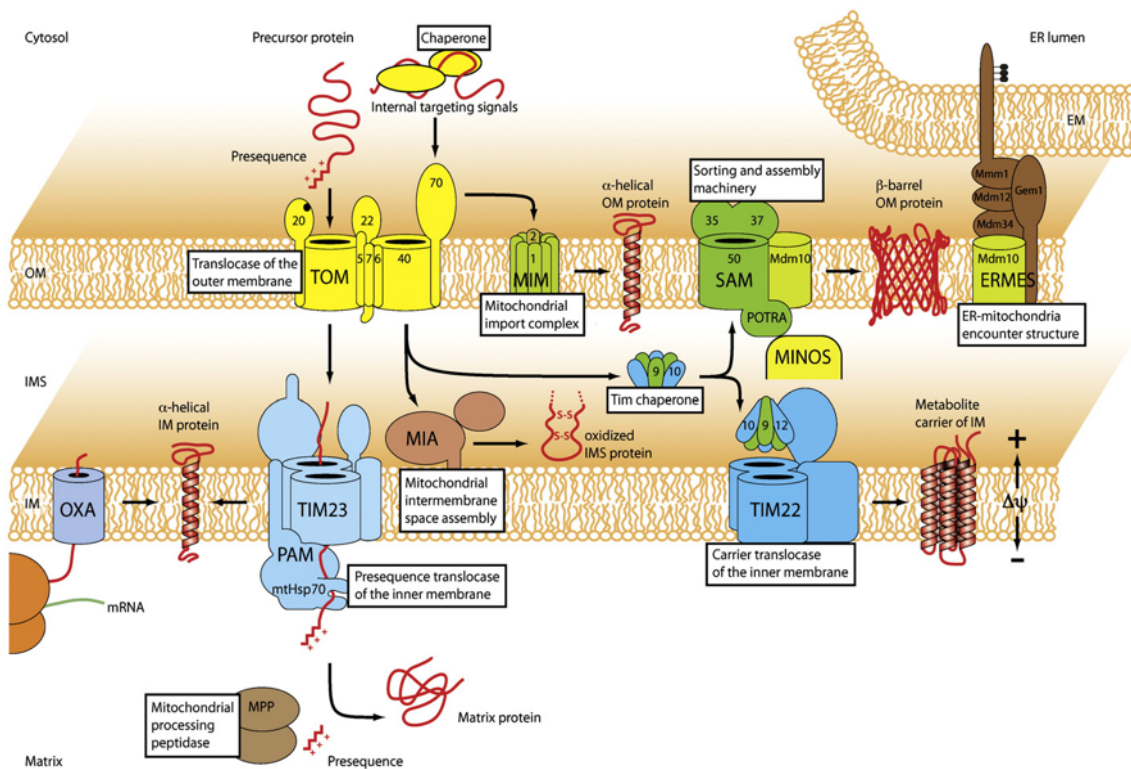


Figure 4: Mitochondrial pathways carried out by aerobic mitochondrion: Protein import machinery (Kulawiak et al., 2013). TOM20 initiates the entry of proteins in the mitochondria. Proteins are translocated across the TOM complex and enter into the intermembrane space where small Tim proteins aids in the delivery of proteins. Proteins with presequence are directed to the TIM23 complex and subsequently cleaved by Hsp70 and MPP.

1.6.2 TCA

The TCA cycle is the most central metabolic pathway for all the aerobic processes required by the organism. Carbohydrates, fatty acids and amino acids are broken down and the acetyl-CoA produced is entered in the TCA cycle. Acetyl-CoA also produced from Glycolysis enters into the TCA cycle where it undergoes oxidation. **Figure 5** Shows that there are at least eight essential enzymes involved in the TCA cycle that produce two CO₂ molecules, three NADHs, one FADH₂ and one GTP (Martínez-Reyes and Chandel, 2020). The TCA cycle starts with the reaction that combines the two-carbon acetyl-CoA with a four-carbon oxaloacetate (OAA) to generate the six-carbon molecule citrate. Aconitase converts the citrate into its isomer, isocitrate. Two oxidative decarboxylation stages take place: i) Isocitrate is converted into the five-carbon α -ketoglutarate (α -KG) by isocitrate dehydrogenase and ii) α -ketoglutarate converted into the four-carbon succinyl-CoA by α -ketoglutarate dehydrogenase (Martínez-Reyes and Chandel, 2020). These stages release two molecules of CO₂ two NADH molecules. Next succinyl CoA synthetase converts succinyl-CoA into succinate generating a GTP molecule, which can be converted into ATP. Succinate is oxidized forming the four-carbon molecule fumarate by succinate dehydrogenase which is also a part of the electron transport chain (**figure 5**). Two hydrogen atoms are transferred to FAD, producing 2FADH. The enzyme fumarase converts fumarate into malate and further into OAA (this conversion is by malate dehydrogenase) that combine with another acetyl-CoA molecule to continue the TCA cycle. The NADH and FADH produced are used in oxidative phosphorylation pathway to produce energy needed for the cells to function.

1.6.3 Oxidative Phosphorylation

The inner membrane of the mitochondria has a series of protein complexes that form the electron transport chain. The electron transport chain is comprised of complex I, II, III, IV and the ATP synthase (**figure 5**).

1.6.3.1 Complex I NADH: ubiquinone oxidoreductase

This is the first enzyme complex of the electron transport chain where ubiquinone is reduced by NADH. When one molecule of NADH binds to complex I, NADH undergoes oxidation forming NAD⁺, ubiquinol and four protons in the intermembrane space. A pair of electrons are transferred to ubiquinone (a mobile electron carrier) thus reducing it to ubiquinol which travels to complex II. The transfer of these electrons causes the translocation of four protons across the inner membrane (Deshpande and Mohiuddin, 2020). A proton gradient is created between the matrix and the intermembrane space which is required for ATP synthesis.

1.6.3.2 Complex II: Succinate Dehydrogenase

Complex II participates in both the TCA cycle and the electron transport chain. In the TCA cycle it oxidises succinate to fumarate and in the electron transport chain it transfers electrons from FADH₂ to a ubiquinone molecule. As FADH₂ does not enter complex I but enters complex II directly, no protons are pumped into the intermembrane space and therefore less energy is produced in comparison to that of NADH (Deshpande and Mohiuddin, 2020).

1.6.3.3 Complex III: Cytochrome c Oxidoreductase

Complex III consists of cytochrome B and iron - sulfur clusters that transfer electrons to cytochrome c. Ubiquinol binds to complex III and pumps two transfers two electrons to cytochrome c, translocating four protons into the intermembrane space. Cytochrome c can only accept one electron and therefore the cytochrome c reductase exists in a dimeric form to accommodate two cytochrome c molecules (Deshpande and Mohiuddin, 2020).

1.6.3.4 Complex IV : Cytochrome c Oxidase

Complex IV like complex III creates a proton gradient, pumping four protons into the intermembrane space during the movement of the electrons. Complex IV consists of heme groups and cofactors. Two reduced cytochrome c molecules bind to complex IV releasing the two electrons. These electrons are transferred to an oxygen atom which functions as the last electron acceptor. Two protons from the matrix are transferred to the reduced oxygen atom forming water and four protons in the intermembrane space (Deshpande and Mohiuddin, 2020).

1.6.3.5 Complex V : ATP Synthase

ATP synthase generates ATP, which provides the cell with the energy needed to function. The energy required for ATP synthase to produce ATP molecules is gained from the translocation of protons across the mitochondrial inner membrane creating a proton gradient. The ATP synthase has three major parts; a membrane-embedded F_0 domain, a catalytic F_1 domain and a joining stalk (**Figure 5**). The F_0 portion (inner membrane of the mitochondria) is hydrophobic and contains a channel for protons to pass through to the F_1 portion. The hydrophilic F_1 domain is comprised of five different subunits, alpha, beta, gamma, epsilon and delta (David L. Nelson). The F_1 domain is the main catalytic site and is formed from the alpha and beta subunits. The gamma and epsilon subunits form a central stalk that is anchored in the F_0 domain and stimulates the synthesis and release of ATP molecules. The delta subunit holds the alpha beta hexamer ring in place to prevent it from rotating. Due to the proton gradient between the intermembrane space and the matrix, protons travel from the F_0 portion to the F_1 portion (Deshpande and Mohiuddin, 2020).

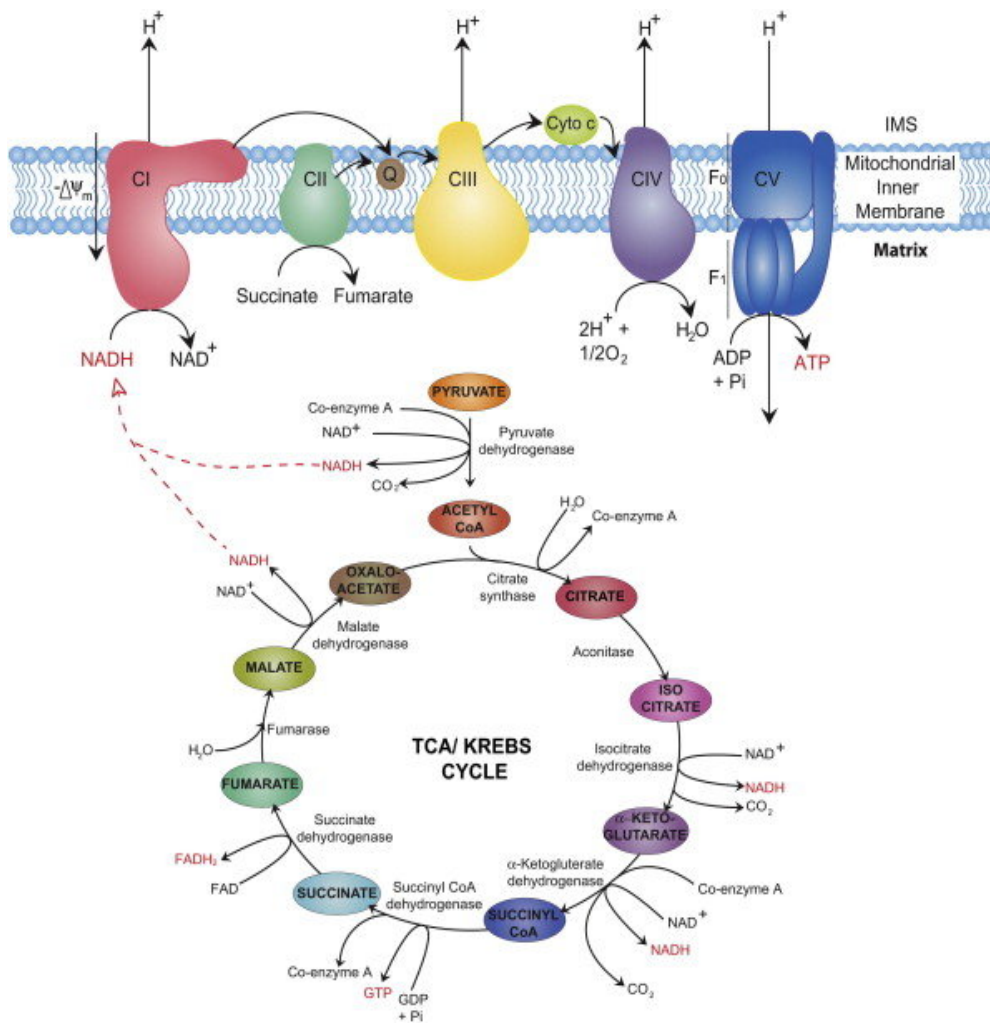


Figure 5: Mitochondrial pathways carried out by aerobic mitochondrion: TCA and ETC (Osellame, Blacker and Duchen, 2012). The ETC cycle results in the transfer of four protons from the matrix into the intermembrane space. Complex II from the ETC does not contribute to a proton gradient and the succinate present is also used in the TCA cycle. The NADH produced in the TCA cycle is utilized in the ETC.

1.6.4 Fe-S Cluster Assembly

The mitochondria plays a key role in the biogenesis of Fe-S clusters (Wachnowsky, Fidai and Cowan, 2018). The first step in Fe-S cluster is the assembly of iron and sulfur on the scaffold protein IscU. Cysteine desulfurase provides the sulfur needed whilst iron is transported via mioferrin 1 and 2 protein carrier. The iron is then transferred to IscU through frataxin (Fxn) to complete the assembly of [2Fe-2S] cluster. This early ISC machinery, also recruits electrons from the electron transfer chain (Arh1) and ferredoxin. A chaperone system comprising of Hsp70 and Jac1 binds and induces a conformational change in IscU, which releases the IscU-bound Fe-S cluster to glutaredoxin (Grx5). The [2Fe-2S] cluster can then be targeted to other proteins within the mitochondria to be converted to [4Fe-4S]. Additional iron sulfur cluster proteins are needed for this and they include : IscA1, IscA2 and Iba57. The release of [2Fe-2S] cluster can also be targeted for export from the mitochondria into the cytosol via the ABCB7 (Atm1) transported (**figure 6**).

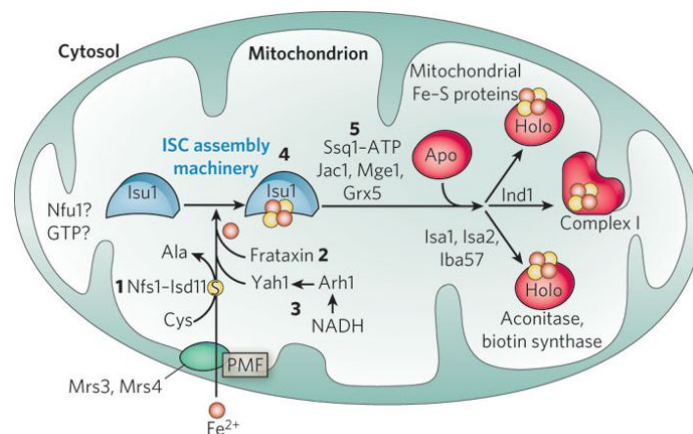


Figure 6 :Mitochondrial pathways carried out by aerobic mitochondrion: Fe-S cluster assembly (Lill, 2009). Early ISC is characterised by ferredoxin, frataxin, Arh1 and the import of sulfur and iron. Subsequent input by glutaredoxin, Jac1 and Hsp70 aids in the release of the 2Fe-2S. Late ISC machinery involves accessory proteins IscA1, IscA2 and Iba57.

1.7 Mitochondrial Diversity

Mitochondria and mitochondria related organelles (MROs) have been classified into five different groups (Muller et al., 2012) based on their energy metabolism, size, function and morphology. These five classes include: aerobic mitochondria, anaerobic mitochondria, hydrogen-producing mitochondria, hydrogenosomes and mitosomes. Mitochondria and MROs have a double membrane, however hydrogenosomes and mitosomes are highly reduced structurally and biochemically in comparison to aerobic and anaerobic mitochondria as shown in **figure 7**.

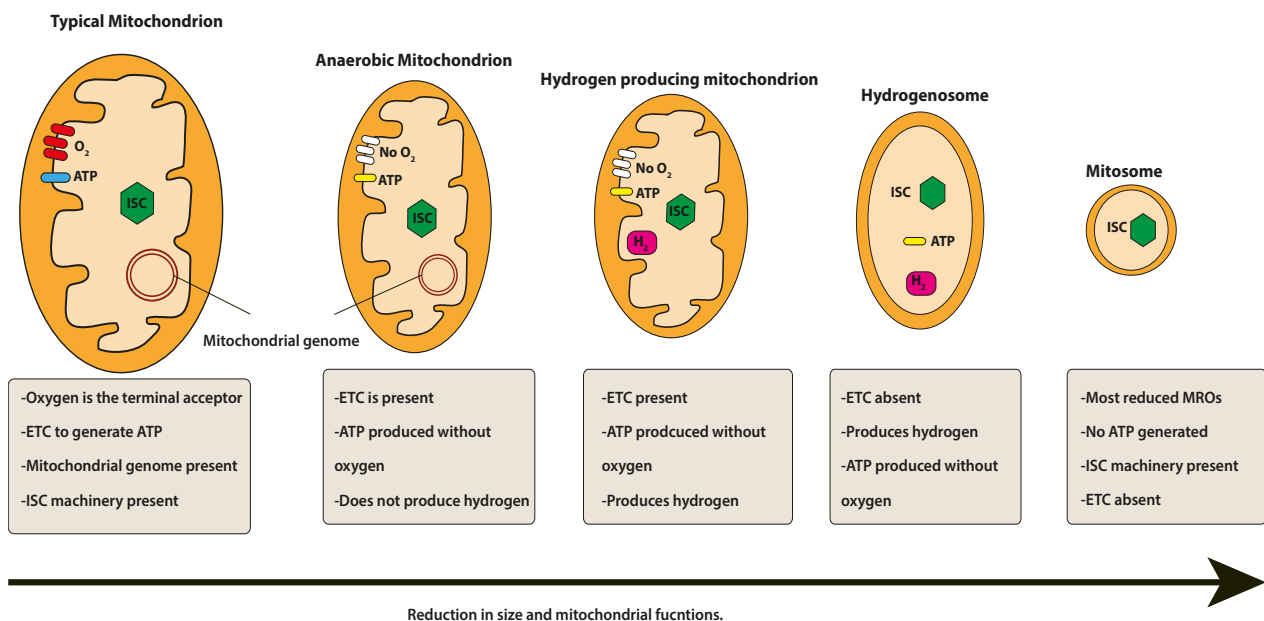


Figure 7: The five different classes of mitochondrion including the MROs (adapted diagram) (Burki, 2016). Present are class I (typical mitochondrion), class II (anaerobic mitochondrion), class III (hydrogen producing mitochondrion), class IV (hydrogenosomes), class V (mitosomes). Red shows the use of oxygen, blue shows ATP production and yellow shows ATP production without oxygen.

1.7.1 Aerobic mitochondria (Class I)

These membrane bound organelles are essential in aerobic eukaryotes and are known as canonical mitochondrion. This typical mitochondrion produces ATP by the TCA cycle, as well as being involved in other cellular processes such as cellular proliferation, apoptosis, steroid and haem synthesis, lipid metabolism and mitochondrial fusion and fission (Wang and Wu, 2014) (Mokranjac et al., 2005). The TCA cycle, oxidative phosphorylation or the electron transport chain (ETC) and β -oxidation are the three commonly associated pathways in the aerobic mitochondria. The ET chain, which is located on the inner mitochondrial membrane, is comprised of five complexes (I-V). Oxygen is the terminal electron acceptor and ATP synthesis is initiated by a proton gradient created from electron transfer through redox reactions. The TCA cycle is carried out in the matrix of the mitochondria by eight essential enzymes. These enzymes are involved in a series of organic reactions leading to the production of two carbon dioxide molecules, three NADH, one FADH₂ and one GTP molecule.

1.7.2 Anaerobic mitochondria (Class II)

Anaerobic mitochondria are just like typical mitochondria, containing an ETC and carrying out other processes like Fe-S cluster assembly. Although ETC is present, they produce ATP using other compounds such as fumarate which is endogenously produced, instead of oxygen as the final electron acceptor (Muller et al., 2012). The fumarate is converted to succinate by fumarate dehydrogenase as an end product that is excreted.

1.7.3 Hydrogen-producing mitochondria (Class III)

Hydrogen producing mitochondria do not contain a complete ETC, however they contain a membrane-associated, proton-pumping electron transport chain (Muller et al., 2012). This allows them to use protons as the terminal electron acceptor instead of oxygen, thus resulting in hydrogen production. Hydrogen producing mitochondria uses pyruvate to produce acetate and succinate end products. They have a conserved Fe-S cluster assembly, protein import and contains subunits for complex I and II of ETC.

1.7.4 Hydrogenosomes (Class IV)

Hydrogenosomes are 0.5-1 μm in diameter and they were first described by Lindmark and Muller in *Tritrichomonas foetus* (Lindmark and Muller, 1973). Hydrogenosomes lack mitochondrial genomes and therefore all the proteins targeted to the organelles have to be encoded by the nuclear genome. These proteins are transported through the double membrane via the protein import machinery that is conserved. They are the site of pyruvate metabolism and they produce ATP by substrate level phosphorylation (Muller et al., 2012).

They decarboxylate pyruvate to hydrogen, carbon dioxide and acetate by pyruvate: ferredoxin oxidoreductase (PFO) and acetate: succinate CoA-transferase.

1.7.5 Mitosomes (Class V)

Mitosomes are the most reduced MROs, which have been found in microbial parasites including *Cryptosporidium*, *Giardia* and the *Entamoeba* (Makiuchi and Nozaki, 2014).

Mitosomes do not produce hydrogen (Germot, Philippe and Le Guyader, 1996) (Tovar, Fischer and Clark, 1999) or ATP and do not use electron acceptors (Muller et al., 2012).

They lack a mitochondrial genome and electron transport chain on the inner membrane, therefore nuclear encoded proteins are directed into the matrix by the protein import machinery that is conserved. It has been suggested that they may retain an alternative respiratory pathway, AOX (Williams et al., 2010) and they synthesize Fe-S cluster proteins, which has been retained in some parasites (Tovar et al., 2003) (Goldberg et al., 2008).

Mitosomes have been recognized as being located at the posterior end of the sporozoite and is close to the nucleus in *C.parvum* (Putignani et al., 2004) . Similar structure of this mitochondrion like structure has been observed in sporozoites (Riordan et al., 1999) merozoites, trophozoites in *C.parvum* (Beyer et al., 2000) and macrogametes in *C. muris* (Uni et al., 1987).

1.8 Diversity of *Cryptosporidium* mitosomes

Cryptosporidium species have lost their mitochondrial DNA and most of them have a mitosome that has undergone reduction in size and function (Liu et al., 2016) (Keithly et al., 2005). *C. parvum* and *C.hominis*, the species that affect the intestine of humans, lack

mitochondrial DNA, pyruvate dehydrogenase (PDH) and the TCA cycle enzymes except malate-quinone oxidoreductase (MQO) and the ATP synthase subunits except alpha and beta. These species therefore rely on glycolysis or substrate level phosphorylation for ATP production. The only conserved function in all mitosomes is the Fe-S cluster assembly as seen in **figure 12**. Comparatively, *C.muris* and *C.andersoni* have retained all the TCA cycle enzymes and a fully functioning ATP synthase (Mogi and Kita, 2010).

A recent study by (Miller, Jossé and Tsaousis, 2018), has demonstrated that three proteins involved in Fe-S cluster assembly have been localised in the mitosome. IscU, IscS and frataxin, were shown to be localised within the mitosome of *C.parvum* sporozoites and merozoites (Miller, Jossé and Tsaousis, 2018). Thus, this is the first and only biochemical function that has been shown to localise in *Cryptosporidium* organelle, and as a result it provides us the tools for further understanding the functions of these reduced mitochondria. These proteins are translocated into the *Cryptosporidium* mitosome by the protein import machinery which has been highly adapted in some *Cryptosporidium* species. The TOM and SAM complexes of the outer membrane and TIM proteins have been identified in *Cryptosporidium* (Alcock et al., 2011). Small Tims can also be seen and they appear to have a single small Tim protein rather than a complex (Gentle et al., 2007).

1.9 Hypothesis

With knowledge of the reduced metabolic capacity of the *Cryptosporidium* species already outlined briefly in the introduction, the aim of this project is to investigate whether the mitochondrial protein composition in various *Cryptosporidium* species is reflected in their mitochondrial protein import machinery. This will be achieved using a combination of bioinformatics tool annotations and sequence analysis of *Cryptosporidium* from various databases, comparative analysis and analysing genomic data to identify mitochondrial proteins present in the *Cryptosporidium* species. This will provide further insight into how this parasite infects hosts, with the possibility of finding treatment for further research to be done.

Chapter 2

Materials

and

Methods

2. Materials and Methods

2.1 Bioinformatics analyses- Gene IDs and protein sequences

The websites for the databases used to generate the gene IDs and protein sequences are shown in **table 3**. To identify the proteins in the different mitochondrial pathways, KEGG was used to aid protein function prediction, providing figures and pathways to visualize what proteins are present. The mitochondrial pathways to be investigated were chosen from KEGG (<https://www.genome.jp/kegg/>) see **table 4**. Through KEGG the mitochondrial pathway for energy and carbohydrate metabolism were identified. The organism was chosen: *C.hominis*, *C.parvum* and *P.falciparum* which were analysed using the highlighted EC numbers in green from the KEGG pathway. The EC numbers gave an identification of the name of the protein, gene ID and the amino acid sequence, which was then used for further analysis in *PlasmoDB* (<https://plasmodb.org/plasmo/>) and *CryptoDB* (<https://cryptodb.org/cryptodb/>). Using BlastP in *PlasmoDB*, identified amino acid sequence were run to show the gene results of all the species of Plasmodium.

Table 3: The websites that used to generate the protein sequences, generate protein coding gene IDs and confirm the name and function of proteins.

Name	Website
KEGG	https://www.genome.jp/kegg/
<i>CryptoDB</i>	https://cryptodb.org/cryptodb/
<i>PlasmoDB</i>	https://plasmodb.org/plasmo/
Uniprot	https://www.uniprot.org/
Interpro	https://www.ebi.ac.uk/interpro/
NCBI BlastP	https://blast.ncbi.nlm.nih.gov/Blast.cgi
Malaria parasite metabolic pathways	http://mpmp.huji.ac.il/

P.falciparum 3D7 was used as the control, therefore the amino acid sequence of each specific protein from the BlastP search in *PlasmoDB*, was then analysed in *CryptoDB* using

BlastP. This was done in order to check for the conserved protein coding genes in *Cryptosporidium*. *CryptoDB* was used to search the database to identify full length sequences of the protein coding genes involved in the different mitochondrial pathways. To confirm the name of the protein, NCBI BLASTP (<https://blast.ncbi.nlm.nih.gov/Blast.cgi>) was used and the top hit with E-value closest to zero, confirmed the name of the protein.

Table 4: The overall pathway IDs used in KEGG to identify the mitochondrial pathway in question.

KEGG Pathways	Pathway ID
Glycolysis/Gluconeogenesis	00010
TCA	00020
Pyruvate metabolism	00620
Oxidative Phosphorylation	00190
Ubiquinone biosynthesis	00130

In addition, the function of the protein was confirmed using Interpro (<https://www.ebi.ac.uk/interpro/>) and Uniprot (<https://www.uniprot.org/>). Signal peptides and transmembrane helices; hidden markov mode (TMHMM) were confirmed using the annotations on *CryptoDB*. The malaria parasite metabolic pathway website (**table 3**) was used to identify the protein coding genes for Fe-S cluster assembly and protein import machinery in *Plasmodium* and the steps explained earlier were used to generate the gene IDs for the six *Cryptosporidium* species. **Figure 8** shows the flow chart showing how the gene IDs were generated.

1 Identify Metabolic Pathways based on Pathway Name/ID

Pathway Source: KEGG

Pathway Name or ID: Citrate cycle (TCA cycle) (ec:00020) (KEGG)

4

CMU_006400

11 Sequences

Transcript ID	Transcript Length	Protein Length	Genomic Length
CMU_006400-t26_1	960	319	960

Predicted Protein Sequence

319aa

```

MPTNRKRIKISLIGAGQIQSTIALLLQGRNLGDIPLFDIILGHPQKALDLIHCNEVINSPTFTQNEYEDLQSDVYVLIIT
NVPKPKPWIKRDLGEMAKIISGVNAINIKFCFQNFVYICVWLDANVYFFKESQFASNNQGMARFVLSNFKCHLS
OKLGVRPNDISAVISGHEDMIPNRSITVQGLALNPIRQQITNDELDALIKRPAFAGGELLDLKTSSAFFAPAAAS
AVANVSAVTKDSKALLVCSAEPNGEVKGLFVGPVYIIGSRQVYVVEHSGSSEQLFKDSISIKELLEPMKSLAL
  
```

Copy predicted protein sequence and run this in BlastP using the non-redundant protein sequence (nr) to confirm the identify of the protein coding gene.

5

Description	Max Score	Total Score	Query Cover	E value	Per. Ident	Accession
lactate/malate dehydrogenase, NAD binding domain-containing protein [Cryptosporidium muris RN66]	645	645	100%	0.0	100.00%	XP_002142056.1
lactate/malate NAD binding domain-containing protein [Cryptosporidium andersoni]	624	624	100%	0.0	96.55%	Q0174953.1
malate dehydrogenase, NAD-dependent [Cryptosporidium meleagridis]	461	461	98%	6e-161	67.30%	PF084182.1
malate dehydrogenase [Cryptosporidium taeni]	454	454	98%	5e-158	66.56%	KAF7456329.1
malate dehydrogenase [Cryptosporidium hominis TU502]	443	443	98%	9e-154	68.89%	XP_666655.1
type 3 Malate dehydrogenase [Cryptosporidium tyzani]	441	441	98%	3e-153	68.57%	TRY50808.1
malate dehydrogenase [Cryptosporidium parvum Iowa II]	442	442	98%	4e-153	68.57%	XP_628237.1
malate dehydrogenase [Cryptosporidium parvum]	441	441	98%	7e-153	68.57%	AAP87358.1
malate dehydrogenase [Cryptosporidium ubiquitum]	439	439	98%	3e-152	67.62%	XP_028875140.1

Search menu on *CryptoDB*, select metabolic pathways then pathway name/ID. Select KEGG as pathway source and input Pathway Name/ID using the KEGG ID.

2

Reaction Source	EC Number	Enzyme Description	Equation	Gene Count
KEGG	1.1.1.286	Isocitrate-homoisocitrate dehydrogenase	isocitric acid <=> 2-oxoglutaric acid	0
KEGG	1.1.1.37	Malate dehydrogenase	oxaloacetic acid + (S)-malic acid <=> oxaloacetic acid + (S)-malic acid	12
KEGG	1.1.1.41	Isocitrate dehydrogenase (NAD ⁺)	isocitric acid <=> 2-oxoglutaric acid	0
KEGG	1.1.1.42	Isocitrate dehydrogenase (NADP ⁺)	isocitric acid <=> oxalosuccinic acid	12
KEGG	1.1.1.42	Isocitrate dehydrogenase (NADP ⁺)	oxalosuccinic acid <=> 2-oxoglutaric acid	12
KEGG	1.1.5.4	Malate dehydrogenase (quinone)	(S)-malic acid => oxaloacetic acid	13
KEGG	1.2.4.1	Pyruvate dehydrogenase (acetyl-transferring)	Enzyme N6-(lipoyl)lysine + 2-(1-hydroxyethyl)thiamine diphosphate => [Dihydropyridopyllysine-residue acetyltransferase] S-acetyl[dihydropyridopyllysine + thiamine(1+) diphosphate	5

Results show the gene count for the pathway selected

3

Organism Filter

Apicomplexa

Chromerida

Gene Results

Gene ID	Transcript ID	Organism	Product Description	EC numbers
ChTU502y2012_407g0240	ChTU502y2012_407g0240-t32_1	<i>Cryptosporidium hominis</i> isolate TU502_2012	lactate/malate dehydrogenase NAD binding domain	1.1.1.37 (Malate dehydrogenase)
ChTU502y2012_407g0245	ChTU502y2012_407g0245-t32_1	<i>Cryptosporidium hominis</i> isolate TU502_2012	lactate/malate dehydrogenase NAD binding domain	1.1.1.37 (Malate dehydrogenase)
CmeUKMEL1_11115	CmeUKMEL1_11115-t37_1	<i>Cryptosporidium meleagridis</i> strain UKMEL1	malate dehydrogenase NAD-dependent	1.1.1.37 (Malate dehydrogenase)
CMU_006400	CMU_006400-t26_1	<i>Cryptosporidium muris</i> RN66	lactate/malate dehydrogenase, NAD binding domain-containing protein	1.1.1.37 (Malate dehydrogenase)
GNI_055910	GNI_055910-t26_1	<i>Gregarina niphadrodes</i> Unknown strain	L-lactate dehydrogenase	1.1.1.37 (Malate dehydrogenase)
GNI_056500	GNI_056500-t26_1	<i>Gregarina niphadrodes</i> Unknown strain	L-lactate dehydrogenase	1.1.1.37 (Malate dehydrogenase)

Filter results to only show apicomplexan. Choose specific strain and select the gene ID selected.

The top hit confirms the name of the protein

Figure 8: Flow chart of basic overview of the steps taken to carry out the comparative analysis to identify the protein coding genes present in the mitosome of six *Cryptosporidium* species. The TCA cycle is used in the flow chart above for simplicity. 1) The TCA cycle was chosen as the metabolic pathway. 2) The results showed all the protein coding genes and the different strains in all *Cryptosporidium* species. 3) Organism filter changed to only show apicomplexan and for example strain *C. muris* RN66 (CMU_) was chosen to be investigated further. 4-5) Predicted protein was copied and run in BlastP to confirm the name of the protein.

2.2 Analysis of genome structure

Six *Cryptosporidium* species and their isolates were used in acquiring the genome of various proteins in different pathways in the mitochondria. *CryptoDB* annotations of *C.ubiquitum* (isolate 39726), *C.andersoni* (isolate 30847), *C.muris* (RN66), *C.hominis* (TU502), *C.parvum* (Iowa II), *C.tyzzeri* (UGA55) were selected for this investigation. *P.falciparum* was used as a control as this was the most common relative of the *Cryptosporidium* parasite, *P.falciparum* (PF3D7).

FASTA sequences for proteins involved in various mitochondrial pathways namely TCA, ETC and Glycolysis were taken from the *PlasmoDB* database using PF3D7 genes. Copied FASTA sequences were placed into the *CryptoDB* and BLASTp from NCBI was used to see the similarities in conserved regions of the genes and steps shown in **figure 8** were followed.

Chapter 3

Results

3. Results

3.1 Genome for *Cryptosporidium*

The complete genome sequences obtained from the *CryptoDB* (<https://cryptodb.org/cryptodb/showApplication.do>) and *PlasmoDB* (<https://plasmodb.org/plasmo/showApplication.do>) genome and data types was used to compare the genomes of all the investigated organisms as shown in **table 5**. The whole-genome shotgun approach from GenBank as seen in **table 5**, was used to obtain the complete genome of the organisms. The resulting genome sequence showed that *C.tyzzeri* has the highest total number of genes (4038) in comparison to the other *Cryptosporidium* species. However in comparison, *P.falciparum* has more genes (5712), with a genome size of 23.3 Mbp. The difference in size is based predominantly on the fact that *Plasmodium* has more genes than the *Cryptosporidium* species investigated. Genome sizes from **table 5** reveal that *C.muris* has the largest, whereas *C.ubiquitum*, *C.tyzzeri* and *C.hominis TU502* has the smallest genome size. Although *C.tyzzeri* has the smallest genome, it has the most protein coding genes, as it contains the most total number of genes. *Cryptosporidium* species lack an apicoplast and mitochondrial genome, therefore this shows the highly reduced total number of genes in comparison to *Plasmodium*, shown in **table 5**. All *Cryptosporidium* genomes presumably have eight chromosomes and are around nine Mb in size and are very compact.

Table 5: General features of the *Cryptosporidium* genome in comparison with that of Plasmodium.

Organism	Genome size (Mbp)	Protein coding genes	Total number of Genes	Source	ID
<i>C.andersoni</i> 30847	9.1	3876	3948	GenBank	LRBS00000000.1
<i>C.muris RN66</i>	9.3	3934	3981	GenBank	AAZY00000000.2
<i>C. parvum Iowa II</i>	9.1	3941	4020	GenBank	AAEE00000000.1
<i>C.hominis isolate 30976</i>	9.1	3949	3994	Xiao-Kissinger	NI
<i>C. hominis TU502</i>	8.7	3886	3956	GenBank	NZ_AAEL00000000.1
<i>C. tyzzeri isolate UGA55</i>	9.0	3977	4038	Striepen-Kissinger	NI
<i>C. ubiquitum isolate 39726</i>	9.0	3766	3811	GenBank	LRBP00000000.1
<i>P. falciparum 3D7</i>	23.3	5305	5712	GeneDB	NI

*NI- not indicated

Table 6: The overall number of predicted proteins present in the *Cryptosporidium* species and *Plasmodium*. Each column shows the number of identified proteins.

Species	TCA	ETC	Fe/S cluster assembly	Protein import	AOX	Glycolysis and Gluconeogenesis	Ubiquinone synthesis	Pyruvate Metabolism
<i>C.andersoni</i>	9	3	16	13	1	12	4	13
<i>C.muris</i>	9	3	16	13	1	12	4	13
<i>C.parvum</i>	2	2	13	12	1	12	5	10
<i>C.hominis</i>	2	2	13	12	1	12	3	9
<i>C.tyzzeri</i>	2	2	14	14	1	11	5	10
<i>C.ubiquitum</i>	2	2	13	12	0	12	0	10
<i>P.falciparum</i>	10	5	13	23	0	13	*	*

* Pathway was not investigated. TCA (KEGG) - Number of identified steps in cycle (not number of proteins identified). ETC - Number of different subunits identified. Fe/S and protein import – number of protein hits from BLAST search.

3.2 Protein Import Machinery

Analysis from BlastP using *CryptoDB* and *PlasmoDB*, showed that the protein import machinery in the *Cryptosporidium* species investigated is very limited in comparison to *Plasmodium*. **Figure 9** shows that *P.falciparum* has a more conserved protein import machinery with 23 proteins involved. **Table 8** shows the number of proteins involved in the protein import machinery investigated. The small TOM complexes 5,6 and 7 are absent from all *Cryptosporidium* species, however TOM 7 is present in *P.falciparum*. TOM40, TIM50,TIM17, TIM14,SAM50 as well as MPP alpha and beta subunit are shown to be present in both *Cryptosporidium* and *P.falciparum* (**table 8**). In addition MIPP and Imp1 were not identified in any of the *Cryptosporidium* species, however these were identified in *P.falciparum*.

Table 8:Proteins present in the protein import machinery of *Cryptosporidium* and *Plasmodium*.

	<i>C. andersoni</i>	<i>C. muris</i>	<i>C. parvum</i>	<i>C. hominis</i>	<i>C. tyzzeri</i>	<i>C. ubiquitum</i>	<i>P. falciparum</i>
TOM40							
TOM20							
TOM22							
TOM 7							
TOM 6							
TOM 5							
TOM 70							
TIM16							
TIM 23	*	*	*	*		*	
TIM 50							
TIM 21							
TIM 17							
TIM 22							
TIM 54							
TIM 9-10			*	*	*	*	
TIM 18							

TIM 16							
TIM 12							
TIM 15 (Hep1)		*					
TIM 14							
TIM 8-13							
SAM50							
SAM37							
SAM35							
MPP- α							
MPP- β							
Hsp70							
GrpE							
Cpn10							
Cpn20							
Cpn60							
MIP							
Imp1							
Total	13	13	12	12	14	12	23

* Indicates proteins that may be present (hypothetical or uncharacterized proteins). Blue shading-protein is identified. Blank protein not identified.

Figure 9 shows that OXA1 is absent from all the *Cryptosporidium* species, whereas it is present in *Plasmodium*. A single member of the Tim17/22/23 family was identified, however it is unclear as to whether this was TIM23 (identified in *C.tyzzeri*) or TIM22. Hsp70, Cpn10, Cpn60, MPP (alpha and beta subunits) and GrpE and Hep1 (which may not be present in *C.muris*) are present in all species. *P.falciparum* seems to be the only parasite that possess PAM16, TOM20 and both Tim8-13, Tim9-10 complexes.

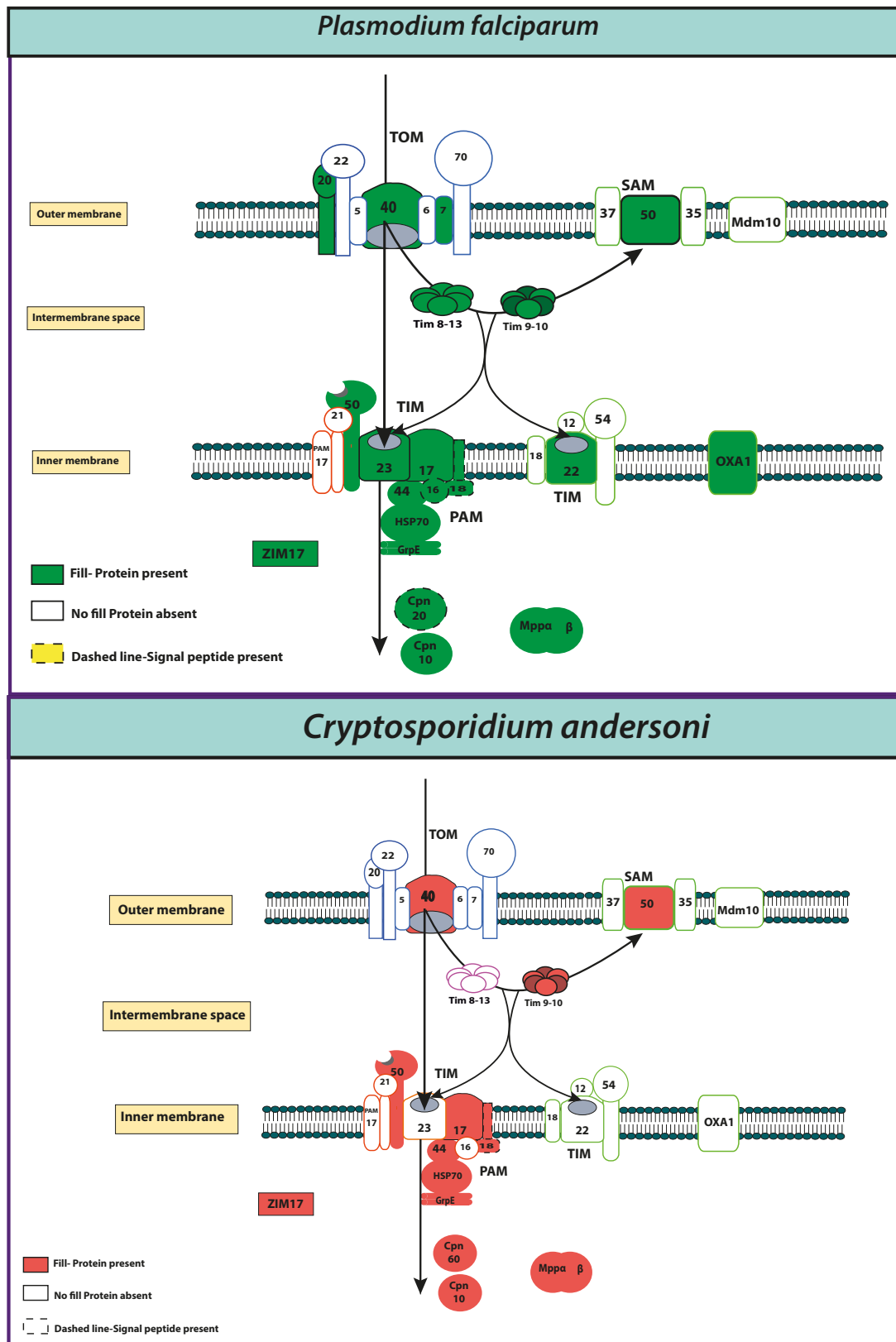


Figure 9: Overview of the five major protein import pathways of the mitosome in *Cryptosporidium* and *Plasmodium*. Presequence- carrying proteins are imported by the TOM complex and the Presequence translocade of the TIM complex. In the genome of *C.parvum*, only a subset of these components were detected , including the single member of the TIM17/22/23 family of proteins. Numbers represent the subunits for each of the protein import components. Arrows indicate the specific routes as to which proteins are imported into the mitosome. Protein identified in each species is shown coloured in red, whereas those without a fill means that the protein has not been identified or annotated properly. Dashed lines shows that a protein signal peptide is present.

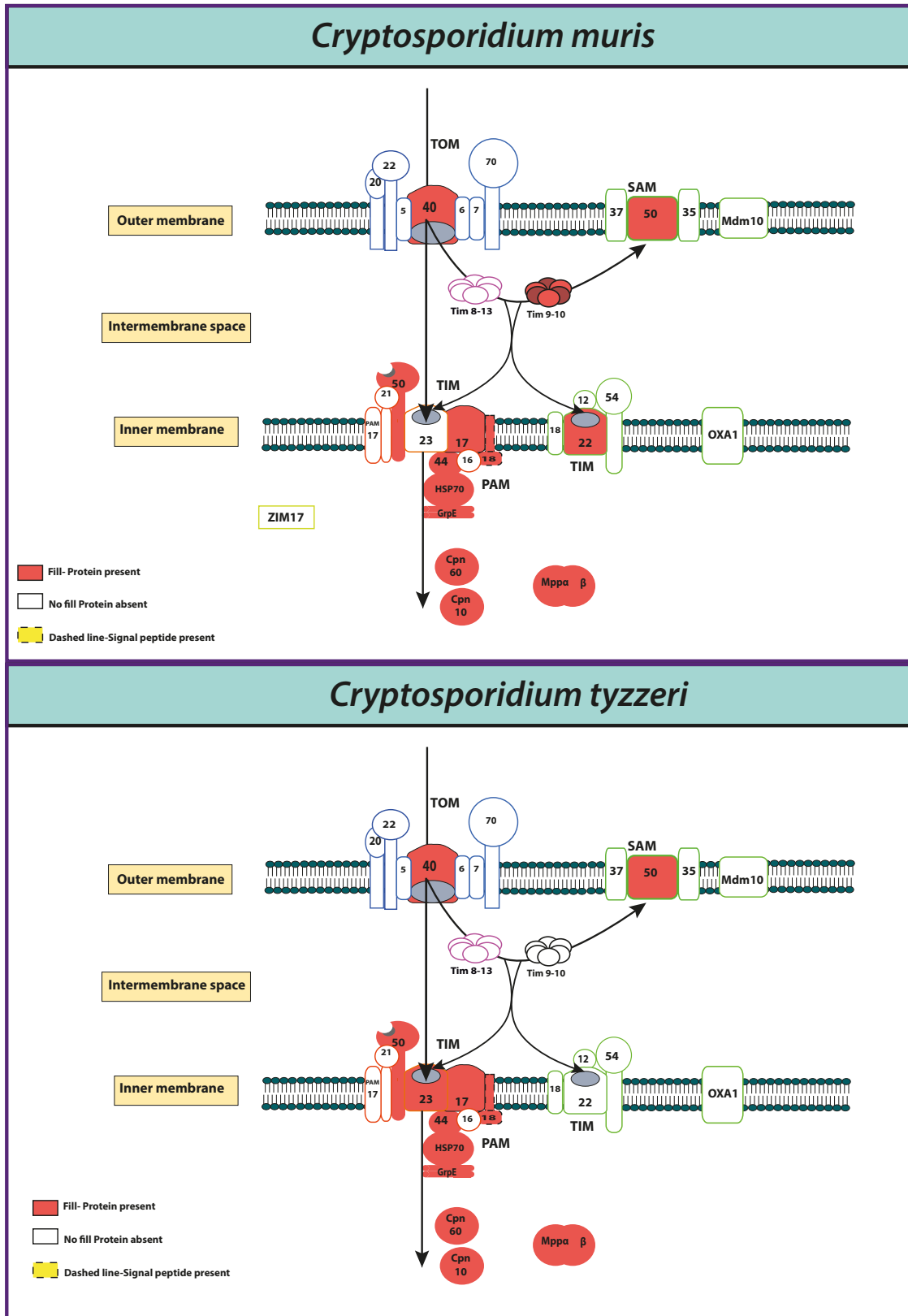


Figure 9: Overview of the five major protein import pathways of the mitosome in *Cryptosporidium* and *Plasmodium*. Presequence- carrying proteins are imported by the TOM complex and the Presequence translocase of the TIM complex. In the genome of *C.parvum*, only a subset of these components were detected , including the single member of the TIM17/22/23 family of proteins. Numbers represent the subunits for each of the protein import components. Arrows indicate the specific routes as to which proteins are imported into the mitosome. Protein identified in each species is shown coloured in red, whereas those without a fill means that the protein has not been identified or annotated properly. Dashed lines shows that a protein signal peptide is present.

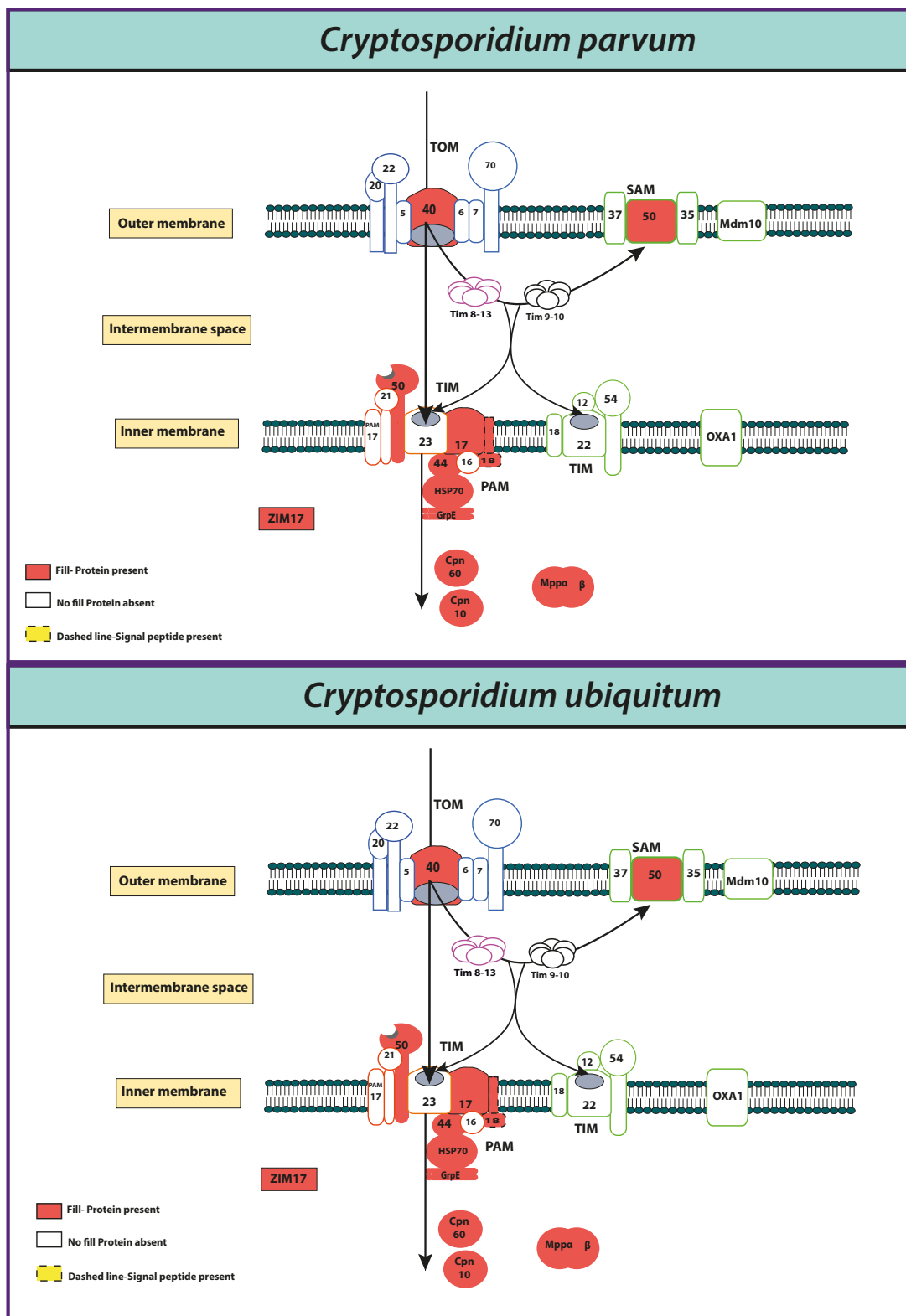


Figure 9: Overview of the five major protein import pathways of the mitosome in *Cryptosporidium* and *Plasmodium*. Presequence- carrying proteins are imported by the TOM complex and the Presequence translocase of the TIM complex. In the genome of *C.parvum*, only a subset of these components were detected , including the single member of the TIM17/22/23 family of proteins. Numbers represent the subunits for each of the protein import components. Arrows indicate the specific routes as to which proteins are imported into the mitosome. Protein identified in each species is shown coloured in red, whereas those without a fill means that the protein has not been identified or annotated properly. Dashed lines shows that a protein signal peptide is present.

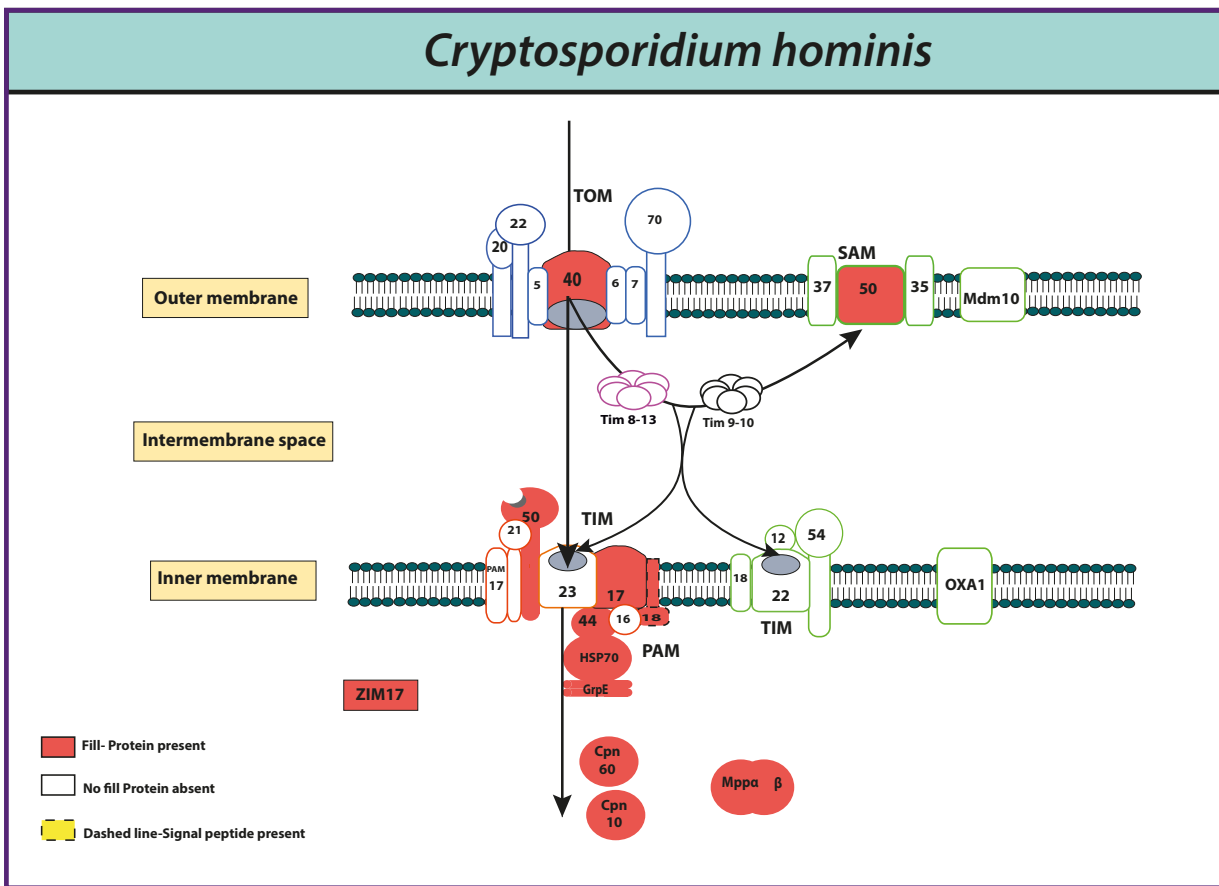


Figure 9: Overview of the five major protein import pathways of the mitosome in *Cryptosporidium* and *Plasmodium*. Presequence- carrying proteins are imported by the TOM complex and the Presequence translocate of the TIM complex. In the genome of *C.parvum*, only a subset of these components were detected , including the single member of the TIM17/22/23 family of proteins. Numbers represent the subunits for each of the protein import components. Arrows indicate the specific routes as to which proteins are imported into the mitosome. Protein identified in each species is shown coloured in red, whereas those without a fill means that the protein has not been identified or annotated properly. Dashed lines shows that a protein signal peptide is present.

3.3 The Citric Acid Cycle

Two of the six *Cryptosporidium* species investigated species contained TCA functioning proteins.

The number of identified proteins of the TCA cycle varied from two to ten as shown in **table 9**.

Four of the *Cryptosporidium* species had a small number of TCA proteins identified: *C.tyzzeri*, *C.andersoni*, *C.ubiquitum*, *C.hominis* (seen in **figure 10**). However the proteins present did not equate to a complete TCA cycle.

Table 9: Proteins present in the TCA cycle of *Cryptosporidium* and *P.falciparum*.

Proteins	EC number	C. pavrum	C. hominis	C. tyzzeri	C. andersoni	C. muris	C. ubiquitum	P. falciparum
Pyruvate synthase	1.2.7.1							
Citrate synthase	2.3.3.1							
Aconitate hydratase	4.2.1.3							
Isocitrate dehydrogenase	1.1.1.42							
Oxoglutarate dehydrogenase	1.2.4.2							
Succinyl-CoA synthetase	6.2.1.5							
Succinate dehydrogenase	1.3.5.1							
Fumarate hydratase	4.2.1.2							
Malate dehydrogenase	1.1.5.4							
Pyruvate carboxylase	4.1.1.1							
Total		2	2	2	9	9	2	10

Shaded regions shows the proteins identified in TCA. Blank- protein not identified. EC numbers for protein identification.

C.andersoni and *C.muris* have a full TCA cycle, however the pyruvate carboxylase protein was not identified, which suggests that another enzyme is utilised in the conversion of pyruvate to oxaloacetate. Pyruvate dehydrogenase, which is present in most eukaryotes, was not identified in any of the *Cryptosporidium* species, however this was present in *Plasmodium*. Pyruvate synthase/ Pyruvate: ferredoxin oxidoreductase (PFO), was identified in all the *Cryptosporidium* species.

Malate dehydrogenase and pyruvate synthase were the only two proteins identified in *C.parvum*, *C.hominis*, *C.ubiquitum* and *C.tyzzeri*. All species in relations to their TCA protein composition can be seen in **figure 10 and table 9**.

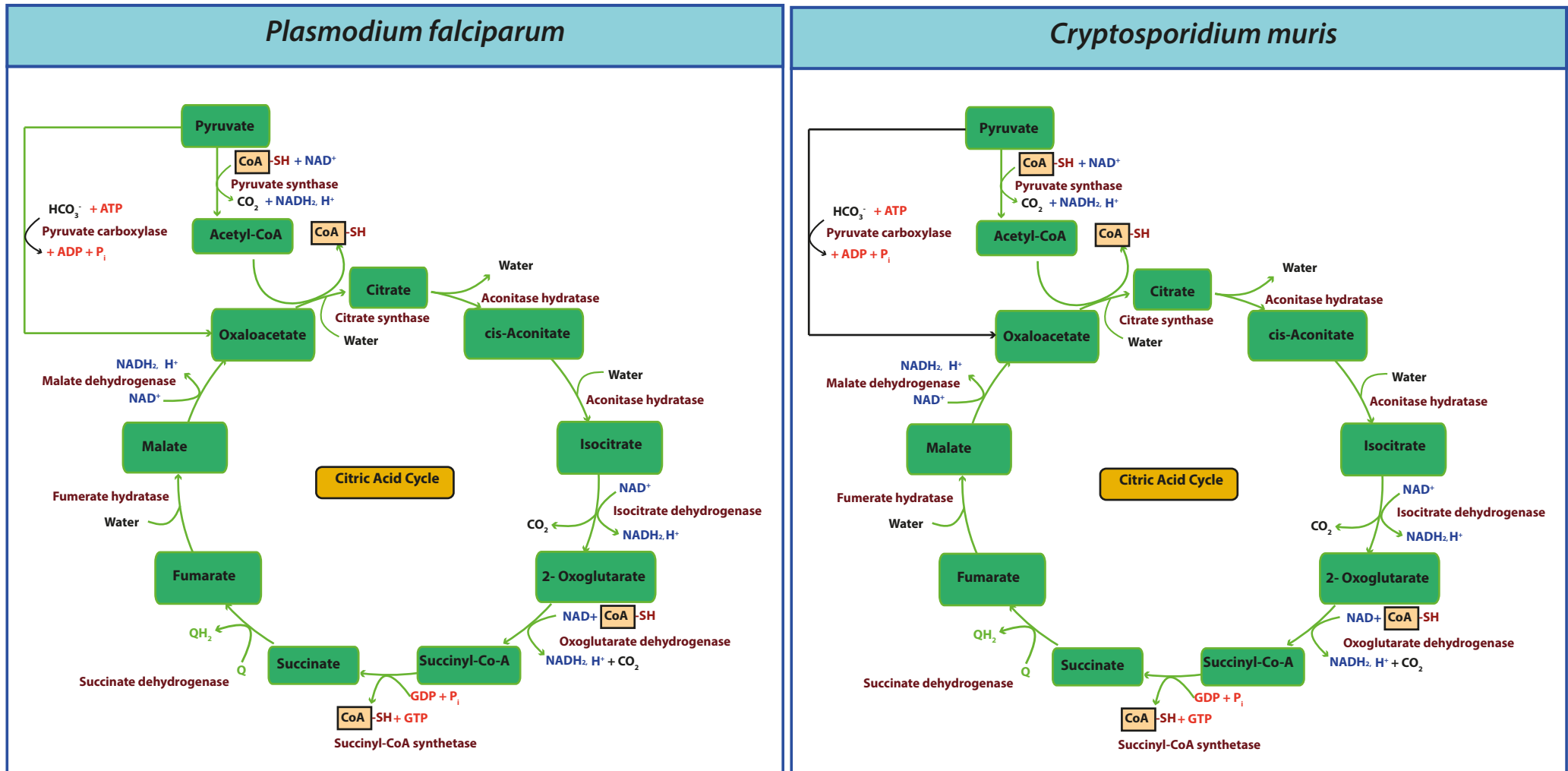


Figure 10: TCA cycle content for each species investigated in *Cryptosporidium* and *P.falciparum*. Steps coloured in green shows when the protein has been identified, red shading suggests that the protein has not been identified. *C.parvum*, *C.tyzzeri*, *C.ubiquitum* and *C.hominis* have lost majority of the proteins used in glycolysis and gluconeogenesis.

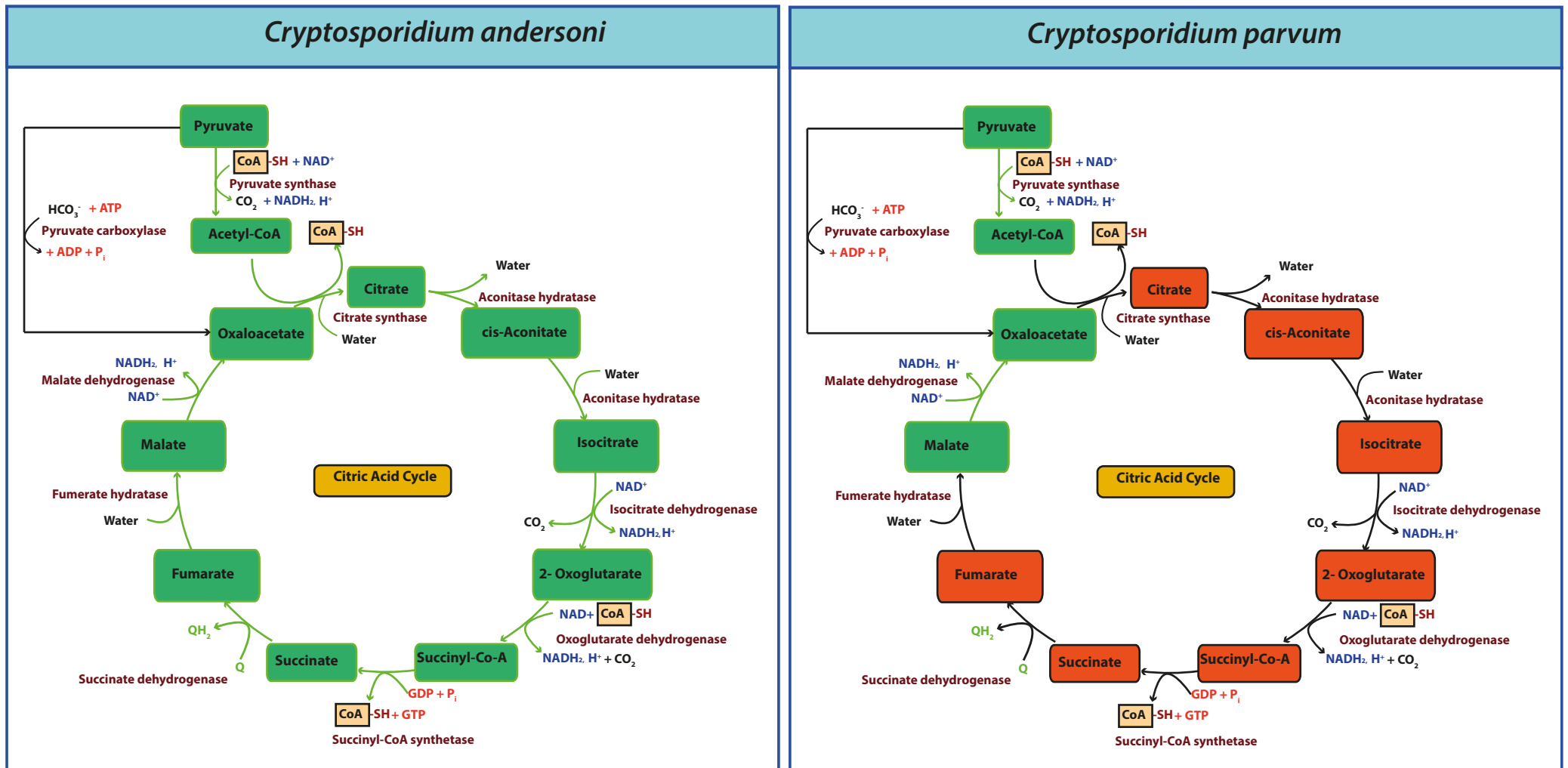


Figure 10: TCA cycle content for each species investigated in *Cryptosporidium* and *P.falciparum*. Steps coloured in green shows when the protein has been identified, red shading suggests that the protein has not been identified. *C.parvum*, *C.tyzzeri*, *C.ubiquitum* and *C.hominis* have lost majority of the proteins used in glycolysis and gluconeogenesis.

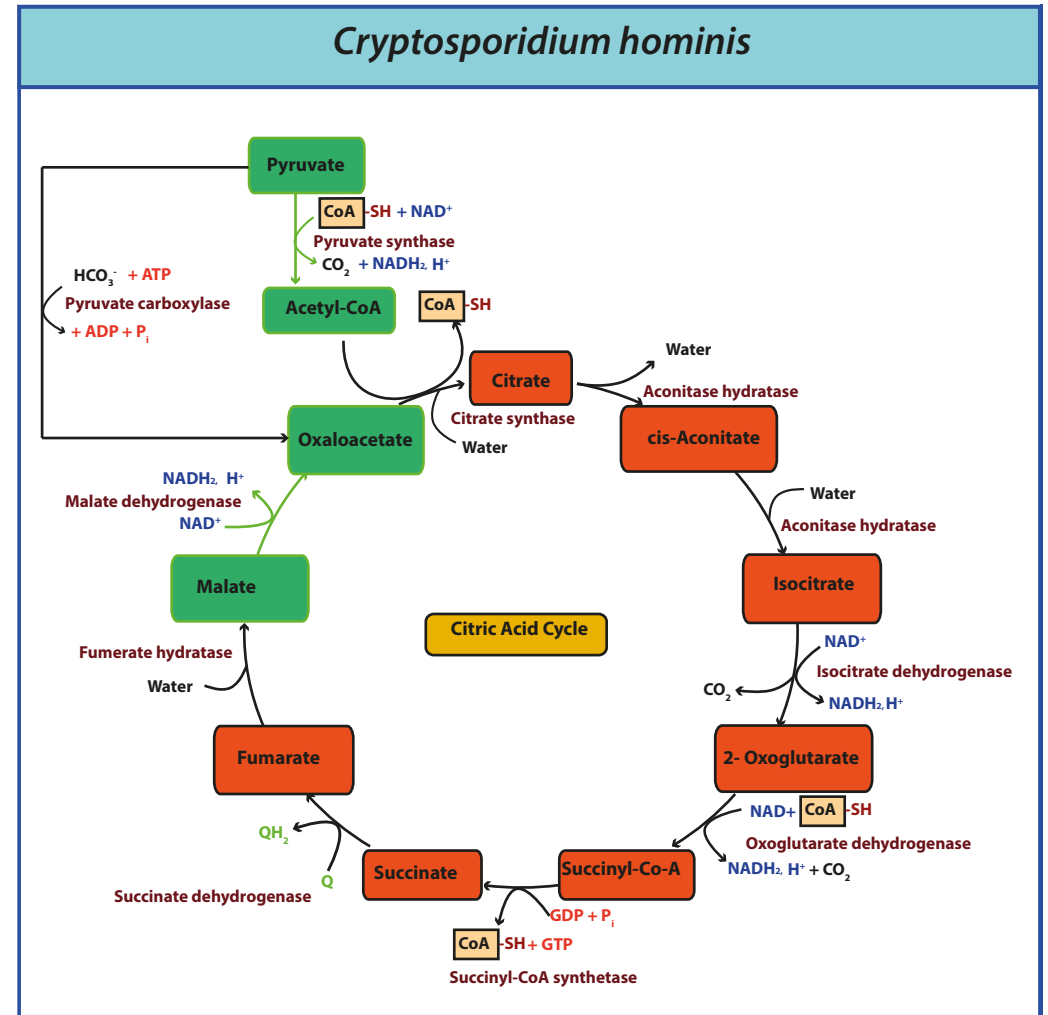
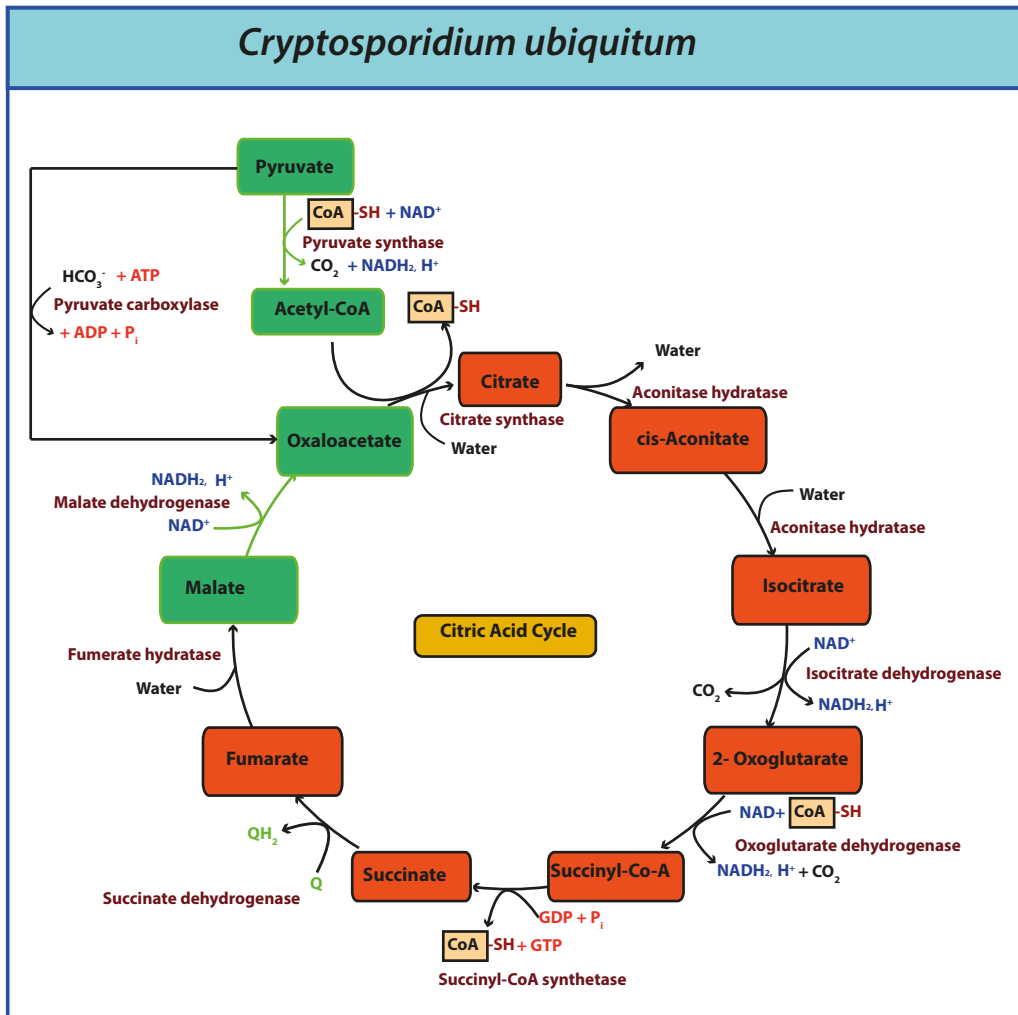


Figure 10: TCA cycle content for each species investigated in *Cryptosporidium* and *P.falciparum*. Steps coloured in green shows when the protein has been identified, red shading suggests that the protein has not been identified. *C.parvum*, *C.tyzzeri*, *C.ubiquitum* and *C.hominis* have lost majority of the proteins used in glycolysis and gluconeogenesis.

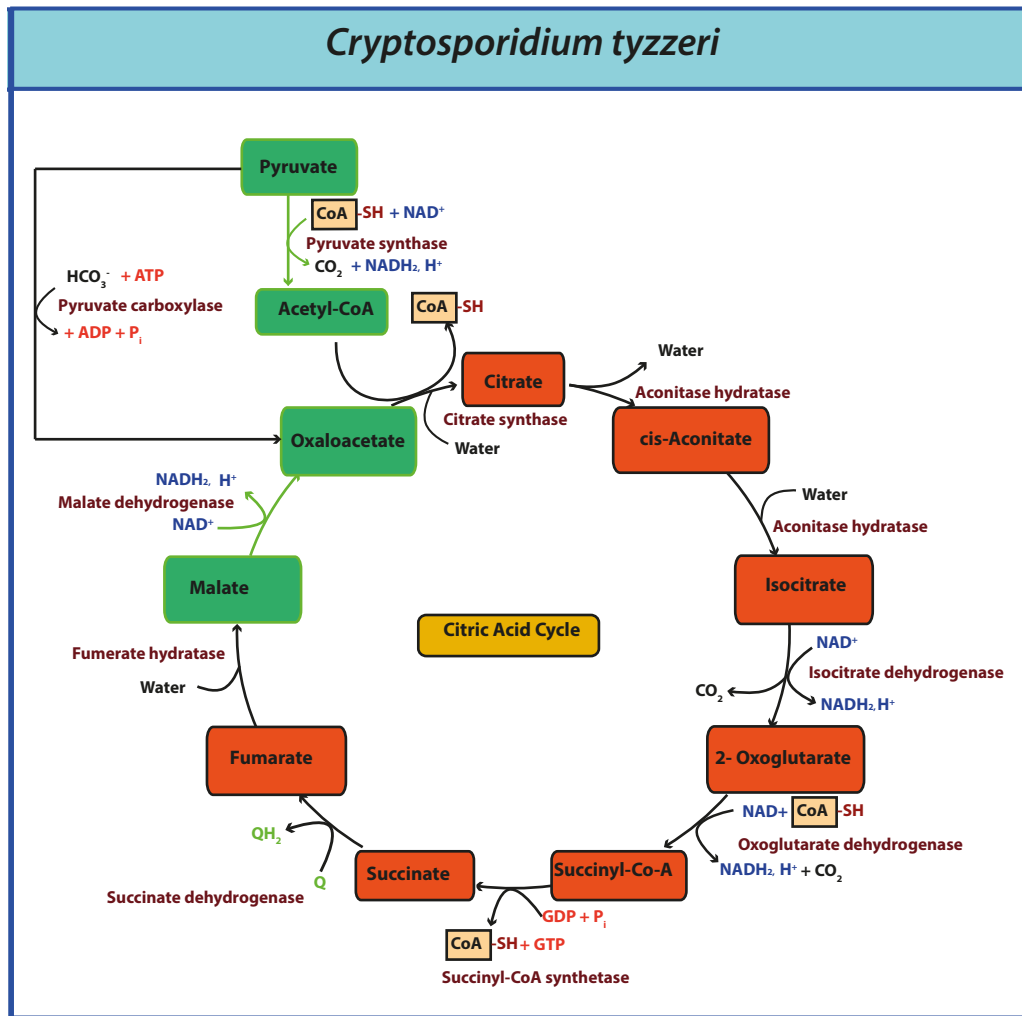


Figure 10: TCA cycle content for each species investigated in *Cryptosporidium* and *P.falciparum*. Steps coloured in green shows when the protein has been identified, red shading suggests that the protein has not been identified. *C.parvum*, *C.tyzzeri*, *C.ubiquitum* and *C.hominis* have lost majority of the proteins used in glycolysis and gluconeogenesis.

3.4 The Electron Transport Chain

All of the *Cryptosporidium* species investigated contained partial ETC proteins. Subunits ranged from one to 13 and this is seen in **figure 11**. Complex III and Complex IV are absent in all species, except for *P.falciparum*, whereas complex II is absent in four of the *Cryptosporidium* species, but is present in the other two (*C.andersoni* and *C.muris*). All six species in relations to their electron transport chain protein composition can be seen in **figure 11 and table 10**.

Table 10: Complexes of the ETC present in *Cryptosporidium* and *Plasmodium*.

Proteins	EC number	<i>C. parvum</i>	<i>C. hominis</i>	<i>C. tyzzeri</i>	<i>C. andersoni</i>	<i>C. muris</i>	<i>C. ubiquitum</i>	<i>P. falciparum</i>
Complex I (NADH dehydrogenase)	1.6.99.3							
Complex II (succinate dehydrogenase)	1.3.5.1							
Complex III (cytochrome bc1 complex)	7.1.1.8							
Complex IV (cytochrome c oxidase)	1.9.3.1							
Complex V (V and F-type ATPase)	7.1.2.2							
AOX								
Total complexes present		2	2	2	3	3	2	5

Shaded regions shows the subunits identified in ETC. EC numbers from KEGG used for identification.

Complex I, only one subunit was identified in both *Cryptosporidium* species and *P.falciparum*. Complex II, two subunits were identified in *Plasmodium* (flavoprotein and iron-sulfur subunit) shown in **supplementary table S1**, whereas only one subunit was identified in *C.muris* and *C.andersoni* (flavoprotein subunit) shown in **supplementary table S1**. Complex III and IV were not identified in any of the *Cryptosporidium* species, however these were present in *Plasmodium* with six to eleven subunits as shown in **figure 11**. AOX (alternative oxidase) was present in all *Cryptosporidium* species except for *C.ubiquitum* (**supplementary table S1**). The ATPase complex containing both F and V type ATPase, was identified in all species. *P.falciparum*, *C.muris* and *C.andersoni* all have 13 subunits in the top part of the ATPase, which was identified as the most subunits present. **Supplementary table S1**, contains more information on the name of the subunits present.

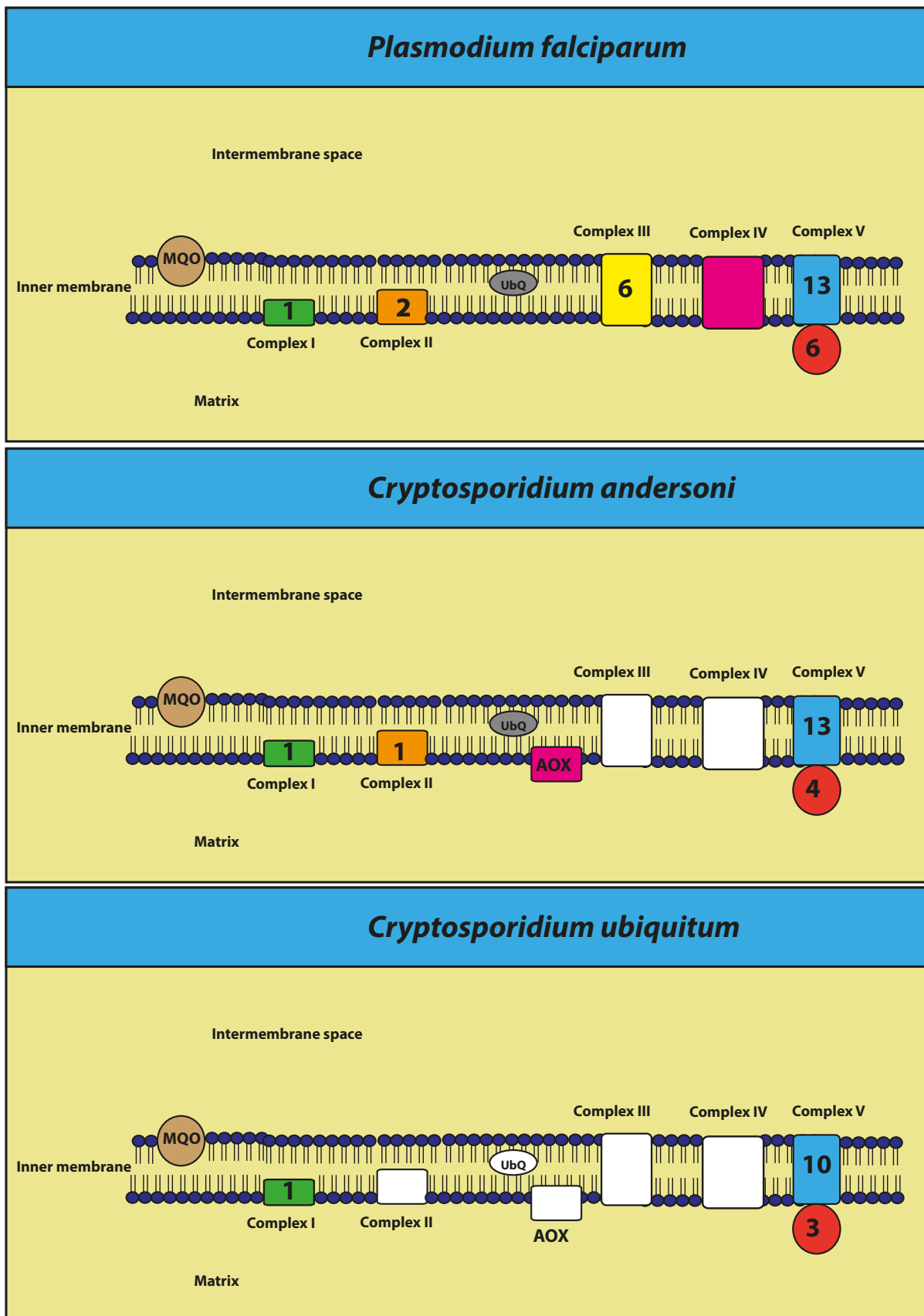


Figure 11: The ETC content for each *Cryptosporidium* and *Plasmodium* species analysed. Each coloured complex shows when the protein forming the complex has been identified. The number present shows the number of protein subunits identified. *Plasmodium falciparum* contains all complexes with varying amounts of subunits present.

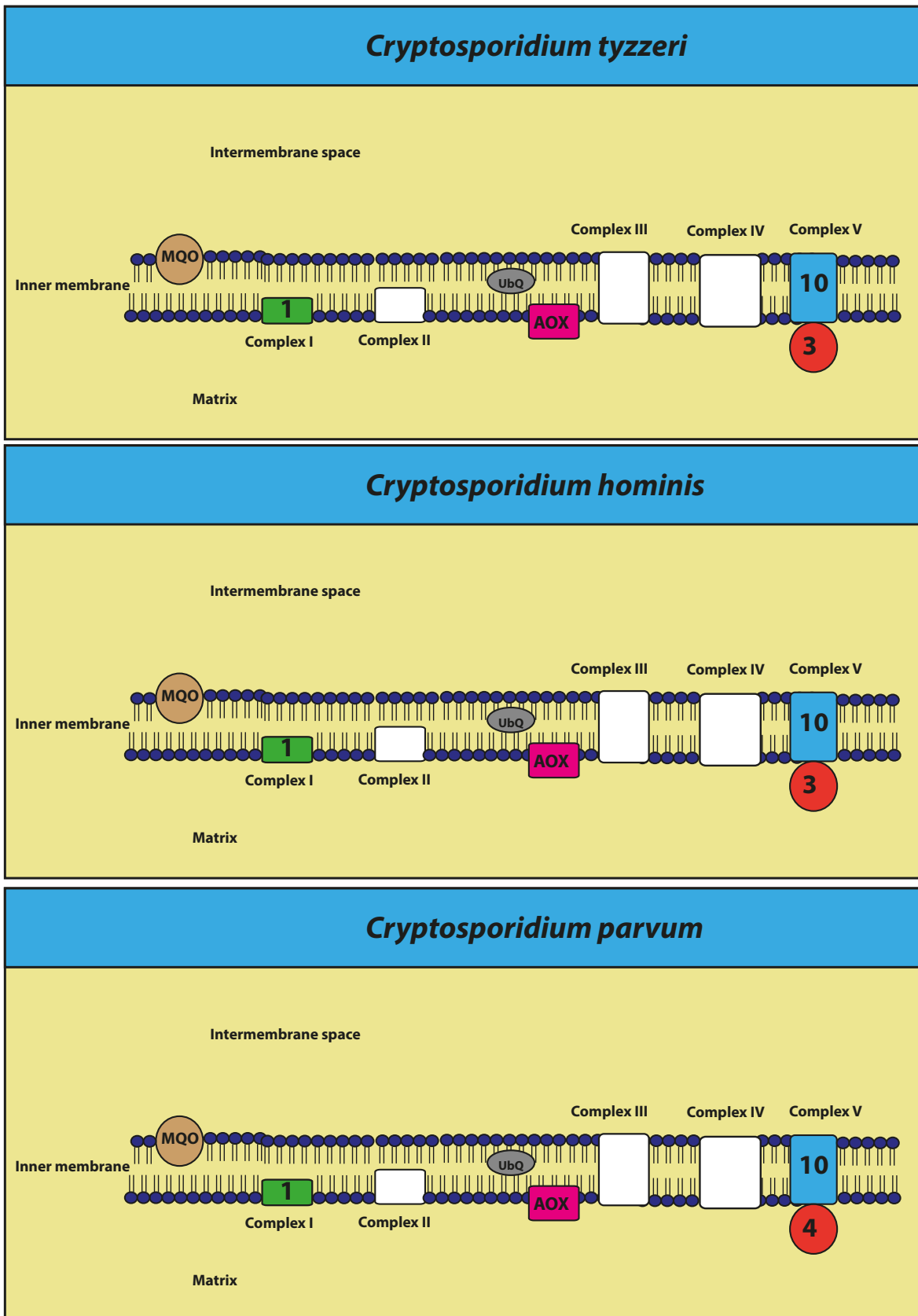


Figure 11: The ETC content for each *Cryptosporidium* and *Plasmodium* species analysed. Each coloured complex shows when the protein forming the complex has been identified. The number present shows the number of protein subunits identified. *Plasmodium falciparum* contains all complexes with varying amounts of subunits present.

Cryptosporidium muris

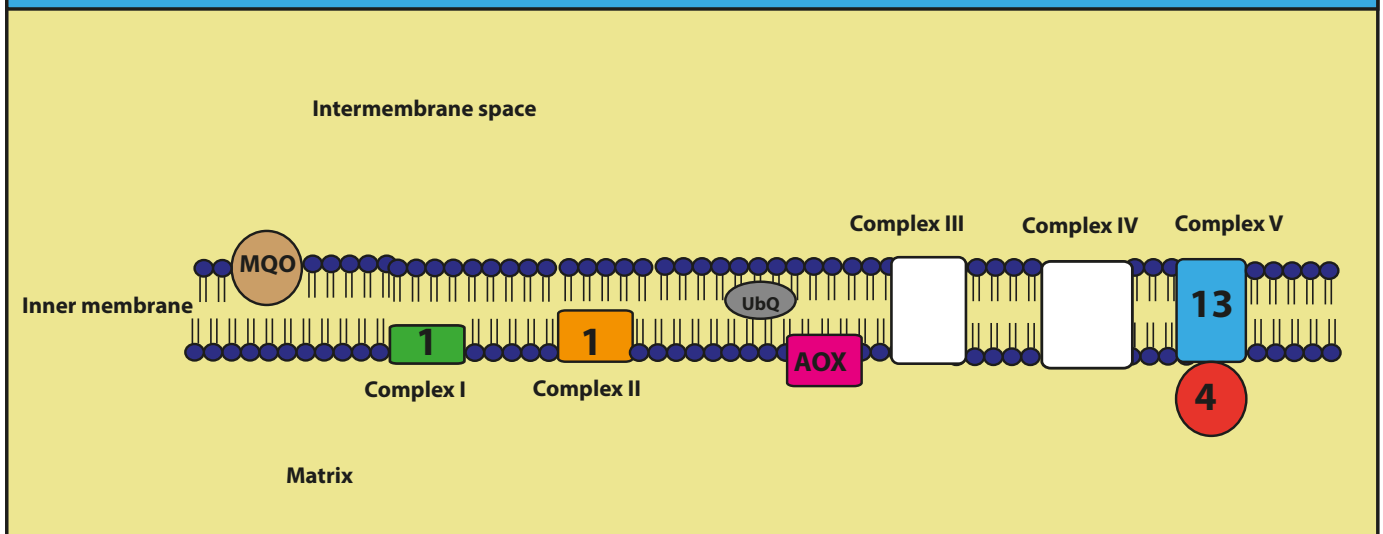


Figure 11: The ETC content for each *Cryptosporidium* and *Plasmodium* species analysed. Each coloured complex shows when the protein forming the complex has been identified. The number present shows the number of protein subunits identified. *Plasmodium falciparum* contains all complexes with varying amounts of subunits present.

3.5 Fe-S Cluster

The protein composition for Fe-S cluster is shown in **figure 12**. A wide range of components of the Fe-S cluster assembly were identified and this pathway is clearly conserved throughout the *Cryptosporidium* species and *Plasmodium* investigated. *C.andersoni* and *C.ubiquitum* may have mitoferrin 2 (MFRN2) present but this has not been fully annotated (**see supplementary table S2**). The chaperone proteins IscA1 and IscA2 were only present in *C.andersoni*, *C.muris* and *P.falciparum*. IBA57 and FDX1L, were not identified in any of the species investigated. *C.muris* and *C.andersoni* contained the most Fe-S cluster assembly proteins (16) as shown in **table 11**. Whereas, *C.parvum*, *C.hominis*, *C.ubiquitum* and *P.falciparum* contained the least number of Fe-S cluster assembly proteins (13 each). All species investigated have a fully functioning and conserved Fe-S cluster assembly machinery. Frataxin (FXN) was identified in all the

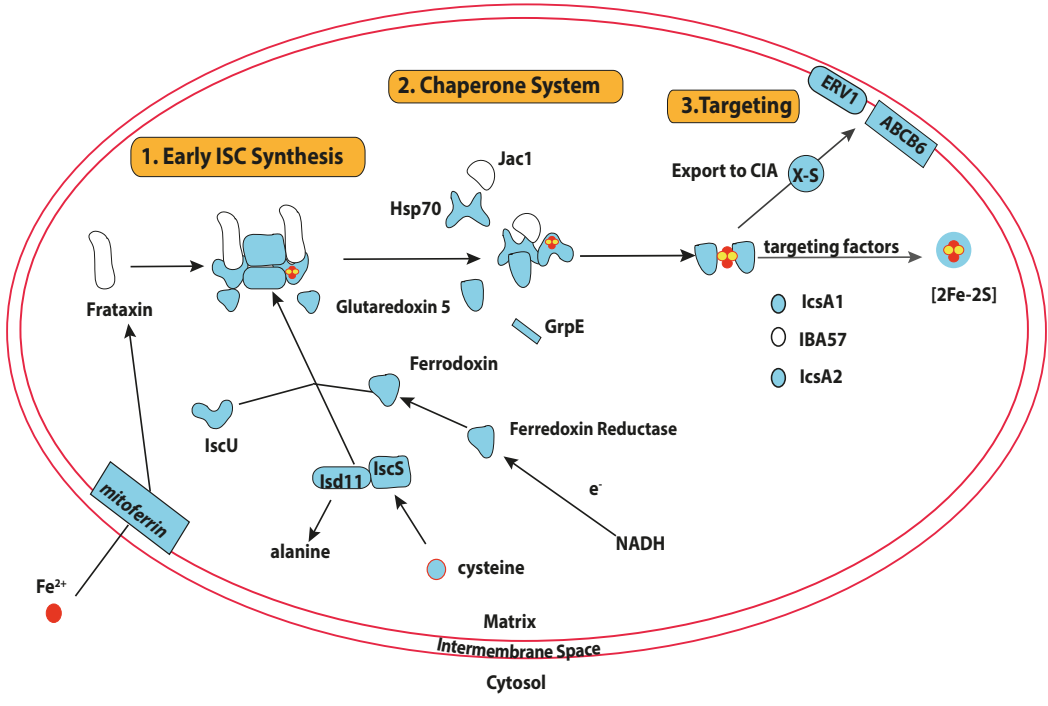
Cryptosporidium species, however it was absent in *P.falciparum*. It should be noted that *P.falciparum* contains an apicoplast, therefore some of the proteins shown not be identified here, may be present in the apicoplast.

Table 11: Proteins that have been identified using BLASTP from NCBI and *CryptoDB*, which may potentially be involved in Fe-S cluster assembly.

	<i>C. andersoni</i>	<i>C. muris</i>	<i>C. hominis</i>	<i>C. parvum</i>	<i>C. tyzzeri</i>	<i>C. ubiquitum</i>	<i>P. falciparum</i>
IscS							
FDXR							
FDX1							
Isc11							
FDX1L							
MFRN1/MRs3 or MFRN2/Mrs4							
FXN							
IscU							
GLRX5							
Hsp70							
Jac1							
GrpE							
Ind1							
IscA1							
IscA2							
IBA57							
ABCB6							
ABCB7/Atm1							
Erv1							
Total proteins	16	16	13	13	14	13	13

Shaded regions shows the proteins identified in Fe-S cluster assembly. **Annotations:** IscS-Cysteine desulfurase, FDXR-ferredoxin reductase, FDX1-ferredoxin, FDX1L-ferredoxin 2, MFRN-mitoferrin, FXN-frataxin, IscU-iron sulfur cluster assembly, GLRX5-glutaredoxin 5, Jac1-J-type co-chaperone, IscA1/2-iron sulfur cluster assembly 1/2, ABCB6/7- ATP Binding Cassette Subfamily B Member 6/7.

Plasmodium falciparum



Cryptosporidium muris

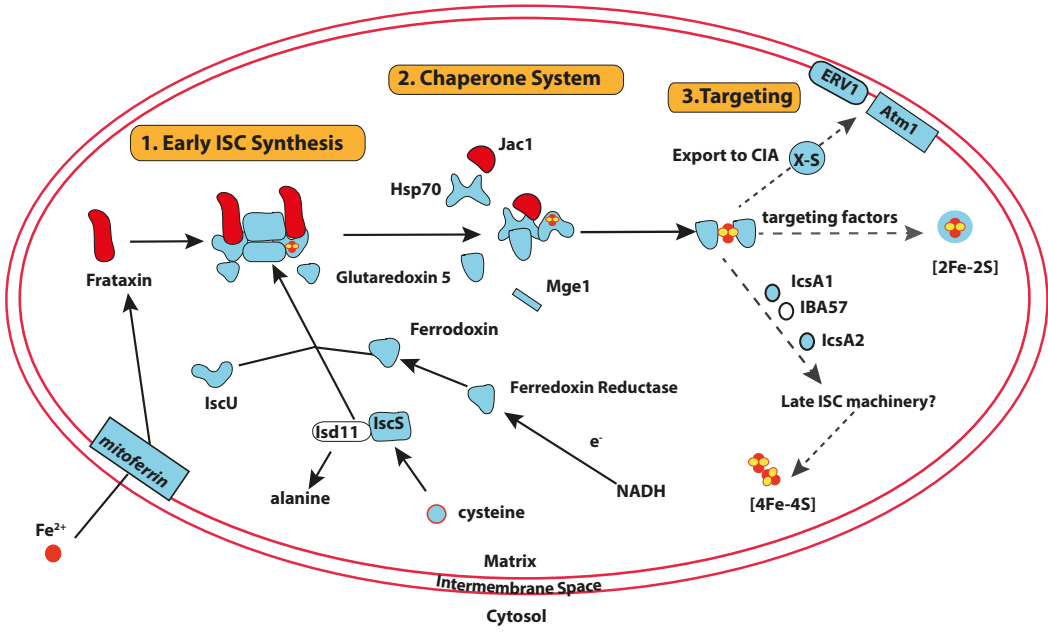


Figure 12: Schematic diagram showing the Fe-S cluster assembly in various *Cryptosporidium* species and *Plasmodium falciparum*. Blue coloured shapes shows the presence of proteins involved in Fe-S cluster assembly. Dashed arrows shows a pathway that has not been fully identified or investigated. Protein that has not been identified is blank and those coloured in red are proteins that are present in *Cryptosporidium* species but not in *Plasmodium*.

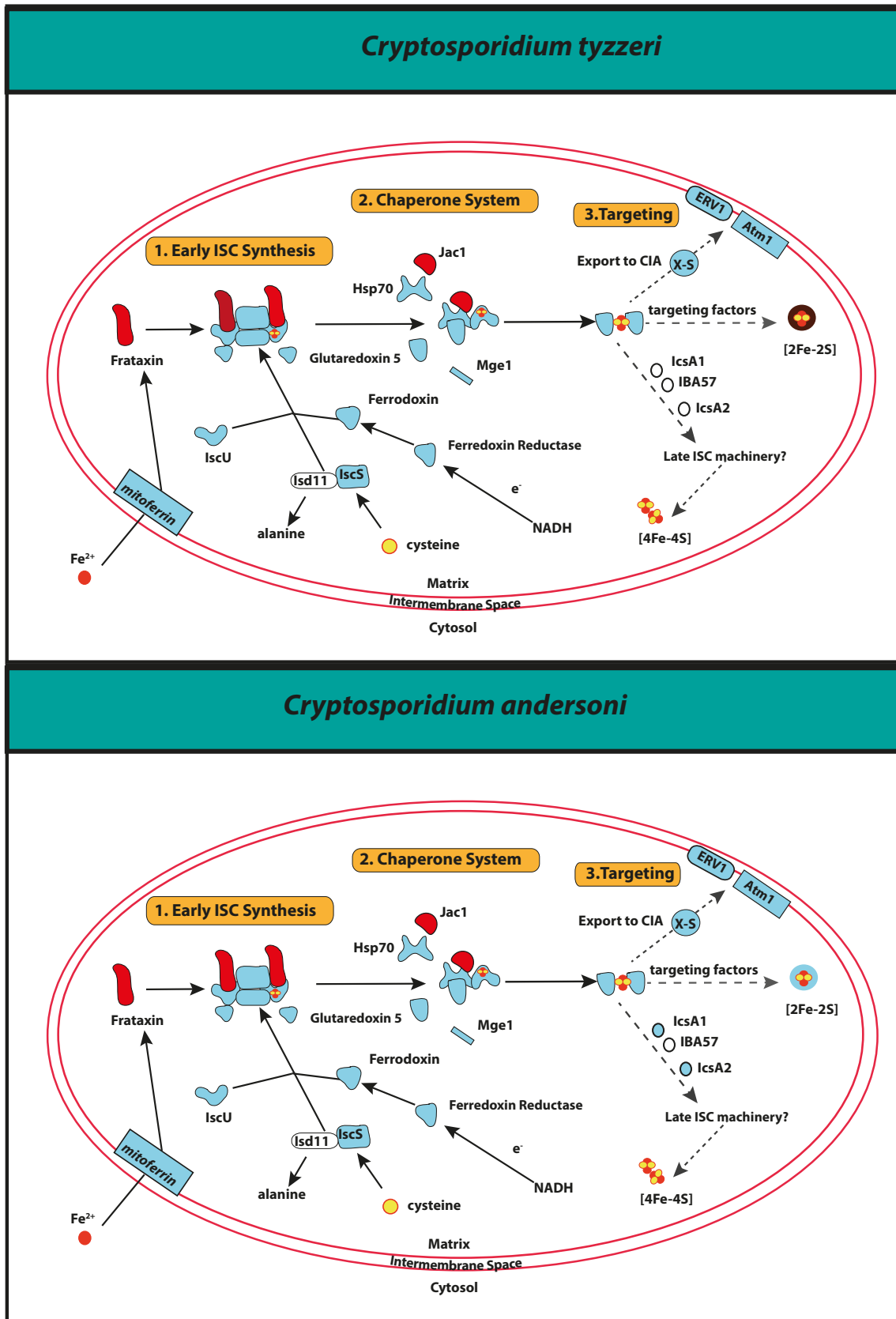
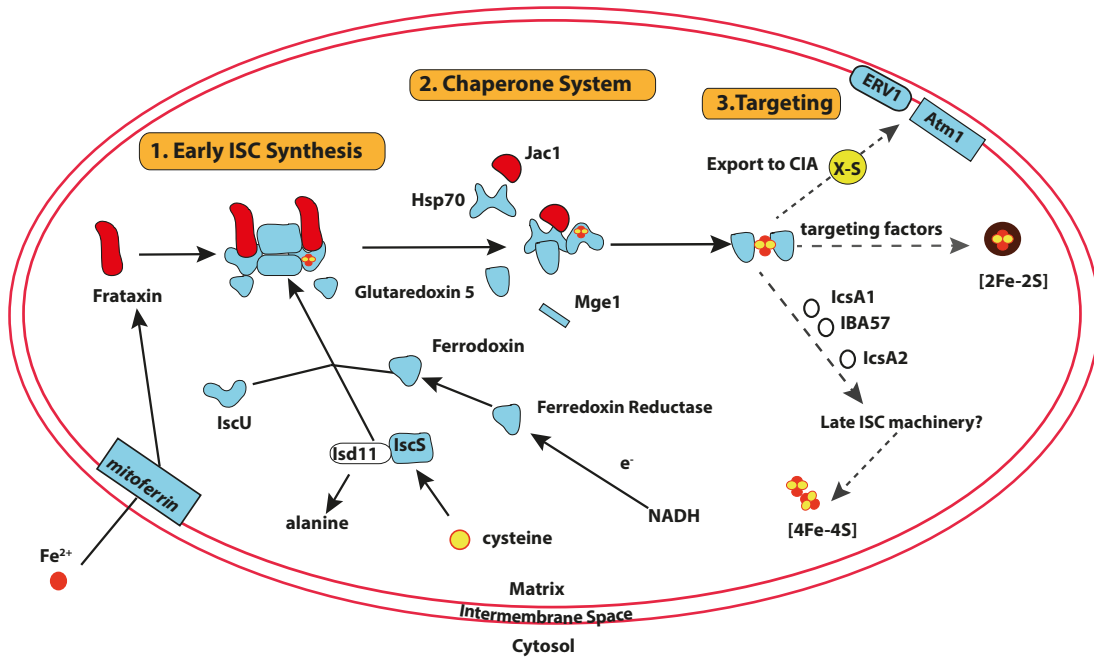


Figure 12: Schematic diagram showing the Fe-S cluster assembly in various *Cryptosporidium* species and *Plasmodium falciparum*. Blue coloured shapes shows the presence of proteins involved in Fe-S cluster assembly. Dashed arrows shows a pathway that has not been fully identified or investigated. Protein that has not been identified is blank and those coloured in red are proteins that are present in *Cryptosporidium* species but not in *Plasmodium*.

Cryptosporidium ubiquitum



Cryptosporidium hominis

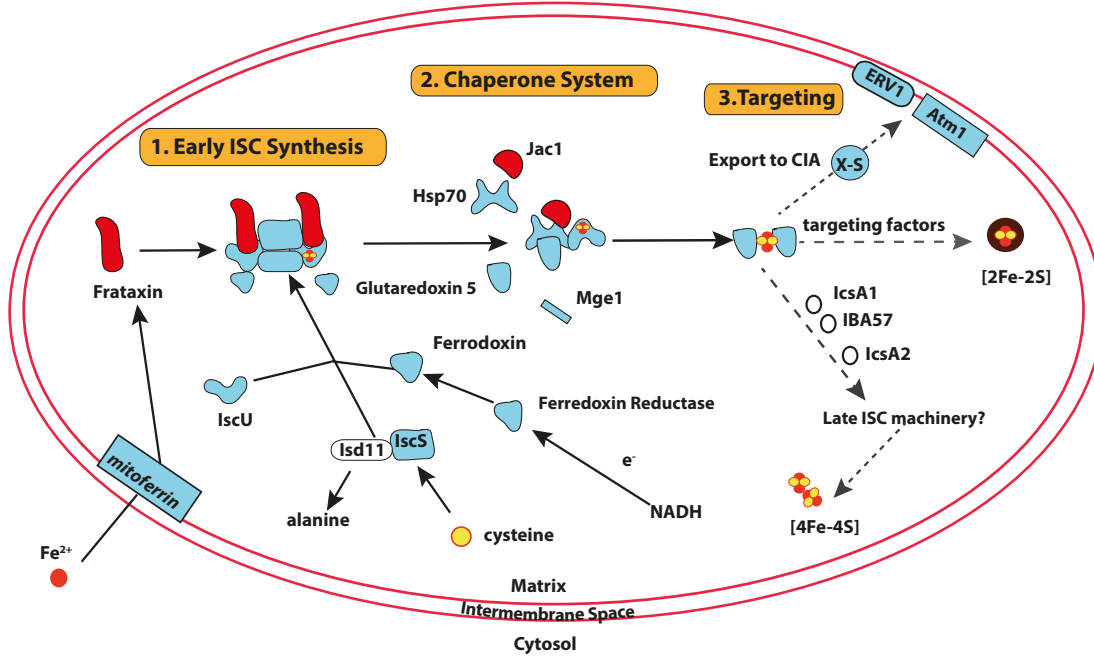


Figure 12: Schematic diagram showing the Fe-S cluster assembly in various *Cryptosporidium* species and *Plasmodium falciparum*. Blue coloured shapes shows the presence of proteins involved in Fe-S cluster assembly. Dashed arrows shows a pathway that has not been fully identified or investigated. Protein that has not been identified is blank and those coloured in red are proteins that are present in *Cryptosporidium* species but not in *Plasmodium*.

Cryptosporidium parvum

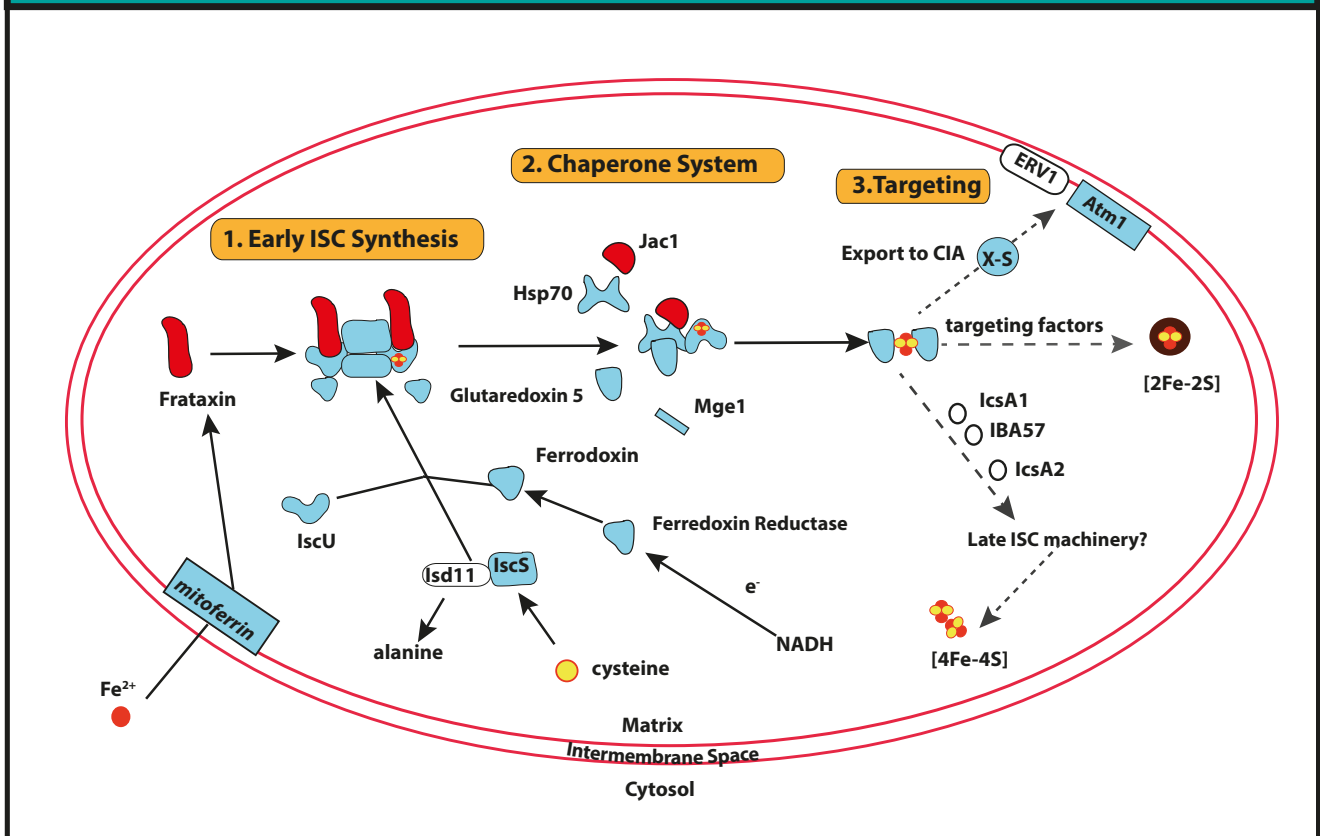


Figure 12: Schematic diagram showing the Fe-S cluster assembly in various *Cryptosporidium* species and *Plasmodium falciparum*. Blue coloured shapes shows the presence of proteins involved in Fe-S cluster assembly. Dashed arrows shows a pathway that has not been fully identified or investigated. Protein that has not been identified is blank and those coloured in red are proteins that are present in *Cryptosporidium* species but not in *Plasmodium*.

3.6 Glycolysis and Gluconeogenesis

Proteins involved in Glycolysis and Gluconeogenesis were also investigated, as *C.hominis* and *C.parvum* rely on this for energy metabolism. Glucose 1-phosphatase was absent in all species, however hexokinase was present in all. Pyruvate kinase was absent in *C.tyzzeri*, however it was present in all other species. **Table 12** and **figure 13**, shows all the proteins present in this pathway.

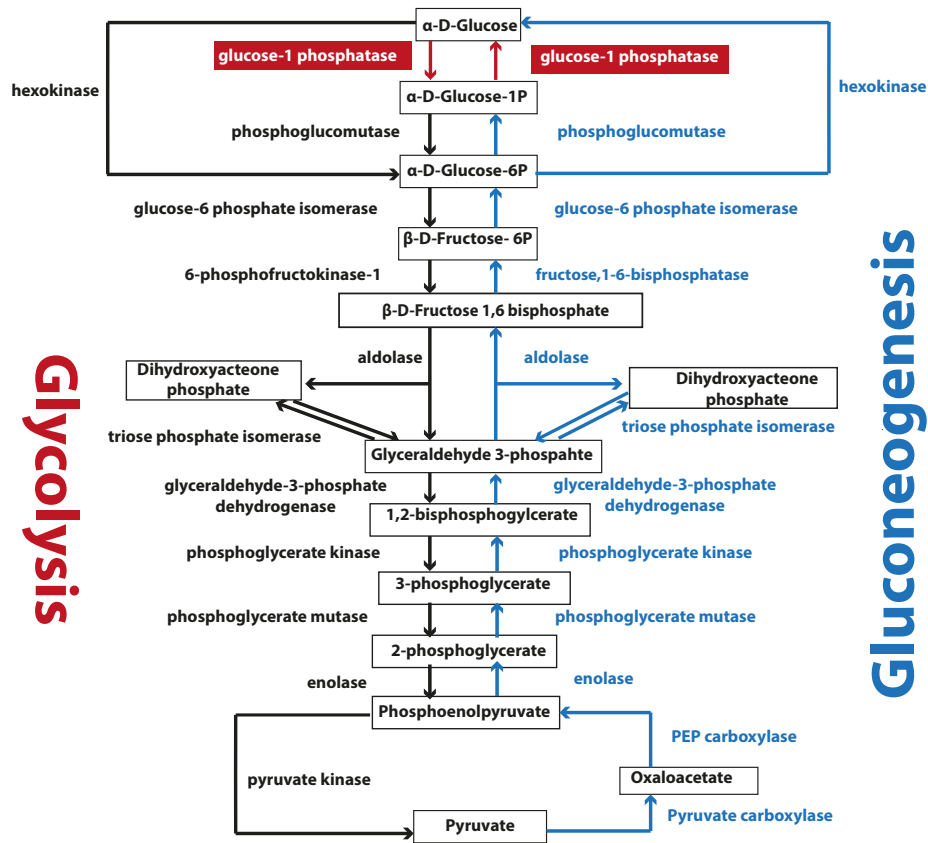
Pyruvate carboxylase as previously mentioned in the TCA cycle results, was not identified in any of the *Cryptosporidium* species, however this was identified in *P.falciparum*.

Table 12: Proteins involved in Glycolysis and Gluconeogenesis.

Protein	EC number	<i>C. andersoni</i>	<i>C. muris</i>	<i>C. parvum</i>	<i>C. tyzzeri</i>	<i>C. hominis</i>	<i>C. ubiquitum</i>	<i>P. falciparum</i>
Phosphoglucomutase	5.4.2.2							
Hexokinase	2.7.1.1							
Glucose-6-phosphate isomerase	5.3.1.9							
Pyrophosphate-dependent phosphofructokinase	2.7.1.90							*
Aldolase	4.1.2.13							
Triose-phosphate isomerase	5.3.1.1							
Glyceraldehyde-3-phosphate dehydrogenase	1.2.1.12							
Phosphoglycerate kinase	2.7.2.3							
Phosphoglycerate mutase	5.4.2.11							
Enolase	4.2.1.11							
Pyruvate kinase	2.7.1.40							
Pyruvate carboxylase	4.1.1.1							
PEP carboxylase	4.1.1.49							
Total proteins		12	12	12	11	12	12	13

* *P.falciparum*, phosphofructokinase-1 identified. Shaded regions shows the proteins identified in Fe-S cluster assembly

Plasmodium falciparum



Cryptosporidium hominis

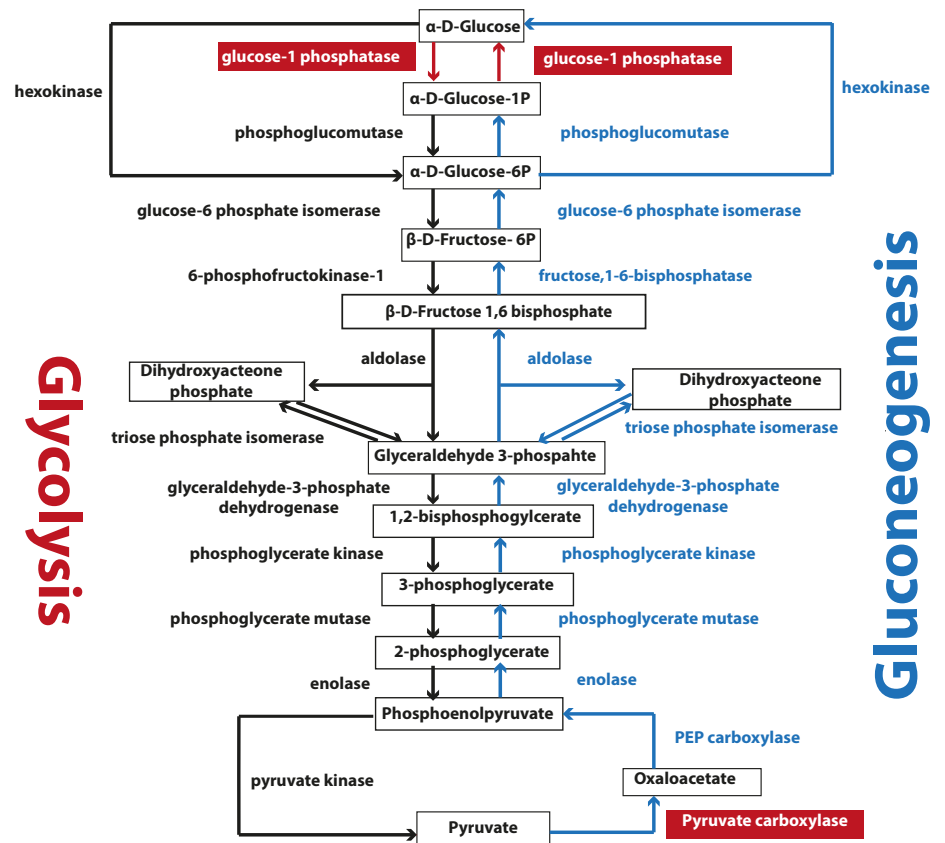
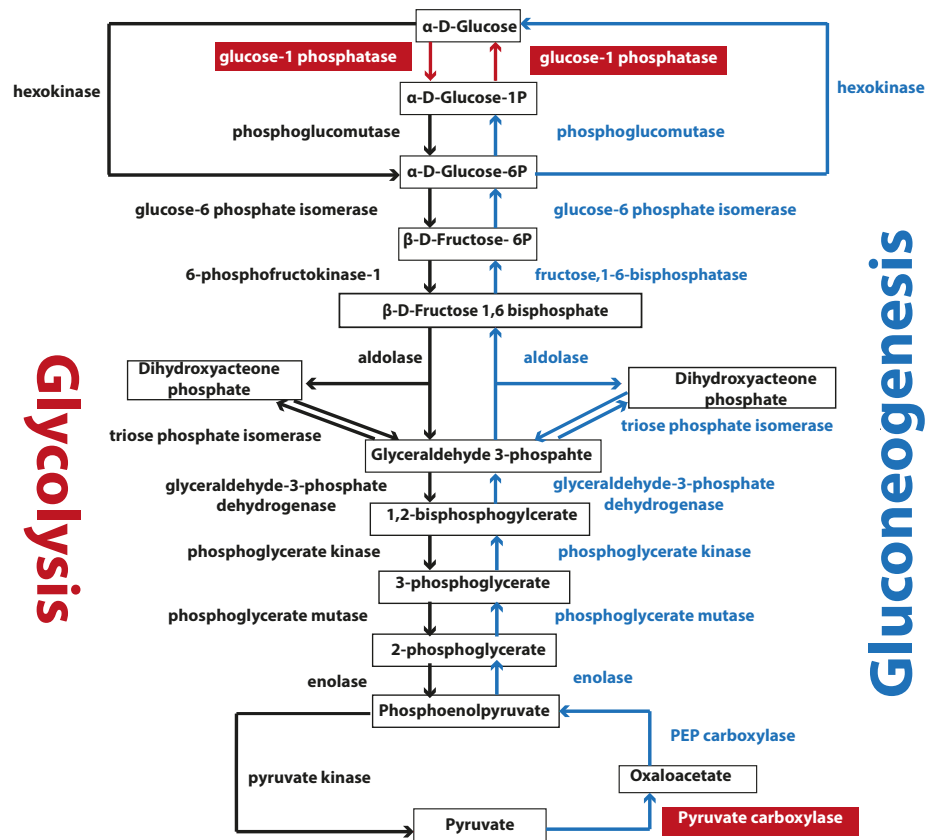


Figure13: Proteins present in Glycolysis and Gluconeogenesis. Black arrows indicate glycolysis and blue arrows indicate gluconeogenesis.

Red shading denotes a protein that is not known to be present in *Cryptosporidium* and *Plasmodium*.

Cryptosporidium muris



Cryptosporidium tyzzeri

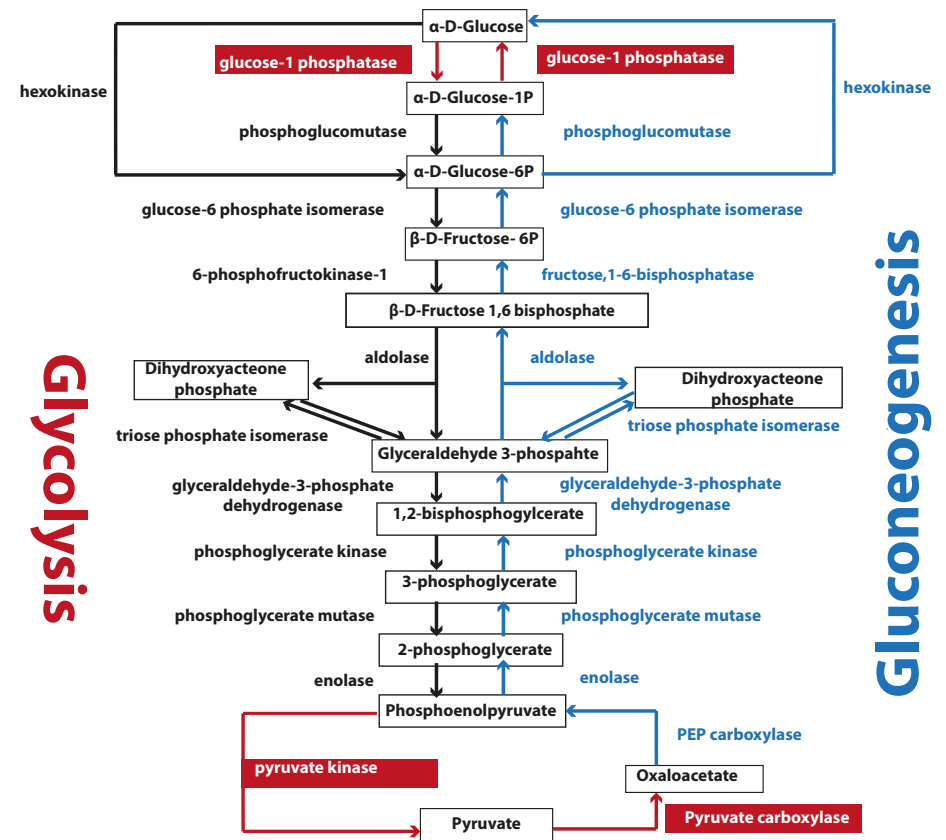


Figure13: Proteins present in Glycolysis and Gluconeogenesis. Black arrows indicate glycolysis and blue arrows indicate gluconeogenesis.

Red shading denotes a protein that is not known to be present in *Cryptosporidium* and *Plasmodium*.

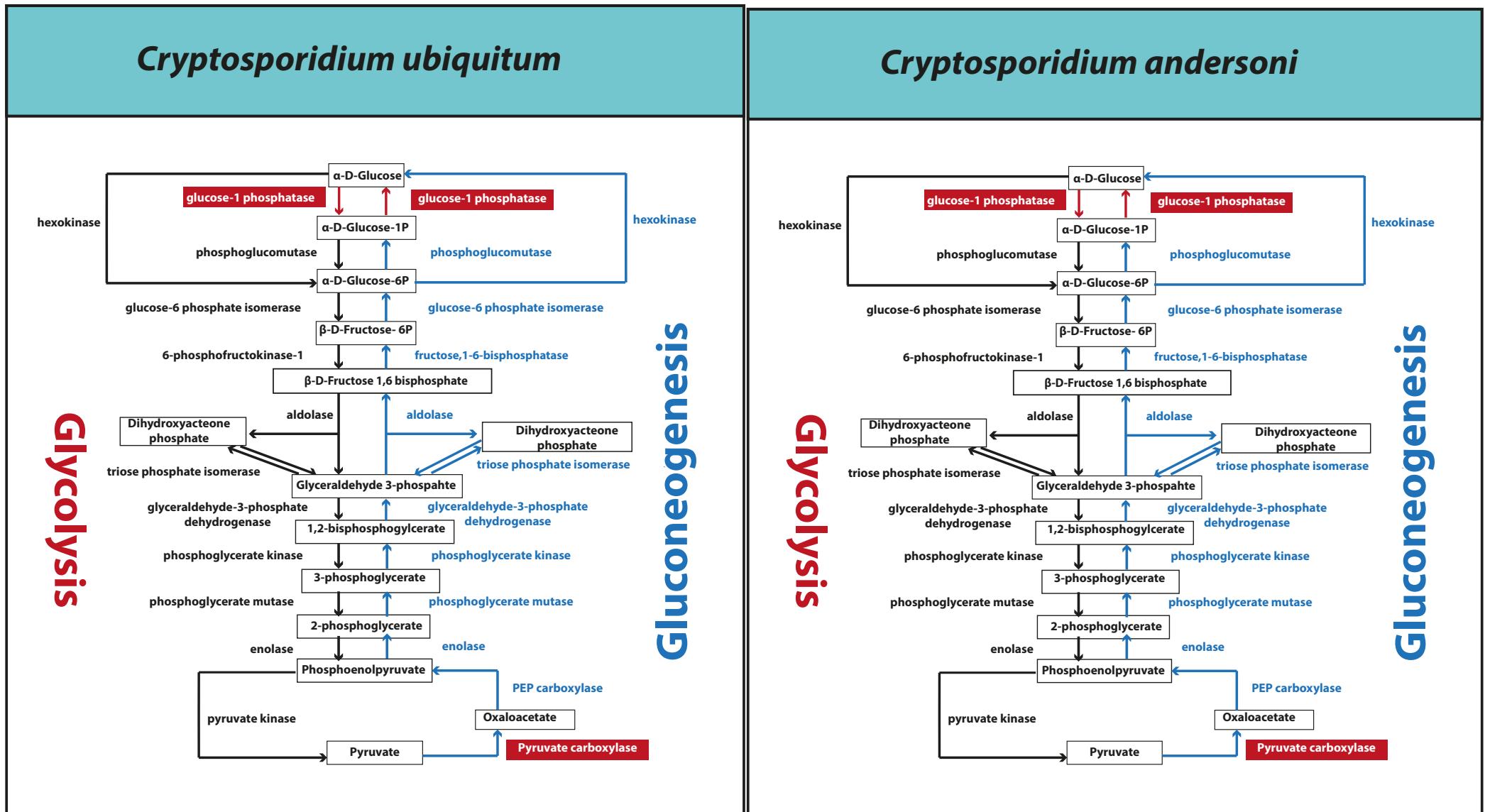


Figure13: Proteins present in Glycolysis and Gluconeogenesis. Black arrows indicate glycolysis and blue arrows indicate gluconeogenesis.

Red shading denotes a protein that is not known to be present in *Cryptosporidium* and *Plasmodium*.

Cryptosporidium parvum

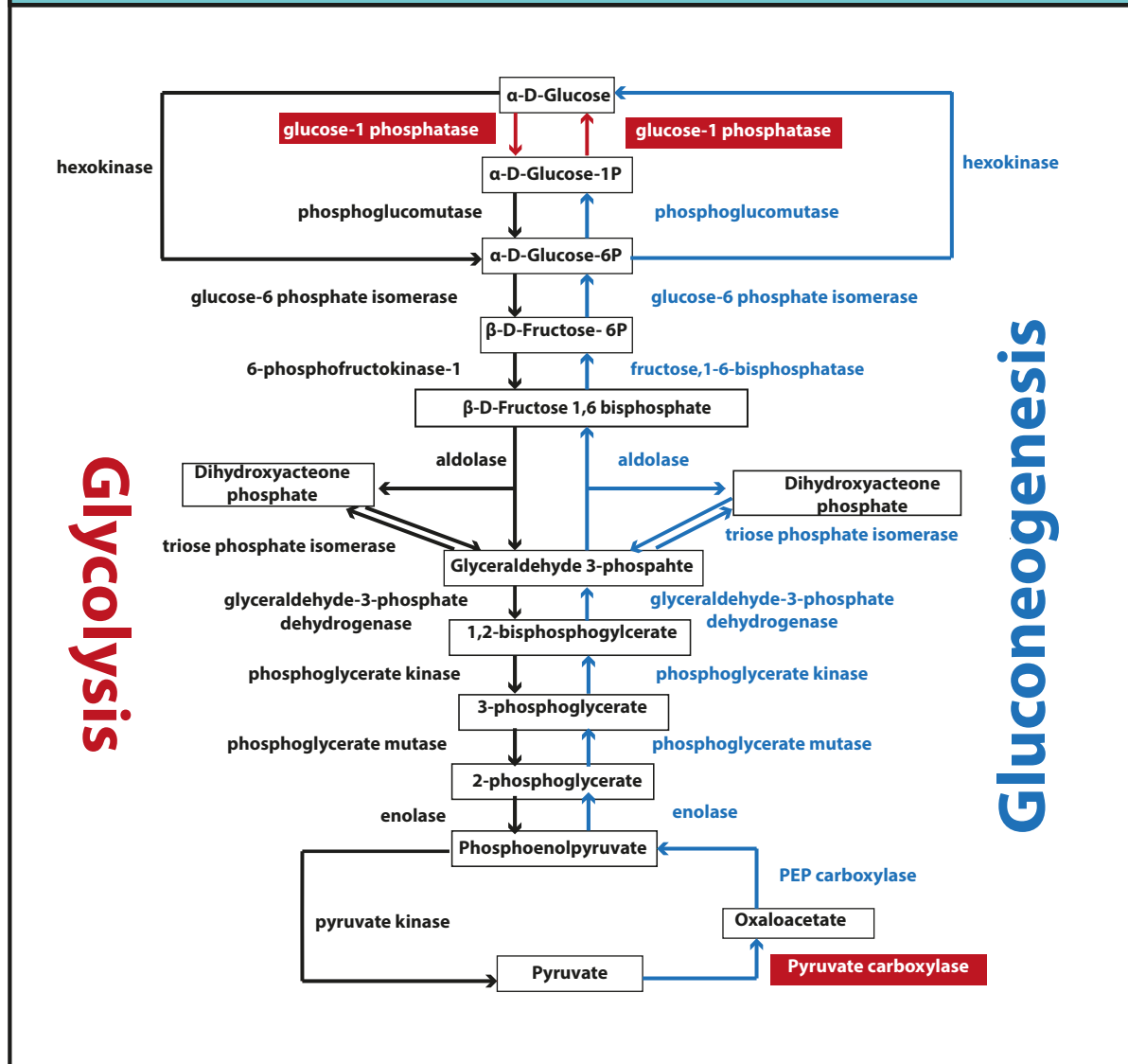


Figure 13: Proteins present in Glycolysis and Gluconeogenesis. Black arrows indicate glycolysis and blue arrows indicate gluconeogenesis. Red shading denotes a protein that is not known to be present in *Cryptosporidium* and *Plasmodium*.

3.7 Overview of mitochondrial pathways

Using the *CryptoDB* database, the protein coding genes for ubiquinone synthesis and pyruvate metabolism were extracted and analysed in order to give a more robust depiction of the proteins present in the *Cryptosporidium* species. No proteins were identified in the ubiquinone synthesis for *C.ubiquitum*. However all the other *Cryptosporidium* species contained two or more proteins necessary for ubiquinone synthesis (**supplementary table S3**). Proteins for pyruvate metabolism were identified in all *Cryptosporidium* species. The mitochondrial carrier proteins can be seen in (**supplementary table S4**), however the exact name of each carrier cannot be distinguished as these may not be annotated precisely. An alternative oxidase was also identified in five of the *Cryptosporidium* species, this was not identified in *C.ubiquitum*. A hexose transporter, adenosine transporter and acetyl Co-A transporter were identified (**figure 14**).

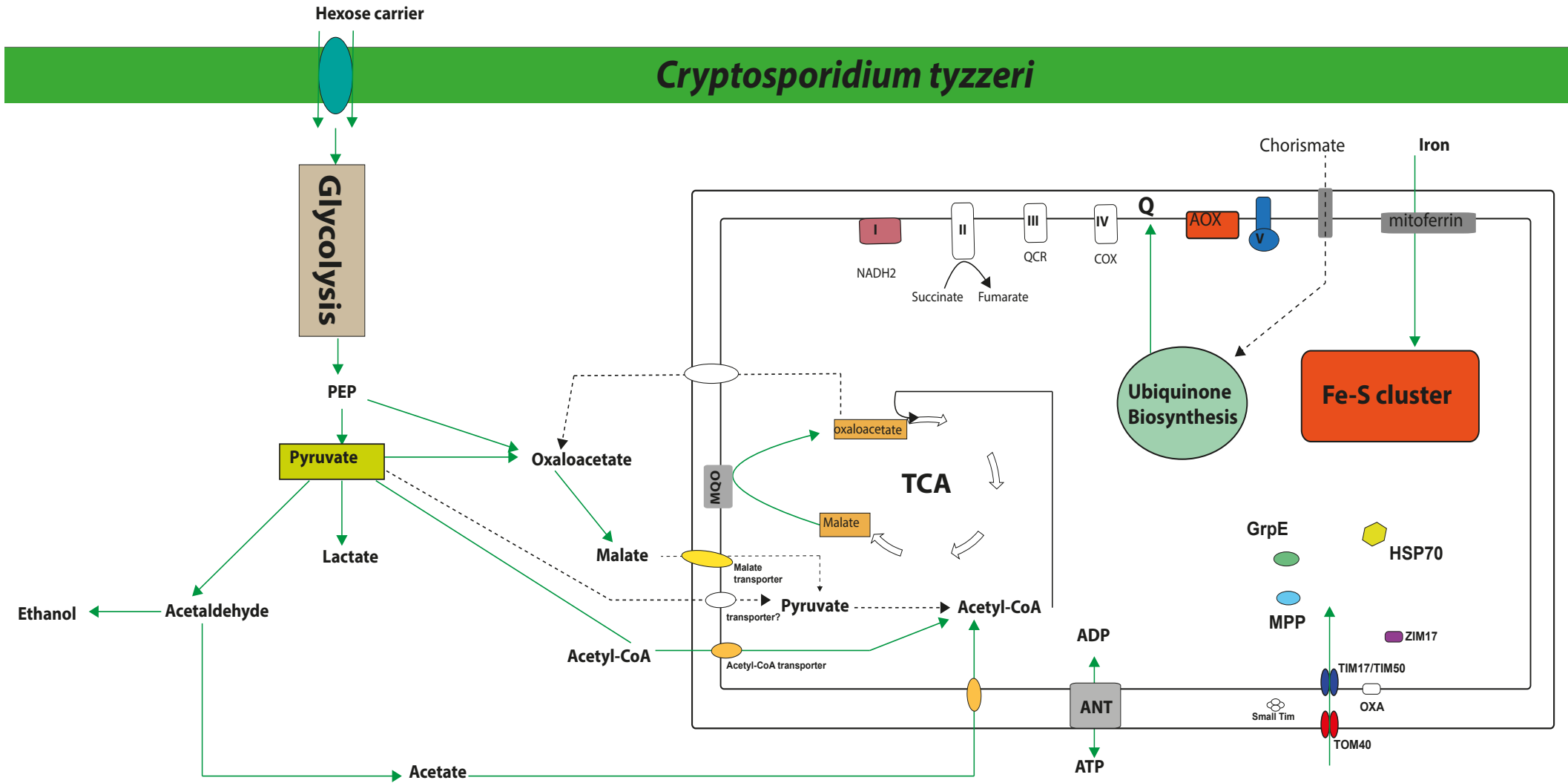


Figure 14: A basic overview of mitochondrial pathways/proteins identified in each *Cryptosporidium* species. Proteins present are shown in colour and the mitochondrial pathways are shown in green. Pathways/proteins shown are: AOX, Glycolysis, pyruvate metabolism, Fe/S cluster assembly, TCA cycle, complex I – V of the electron transport chain, and proteins involved in protein import (TIM, TOM, small TIMs, OXA1L, HSP, MPP, GrpE).

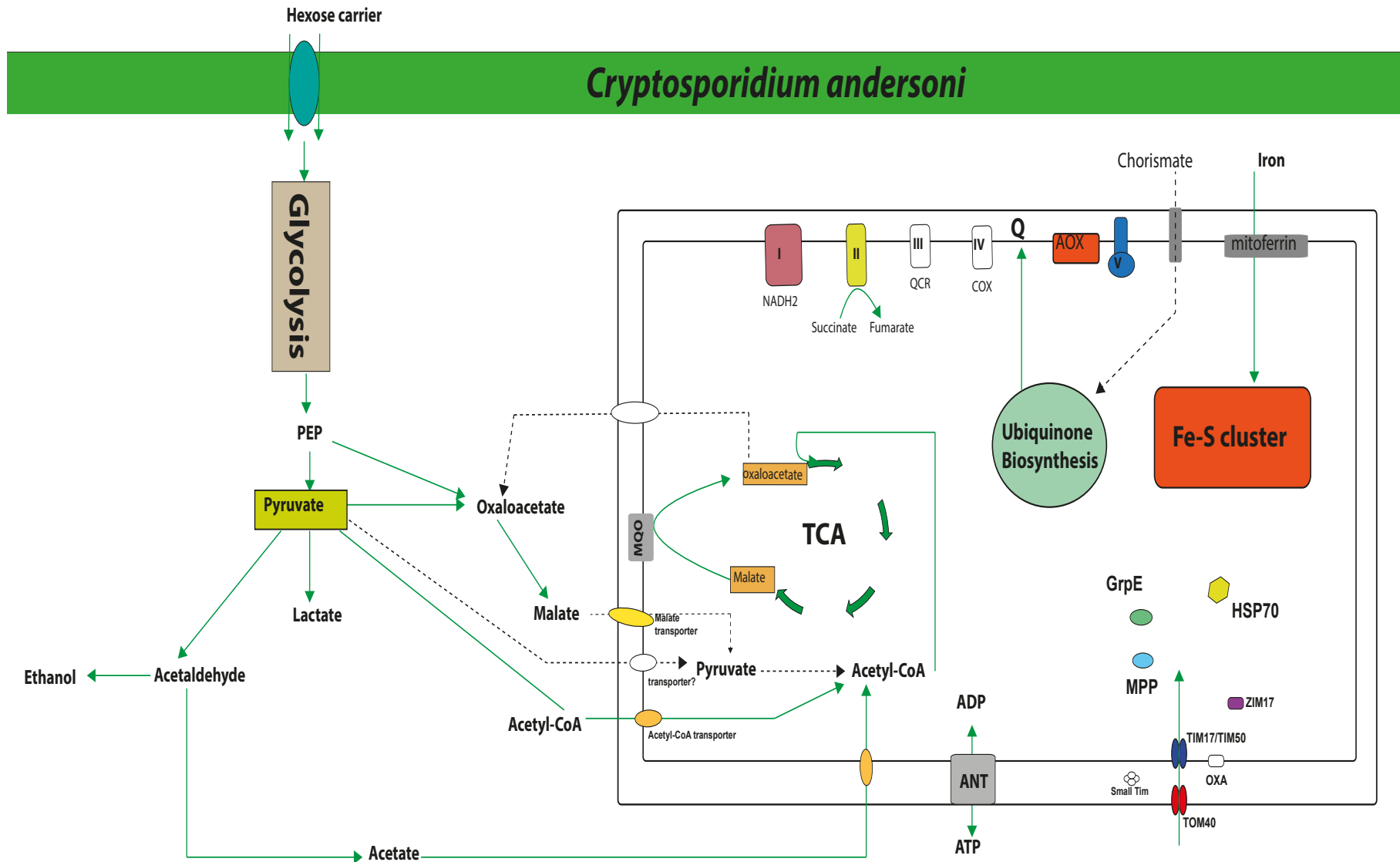


Figure 14: A basic overview of mitochondrial pathways/proteins identified in each *Cryptosporidium* species. Proteins present are shown in colour and the mitochondrial pathways are shown in green. Pathways/proteins shown are: AOX, Glycolysis, pyruvate metabolism, Fe/S cluster assembly, TCA cycle, complex I – V of the electron transport chain, and proteins involved in protein import (TIM, TOM, small TIMs, OXA1L, HSP, MPP, GrpE).

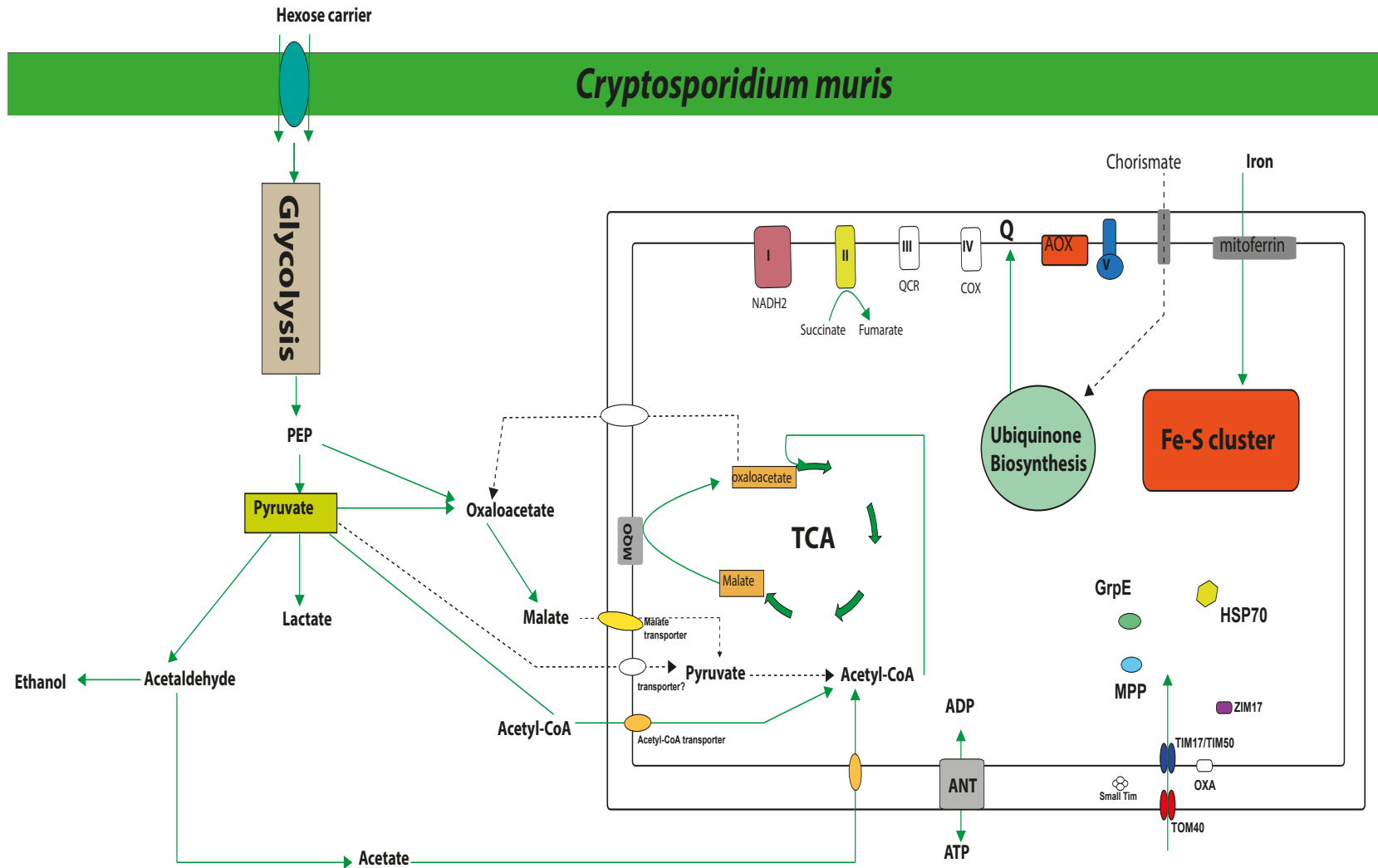


Figure 14: A basic overview of mitochondrial pathways/proteins identified in each *Cryptosporidium* species. Proteins present are shown in colour and the mitochondrial pathways are shown in green. Pathways/proteins shown are: AOX, Glycolysis, pyruvate metabolism, Fe/S cluster assembly, TCA cycle, complex I – V of the electron transport chain, and proteins involved in protein import (TIM, TOM, small TIMs, OXA1L, HSP, MPP, GrpE).

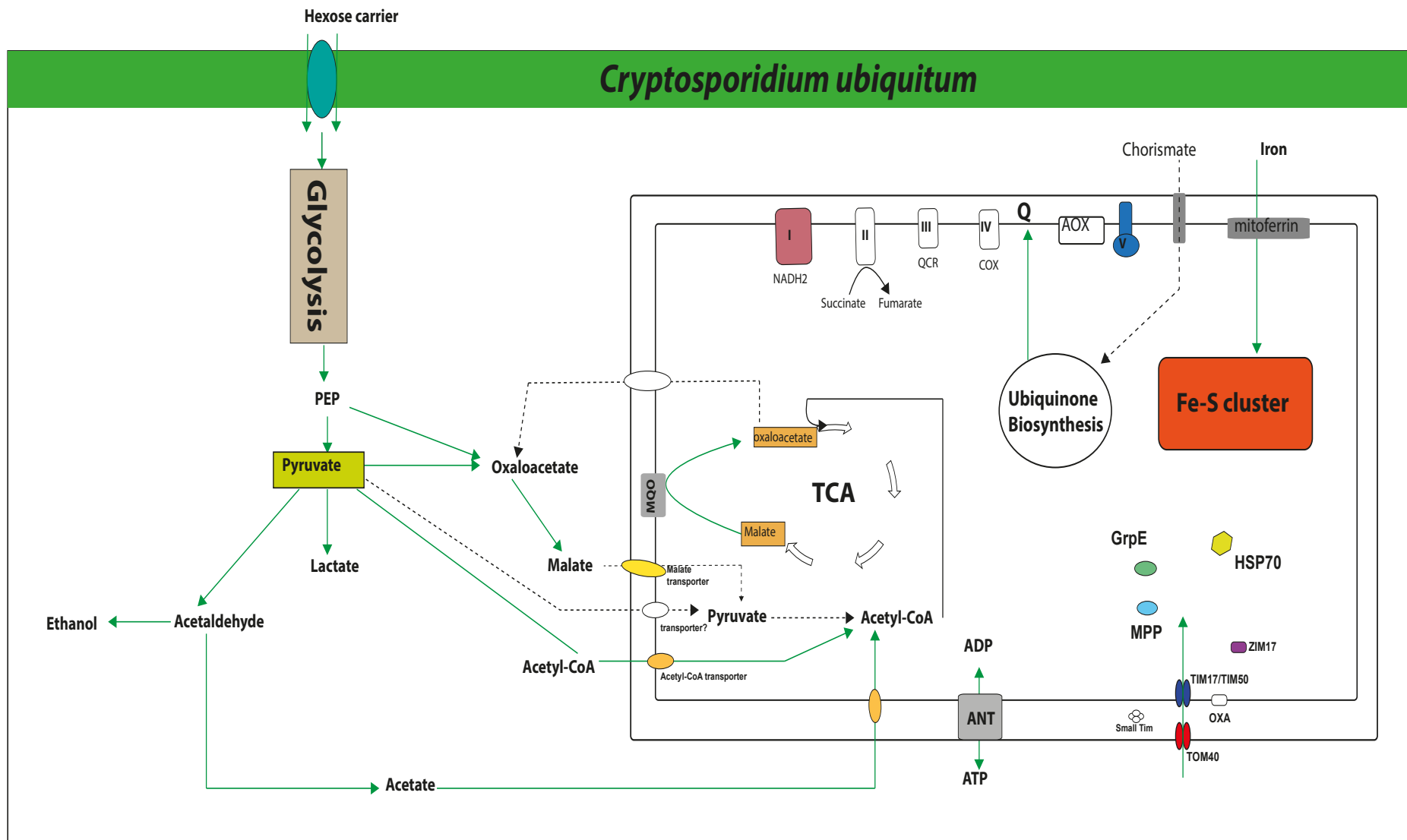


Figure 14: A basic overview of mitochondrial pathways/proteins identified in each *Cryptosporidium* species. Proteins present are shown in colour and the mitochondrial pathways are shown in green. Pathways/proteins shown are: AOX, Glycolysis, pyruvate metabolism, Fe/S cluster assembly, TCA cycle, complex I – V of the electron transport chain, and proteins involved in protein import (TIM, TOM, small TIMs, OXA1L, HSP, MPP, GrpE).

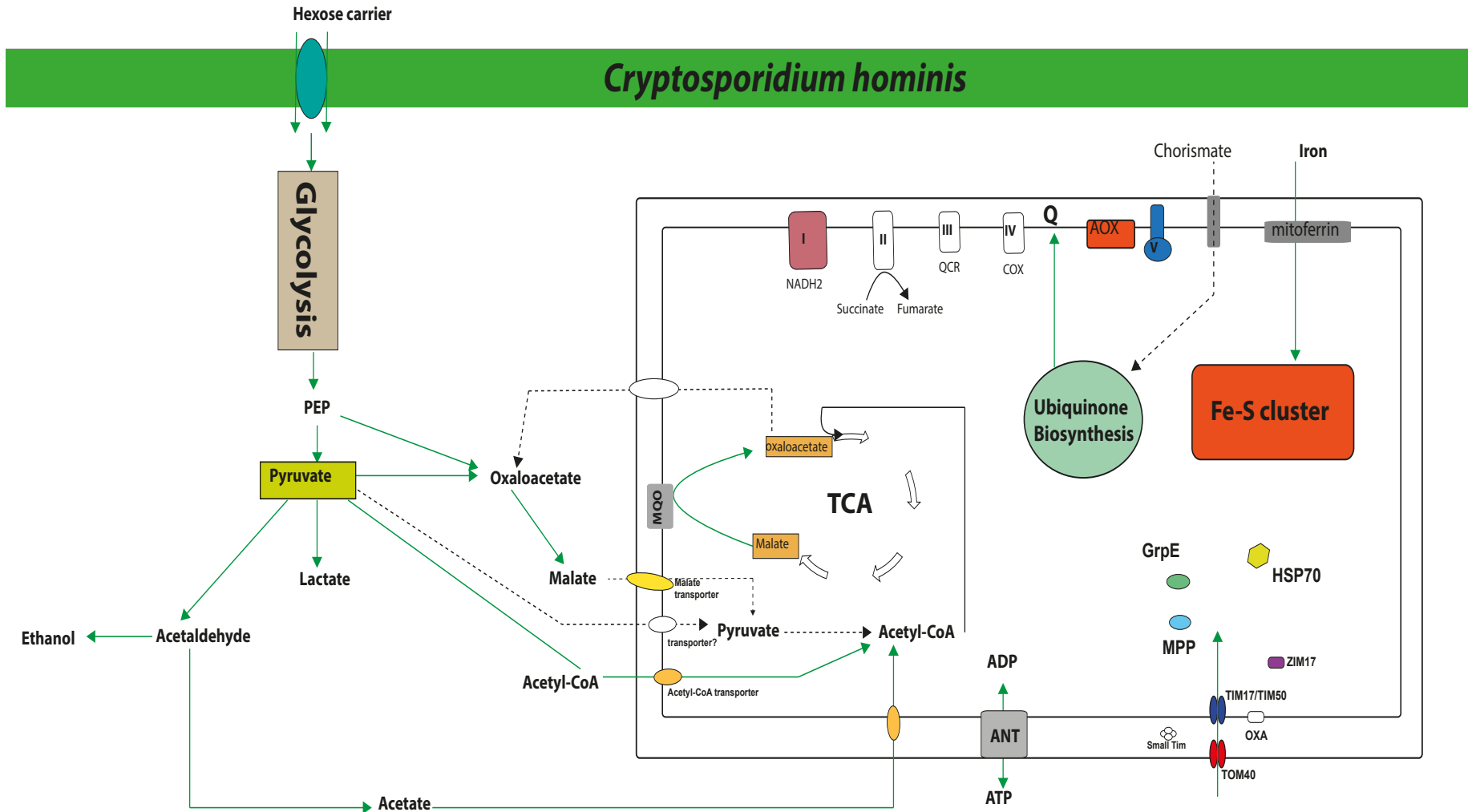


Figure 14: A basic overview of mitochondrial pathways/proteins identified in each *Cryptosporidium* species. Proteins present are shown in colour and the mitochondrial pathways are shown in green. Pathways/proteins shown are: AOX, Glycolysis, pyruvate metabolism, Fe/S cluster assembly, TCA cycle, complex I – V of the electron transport chain, and proteins involved in protein import (TIM, TOM, small TIMs, OXA1L, HSP, MPP, GrpE).

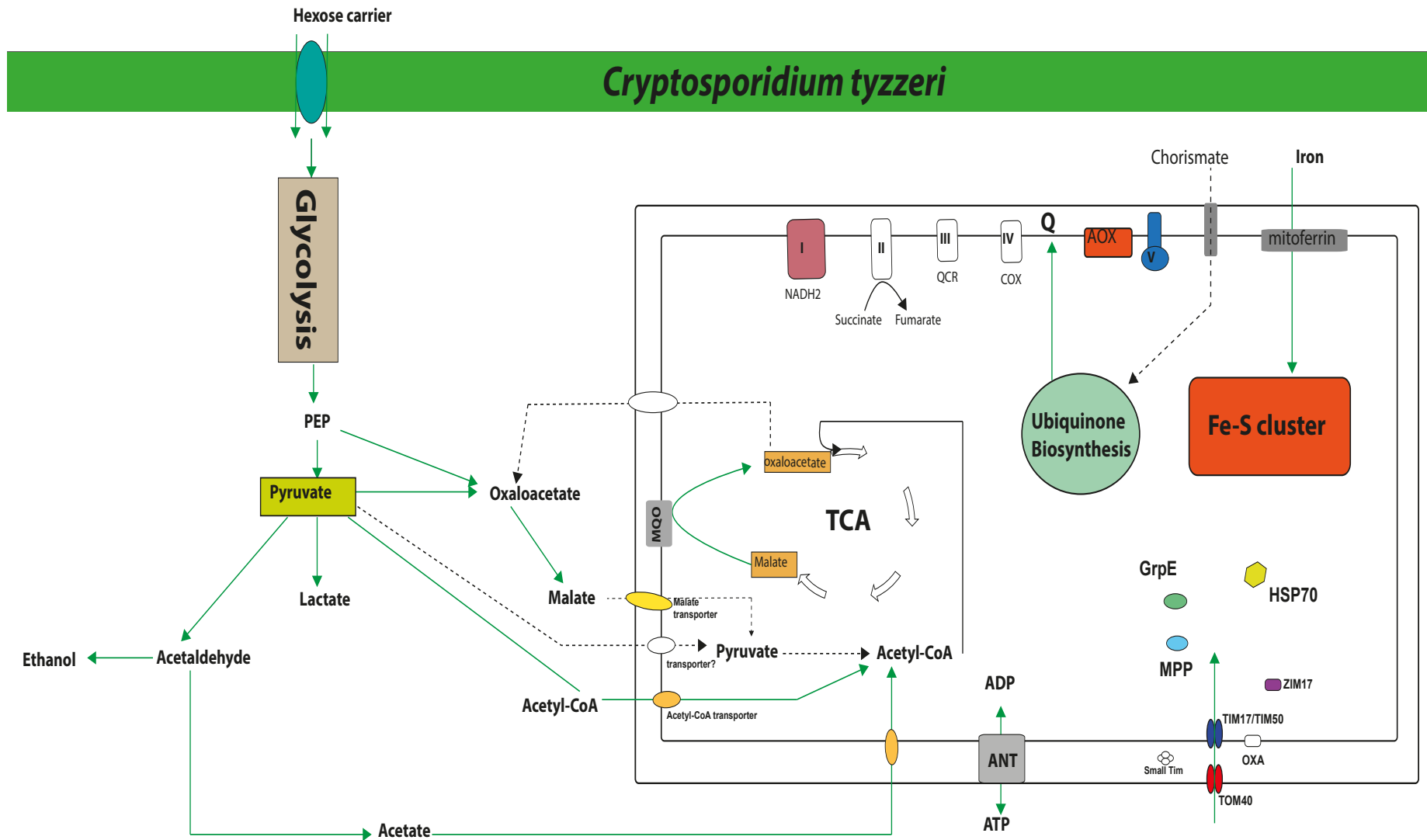


Figure 14: A basic overview of mitochondrial pathways/proteins identified in each *Cryptosporidium* species. Proteins present are shown in colour and the mitochondrial pathways are shown in green. Pathways/proteins shown are: AOX, Glycolysis, pyruvate metabolism, Fe/S cluster assembly, TCA cycle, complex I – V of the electron transport chain, and proteins involved in protein import (TIM, TOM, small TIMs, OXA1L, HSP, MPP, GrpE).

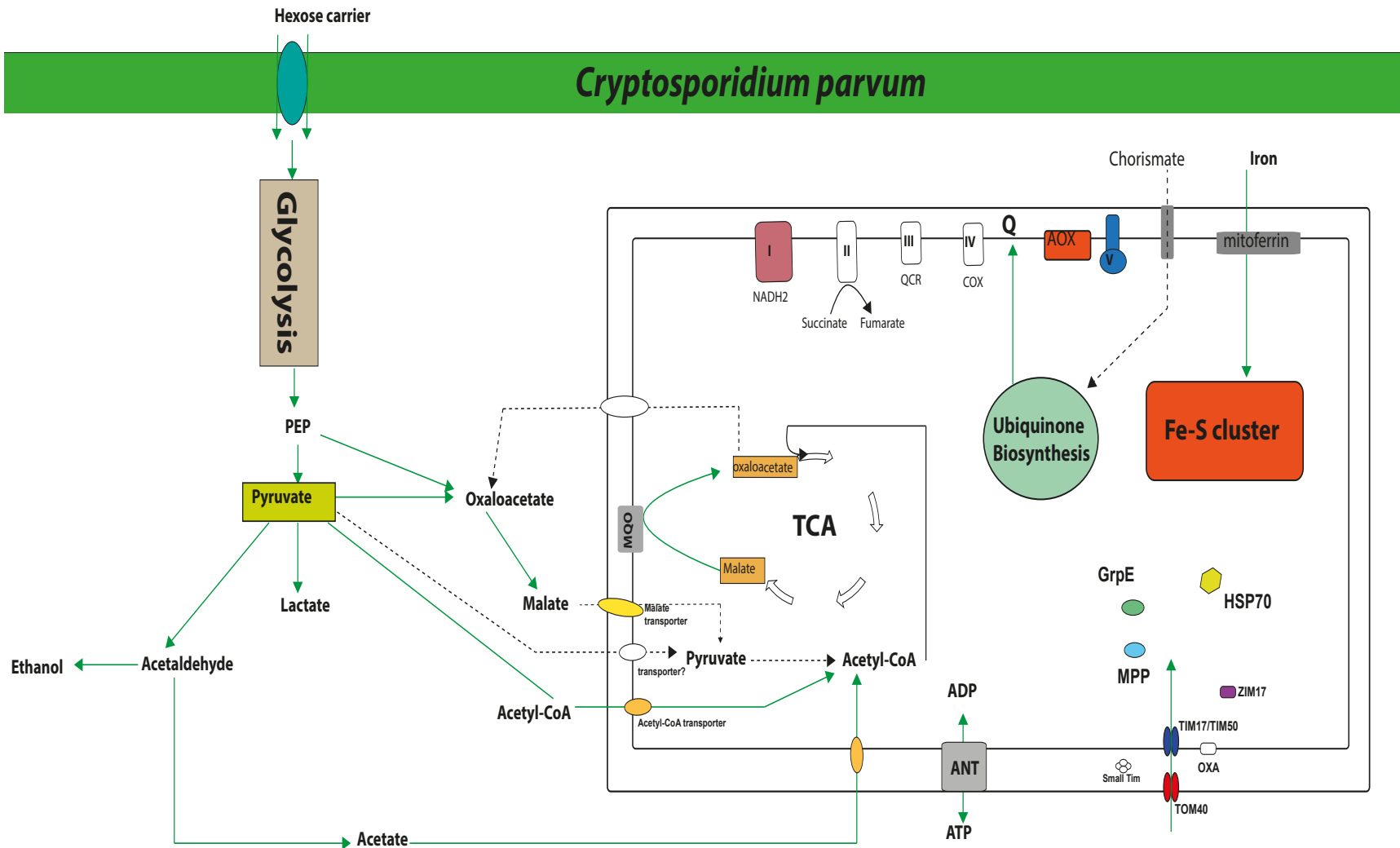


Figure 14: A basic overview of mitochondrial pathways/proteins identified in each *Cryptosporidium* species. Proteins present are shown in colour and the mitochondrial pathways are shown in green. Pathways/proteins shown are: AOX, Glycolysis, pyruvate metabolism, Fe/S cluster assembly, TCA cycle, complex I – V of the electron transport chain, and proteins involved in protein import (TIM, TOM, small TIMs, OXA1L, HSP, MPP, GrpE).

Chapter 4

Discussion

4. Discussion

In this investigation six different *Cryptosporidium* species and a *Plasmodium* species were analysed to predict the mitochondrial composition of various mitochondrial pathways present in each. It has been observed that *Cryptosporidium* have lost their mitochondrial genome and thus they contain a relict mitochondria, the mitosome (Putignani et al. 2004). Mitosomes are the most reduced MROs and they lack ETC proteins as well as TCA cycle proteins (Makiuchi and Nozaki, 2014). Thus, with a reduced mitochondrion, the composition of the genes encoding for various mitochondrial pathways will be reduced in comparison to other apicomplexans, such as *Plasmodium* which is the closest relative of *Cryptosporidium*. By comparing and analysing various mitochondrial protein coding genes present in *Cryptosporidium* and *Plasmodium*, the mitochondrial compositions of various mitochondrial pathways such as Fe-S cluster assembly, TCA cycle, ETC and ubiquinone synthesis can be predicted. This study allows for the prediction of proteins that have been conserved with a focus on the protein import machinery, giving more insight into how the parasite uses energy. It also allows the proposal of possible approaches in which the parasite interacts with the host as well as provides the opportunity for more research to be carried out on possible drug targets.

To carry out the study, genomic data gathered from various *Cryptosporidium* species and *Plasmodium* using *CryptoDB* and *PlasmoDB*, were analysed using BLASTP, KEGG, Interpro and Uniprot to identify the mitochondrial functioning proteins (**tables 3 and 4**). Through this we have been able to predict the composition of the mitochondrial proteins that have been conserved in the *Cryptosporidium* species using *Plasmodium* protein sequences as a reference point. These predictions showed clear distinctions between the *Cryptosporidium* species as well as differences between *Cryptosporidium* and *Plasmodium*. *Cryptosporidium* has lost the apicoplast (Abrahamsen, 2004), however this is present in *Plasmodium*, therefore more metabolic processes will be present. As a result of this loss of apicoplast the *Cryptosporidium* species rely on the host for basic nutrients. Phylogenetic tree from Tsoulos and Keithly, (2019) of the six *Cryptosporidium* species

investigated shows that *C.andersoni* and *C.muris* may have been earlier members as they share a similar mitochondrial protein composition, possessing fully functioning TCA cycle proteins, glycolysis proteins and a functioning ETC (**table 7**). Whereas, *C.hominis*, *C.parvum* and *C.tyzzeri* are more related, with *C.ubiquitum* being a recent member that has lost all TCA cycle proteins, AOX and ubiquinone biosynthesis (**table 6 and 7**).

TOM40 was shown to be present in all *Cryptosporidium* species and contains no transmembrane domain. The three small subunits of the TOM complex in the outer membrane Tom5, Tom6 and Tom7 were not identified in any of the *Cryptosporidium* species investigated, however Tom7 was present in *P.falciparum*. These subunits are not essential for TOM functions, however they are thought to be involved in the assembly and stability of TOM complex (Wiedemann and Pfanner, 2017). TOM20 which is the initial receptor for the proteins with pre-sequences and TOM70 (recognition and translocation of cytosolic synthesized mitochondrial preprotein), were not identified in any of the *Cryptosporidium* species investigated. However the TOM22 complex which is the central receptor was identified in all *Cryptosporidium* species. This receptor most likely substitutes for the lack of TOM20 and TOM70 in the mitosome of *Cryptosporidium*. However further research needs to be carried out in order to confirm the presence TOM20 and also its likely adapted function in the mitosome of *Cryptosporidium*. As these TOM subunits such as TOM70, TOM5,6,7 and TOM20, were not identified in any of the *Cryptosporidium* species. This raises the question as to whether the TOM complex is conserved in these parasites. Proteins required for translocation to the mitochondrial outer membrane are facilitated by the SAM50 complex which was identified in both *Plasmodium* and *Cryptosporidium* species. Although other TOM complexes have not been identified, the results indicate that TOM40 and TOM20 have been modified or adapted in a way that facilitates the movement of pre-proteins and carrier proteins into the mitosome (**figure 9**).

The annotations for Tim10 gathered from our research could be a potential target for further investigations as to whether this TimS (which could be Tim10) is also identified in other *Cryptosporidium* species. This Tim identified could possibly be involved in the transfer of proteins to SAM and TIM complexes, thus aiding in the reduced protein translocation of the TOM complex.

The subunits of TIM23: Tim50, Tim23 and Tim21, were identified in the *Cryptosporidium* species investigated except from Tim21 and Tim 23. In our study, we observed that in *C.tyzzeri* both TIM23 and TIM17 were identified, however in the other species only TIM17 was identified. It should be noted that there were annotations for a translocase of the inner membrane, which could either be TIM23 or TIM22, further study needs to be carried out to confirm the presence of this. TIM23 translocates proteins into the matrix and also in the inner membrane, and although this was not identified in most *Cryptosporidium* species, the presence of a single family of the TIM17 protein (member of the TIM17/22/23 family) is thought to accommodate for this. The absence of TIM22, which translocates proteins in the inner membrane, suggests that TIM17 has been adapted to both translocate proteins into the matrix and the inner membrane of the mitosome of *Cryptosporidium*. Further research needs to be carried out in order to validate this hypothesis. SAM50 which has been identified in all the *Cryptosporidium* species aids in the insertion of proteins directed for translocation into the outer membrane. PAM18 complex, Hsp70, GrpE and other matrix chaperones identified, aid in the import and cleaving of pre-sequence carrying proteins translocated through the TIM17/22/23 complex.

The presence of TIM50, PAM18 and SAM50 in all six species, confirms recent work that identified these proteins (Alcock et al., 2011). TOM40, TIM17, TIM44 and the alpha and beta subunit of MPP were the first proteins of the protein import machinery annotated in the genome of *C.parvum* (Abrahamsen, 2004) and our results confirms the findings. Whilst the *Cryptosporidium*

mitochondrial protein import machinery is reduced, as shown from our findings, it appears that some of the proteins or complexes have been adapted to accommodate the need of importing proteins into the organelle.

In the intestinal species of *Cryptosporidium*, *C.parvum*, *C.ubiquitum*, *C.tyzzeri* and *C. hominis* there is no TCA cycle present (**figure 10**), as the main proteins needed for a fully functioning TCA cycle is not present, which suggests that these species rely on glycolysis for energy metabolism. In *C.parvum*, pyruvate is converted to acetyl-CoA using pyruvate: NADP⁺ oxidoreductase (PNO) (Rotte et al., 2001). This protein contains two domains that are fused together: N terminal pyruvate: ferredoxin oxidoreductase (PFO) and C terminal NADPH-cytochrome P450 reductase (CPR). The C terminal domain of this PNO enzyme was not identified in the *Cryptosporidium* species, therefore more research needs to be carried out in order to confirm its presence in the mitosome. On the other hand the N terminal domain (PFO) was identified in all *Cryptosporidium* species, which compensates the lack of the pyruvate dehydrogenase (PDH) enzyme that is normally present in most eukaryotes. *C.muris*, *C.andersoni* and *P.falciparum* each contain fully functioning proteins in the TCA cycle as shown **in table 9 and figure 10**. In the *Cryptosporidium* species investigated, the acetyl CoA is thought to be delivered into the mitosome through the acetyl CoA transporter protein that is embedded in the mitosome membrane (**supplementary table S3 and figure 14**). Conversely, a pyruvate transporter may be present in these species to supplement the transport of pyruvate into the mitosome, where it can be converted to acetyl Co-A by PNO. However, this predicted pyruvate transporter was not identified, therefore more research needs to be carried out to confirm whether this is present or not.

The *Cryptosporidium* species genome contains a hexokinase gene to that phosphorylate hexoses before they enter glycolysis. A hexokinase transporter was shown to be present in all

Cryptosporidium species (**supplementary table S3**). In the glycolytic pathway, *Cryptosporidium* species uses a pyrophosphate-dependent phosphofructokinase instead of the typical phosphofructokinase to convert fructose-6-phosphate into fructose-1,6-bisphosphate (Rotte et al. 2001) (Thompson et al. 2005) (**table 12, figure 13**). The conversion of phosphoenolpyruvate to pyruvate is facilitated by pyruvate kinase which yields ATP molecules. This seems to be the main source of energy for *Cryptosporidium* species, especially in *C.hominis*, *C.parvum*, *C.tyzzeri* and *C.ubiquitum* where the TCA cycle is absent. Glycolysis links to the TCA cycle where pyruvate is converted to oxaloacetate using malate dehydrogenase thought to be present in the cytosol. This oxaloacetate is also converted in the cytosol by malate dehydrogenase and enters mitosome via a malate transporter (identified in **supplementary table S3**) where it enters the TCA cycle. In addition, the pyruvate is converted to acetyl-Co-A via PNO. Malate: quinone oxidoreductase (MQO) is thought to be membrane bound and has been identified in all *Cryptosporidium* species. This converts mitochondrial malate to oxaloacetate, which can exit the mitochondria via a transporter (**figure 14**). This mechanism has not been fully investigated and therefore further research needs to be carried out in order to confirm this.

It is clear from the results that *C. andersoni* and *C.hominis* have the complete complex II, succinate dehydrogenase, which is involved in the TCA cycle, converting succinate to fumarate and produces ubiquinol. However, *C.parvum*, *C.hominis*, *C.ubiquitum* and *C.tyzzeri* have lost these enzymes completely. In the NADH dehydrogenase complex, electrons are removed and transferred to coenzyme Q (ubiquinone) which transfers electrons from to complex II and complex III. It is synthesized from chorismate, which is predicted to be taken from the host as the shikimate pathway is absent in the *Cryptosporidium* species (Liu et al., 2016). In the succinate dehydrogenase complex (complex II) only one subunit was identified in *C.muris* and *C.andersoni*-the flavoprotein subunit. *C.parvum*, *C.hominis*, *C.andersoni*, *C.muris* and *C.tyzzeri* all have all enzymes and proteins that are involved in ubiquinone biosynthesis see **supplementary table S4**. Five of the essential enzymes needed are missing in *C.ubiquitum* which suggests that it lacks the capability of ubiquinone biosynthesis. *C.ubiquitum* does not contain AOX, however all other

Cryptosporidium species do. The presence of AOX compensates for the lack of complex III and IV, where it takes electrons from the quinone pool generated from complex II. This subsequently feeds into ATP synthase where ATP is generated.

Most of the components of the Fe-S cluster machinery are encoded by the *Cryptosporidium* genome (**figure 12**). There are three main processes which include: ISC synthesis, cluster assembly and targeting. Frataxin, IscU and IscS have been experimentally found to be localised in *C.parvum* (Miller, Jossé and Tsaousis, 2018). As shown in **figure 12** ISC proteins are needed for the synthesis of Fe-S cluster proteins. Early ISC synthesis is generated by IscU scaffold protein, cysteine desulfurase complex (IscS-IscD), frataxin, ferredoxin and electrons from ferredoxin reductase. All these proteins except for IscD, were not identified in any of the *Cryptosporidium* species investigated. Iron is transported into this relict mitochondrion via mitoferrin transporter. This bound IscU iron sulfur cluster assembly is then delivered to Glutaredoxin 5, via the chaperone system consisting of Jac-1 and Hsp70 (**figure 12**). GrpE the exchange factor facilitates the exchange of ADP to ATP which is needed for the chaperone system. IscA1, IscA2 and IBA57 are required for the generation of other iron sulfur cluster proteins, however the absence of IBA57 in all of the species investigated raises the question as to whether these late ISC machinery proteins are generated.

5. Conclusion and further research

Our study successfully predicted the mitochondrial protein composition of six *Cryptosporidium* species. The gastric species of *Cryptosporidium*, *C.andersoni* and *C.muris* contain the most conserved mitochondrial proteins, followed directly after *C.parvum* and *C.hominis*, *C.tyzzeri* and then *C.ubiquitum* which contained the least amount of predicted proteins (reflected in the number of protein coding genes in **table 5**). More studies can be carried out on these species that in turn may lead to the development of intervention strategies against these waterborne and zoonotic pathogens in developing and industrialised nations. Alongside this, possible drug targets could be

made to target various pathways that have been identified for example, as the intestinal *C.ubiquitum* lacks an AOX, inhibitors of this enzyme will not affect its metabolism. Although our study has provided some a framework for further research, it should be noted that there may be some limitations as some proteins may have been misannotated. Although proteins have been identified, MitoProt could be used to confirm in silico presence or absence of these proteins in the mitosome. In addition, antibodies against the proteins identified could be used to confirm the presence of these mitochondrial proteins and their locations in the mitosome.

Using a bioinformatics only approach as seen in our study provided some limitations, as some protein coding genes were seen as putative or hypothetical, meaning that further tests have to be carried out experimentally to test the function and presence of these proteins.

To test the function of such hypothetical proteins, a combination of both experimental and computational approaches need to be employed. Experimental tests such as antibody testing can be used to confirm the presence of the hypothetical proteins and fluorescent labelling can also be used predict the interaction with host cell which will give a better understanding of targets that could be used for possible drug treatment. Additionally identification of host cell receptors can also aid in understanding the such host- pathogen interactions.

Our research findings show that the TCA cycle and ETC is present in *C.andersoni* and *C.muris*, but absent in *C.tyzzeri*, *C.ubiquitum*, *C.parvum* and *C.hominis*. Furthermore, ubiquinone biosynthesis and AOX is absent from *C.ubiquitum*. This study successfully predicted that the most recent *C.ubiquitum* species contains the least mitochondrial pathways, therefore suggesting that it may not be as detrimental to the host in comparison to *C.hominis* and *C.parvum* which infect mostly humans.

Supplementary Information

6. Supplementary information

These supplementary tables supplies the annotations from CryptoDB and PlasmoDB for Fe-S cluster assembly, ETC, ubiquinone synthesis, pyruvate metabolism and carrier proteins. The protein coding genes are present for identification in these databases, as well as the EC numbers are supplied for protein function and identification. An extra *C.hominis* isolate (30976) was used for further comparative analysis.

Supplementary Table S 1: Identified proteins subunits potentially involved in ETC in six *Cryptosporidium* species as extracted from PlasmoDB and CryptoDB using BLASTP.

Protein	EC number	C.muris	C.andersoni	C.hominis	C.hominis	C.parvum	C.ubiquitum	C.tyzzeri	P.falciparum
		RN66	30847	TU502	30976	Iowa II	39726	UGA55	3D7
AOX (Alternative Oxidase)		CMU_000270	cand_000250	Chro.30354	GY17_00002541	cgd3_3120		CTYZ_00003035	
NADH dehydrogenase (Complex I)	1.6.99.3	CMU_033930	cand_030010	Chro.70218	GY17_00001984	cgd7_1900	cubi_02867	CTYZ_00000789	PF3D7_0915000
Succinate dehydrogenase (Complex II)-flavoprotein subunit	1.3.5.1	CMU_043190	cand_038900						PF3D7_1034400
Succinate dehydrogenase (Complex II)-iron-sulfur subunit	1.3.5.1								PF3D7_1212800
cytochrome b-c1 complex subunit 7 (Complex III)	7.1.1.8								PF3D7_1012300
cytochrome c reductase iron-sulfur subunit (complex III)	7.1.1.8								PF3D7_1439400
cytochrome c reductase cytochrome b subunit (Complex III)	7.1.1.8								mal_mito_3
cytochrome c1 precursor (Complex III)	7.1.1.8								PF3D7_1462700
cytochrome c reductase subunit 6 (Complex III)	7.1.1.8								PF3D7_1426900
cytochrome c reductase subunit 7 (Complex III)	7.1.1.8								PF3D7_1012300
cytochrome c oxidase subunit 5B (Complex IV)	1.9.3.1								PF3D7_0927800
cytochrome c oxidase assembly protein (Complex IV)	1.9.3.1								PF3D7_0519300
cytochrome oxidase subunit III (Complex IV)	1.9.3.1								mal_mito_1

cytochrome c oxidase subunit 1 (Complex IV)	1.9.3.1								mal_mito_2
cytochrome c oxidase subunit 2 (Complex IV)	1.9.3.1								PF3D7_1430900
cytochrome c oxidase subunit 5b (Complex IV)	1.9.3.1								PF3D7_0927800
cytochrome c oxidase subunit 6b (Complex IV)	1.9.3.1								PF3D7_0928000
cytochrome c oxidase assembly protein subunit 11 (Complex IV)	1.9.3.1								PF3D7_1475300
cytochrome c oxidase assembly protein subunit 15 (Complex IV)	1.9.3.1								PF3D7_1435000
cytochrome c oxidase assembly protein subunit 17 (Complex IV)	1.9.3.1								PF3D7_1025600
cytochrome c oxidase assembly protein (Complex IV)	1.9.3.1								PF3D7_0519300
F-type H ⁺ -transporting ATPase subunit gamma	7.1.2.2	CMU_017340	cand_015060						PF3D7_1311300
F-type H ⁺ -transporting ATPase subunit delta	7.1.2.2	CMU_008960	cand_007400						PF3D7_1147700
F-type H ⁺ -transporting ATPase subunit epsilon	7.1.2.2	CMU_002850	cand_002490						PF3D7_0715500
F-type H ⁺ -transporting ATPase subunit O	7.1.2.2								PF3D7_1310000
F-type H ⁺ -transporting ATPase subunit c	7.1.2.2	CMU_016520	cand_014260						PF3D7_0705900
Vacuolar ATP synthetase subunit	7.1.2.2	CMU_011240	cand_009490	Chro.10062	GY17_00001053	cgd1_520	cubi_00048	CTYZ_00003636	
Vacuolar ATP synthase, subunit C (ATP synthase)	7.1.2.2	CMU_005350	cand_003910			cgd4_540			PF3D7_0106100
F-type ATPase, beta chain (ATP synthase)	7.1.2.2	CMU_008950	cand_007390	Chro.20148	GY17_00003496	cgd2_1360	cubi_00515	CTYZ_00002375	PF3D7_1235700
F-type ATPase, alpha chain (ATP synthase)	7.1.2.2	CMU_027630	cand_024370	Chro.60082	GY17_00000059	cgd6_610	cubi_02187	CTYZ_00001233	PF3D7_0217100
Vacuolar ATPase synthetase subunit A	7.1.2.2.	CMU_019130	cand_016810	Chro.70559	GY17_00002386	cgd7_5000	cubi_03172	CTYZ_00001121	PF3D7_1311900
Vacuolar ATPase synthetase subunit B	7.1.2.2	CMU_025620	cand_022390	Chro.80195	GY17_00000596	cgd8_1670	cubi_03395	CTYZ_00000180	PF3D7_0406100
Vacuolar ATP synthase subunit C	7.1.2.2	CMU_012660	cand_010580	Chro.40070	GY17_00003173	cgd4_540	cubi_01300	CTYZ_00001820	PF3D7_0106100
Vacuolar H-ATpase subunit D	7.1.2.2	CMU_041380	cand_037120	Chro.50340	GY17_00002934	cgd5_530	cubi_01745	CTYZ_00003216	PF3D7_1341900
Vacuolar ATP synthase subunit E	7.1.2.2	CMU_024280	cand_021060	Chro.80048	GY17_00002780	cgd8_360	cubi_03259	CTYZ_00000040	PF3D7_0934500
Vacuolar ATP synthase subunit F	7.1.2.2	CMU_041040	cand_036790	Chro.50302	GY17_00002967	cgd5_850	cubi_01775	CTYZ_00003250	PF3D7_1140100
Vacuolar ATP synthase subunit G	7.1.2.2	CMU_010180	cand_008620	Chro.20032	GY17_00000672	cgd2_250	cubi_00402	CTYZ_00002263	PF3D7_1323200

V-type H ⁺ -transporting ATPase subunit H	7.1.2.2	CMU_003000	cand_002640	Chro.20424	GY17_00003569	cgd2_3960	cubi_00771	CTYZ_00002649	PF3D7_1306600
V-type H ⁺ -transporting ATPase subunit a	7.1.2.2	CMU_028580	cand_025140	Chro.40167	GY17_00001877	cgd4_1470	cubi_01559	CTYZ_00002170	PF3D7_0806800
V-type H ⁺ -transporting ATPase subunit c	7.1.2.2	CMU_011240	cand_003910	Chro.80551	GY17_00001051	cgd1_520	cubi_00048		PF3D7_0519200
V-type H ⁺ -transporting ATPase subunit d	7.1.2.2	CMU_015820	cand_013600	Chro.50039	GY17_00001616	cgd5_3340	cubi_02101	CTYZ_00004016	PF3D7_1464700
V-type H ⁺ -transporting ATPase subunit e	7.1.2.2				GY17_00001850	cgd4_3723		CTYZ_00002141	PF3D7_0721900

* These protein annotations were used to predict the presence of the proteins. Kegg EC numbers are present for the complex name and function.

Supplementary Table S 2: Showing the predicted proteins identified in Fe-S cluster assembly in six *Cryptosporidium* species as extracted from PlasmoDB and CryptoDB using BLASTP.

Protein	EC number	C.muris	C.andersoni	C.parvum	C.ubiquitum	C. tyzzeri	C.hominis	C.hominis	P.falciparum
		RN66	30847	Iowa II	39726	UGA55	TU502	30976	3D7
Cysteine Desulfurase/IscS	2.8.1.7	CMU_018170	cand_015850	cgd4_3040	cubi_00423	CTYZ_00002241	Chro.40346	GY17_00003685	PF3D7_0716600
Isc11		CMU_009960	cand_008400	cgd2_30		CTYZ_00002068	Chro.20011	GY17_00001778	PF3D7_1311000
GLRX5/Grx5) Glutaredoxin 5		CMU_037450	cand_033360	cgd2_2540	cubi_00634	CTYZ_00002502	Chro.20270	GY17_00002209	PF3D7_0304500
(IscU/IscU) Iron-Sulfur Assembly		CMU_027160	cand_023910	cgd6_1050	cubi_02231	CTYZ_00001280	Chro.60135	GY17_00000104	PF3D7_1128500
(FDX1) Ferredoxin		CMU_031030	cand_027210	cgd6_3000	cubi_02428	CTYZ_00001491		GY17_00000310	PF3D7_1318100
(FDXR) Ferredoxin Reductase	1.18.1.2	CMU_026730	cand_023500	cgd8_2710	cubi_03495	CTYZ_00000293	Chro.80316	GY17_00000705	PF3D7_1139700
Fra1 (FXN)		CMU_03778	cand_033600	cgd5_4320	cubi_02009	CTYZ_00003501	Chro.50410	GY17_00001513	
MFRN1/MRs3 (mitochondrial carrier protein)		CMU_009340	cand_007780	cgd2_1030	cubi_00483	CTYZ_00002344	Chro.20115	GY17_00003465	PF3D7_0905200
MFRN2/Mrs4 (mitochondrial carrier protein)		CMU_012200	cand_005980	cgd6_2350		CTYZ_00001418	Chro.60274	GY17_00000239	PF3D7_0905200
		CMU_007520							
Grp75/Ssq1/Hsp70		CMU_010560	cand_008820	cgd3_3440	cubi_01153	CTYZ_00003068	Chro.30389	GY17_00002573	PF3D7_0818900
Hsp20									PF3D7_0816500
HSCB/Jac1		CMU_005860	cand_004420	cgd8_3770	cubi_03606	CTYZ_00000413	Chro.80434	GY17_00000821	
GrpE-L1/Mge1		CMU_015580	cand_013360	cgd5_3510	cubi_02117	CTYZ_00003999	Chro.50021	GY17_00001633	PF3D7_1124700
Ind1		CMU_023680	cand_020440	cgd8_3140	cubi_03543	CTYZ_00000342	Chro.80366	GY17_00000752	
IscA1/IscA1 (Iron sulfur cluster assembly 1)		CMU_003090	cand_002740						PF3D7_1209400
IscA2/IscA2 (Iron-sulfur cluster assembly 2)		CMU_001480	cand_001440						PF3D7_0322500
ABC7/Atm1		CMU_036080	cand_032010	cgd1_1350	cubi_00131	CTYZ_00003722	Chro.10157	GY17_00001140	

* These protein annotations were used to predict the presence of the proteins. Kegg EC numbers are present for the complex name and function.

Supplementary Table S 3: Showing the predicted carrier proteins in six *Cryptosporidium* species as extracted from PlasmoDB and CryptoDB using BLASTP.

Protein	<i>C.andersoni</i>	<i>C.hominis</i>	<i>C.muris</i>	<i>C.parvum</i>	<i>C.ubiquitum</i>	<i>C.tyzzeri</i>	<i>P.falciparum</i>
	30847	TU502	30976	RN66	lowa II	39726	UGA55
Hexose transporter	cand_028430	Chro.30458	CTYZ_00003132	CMU_032230	cgd3_4070	cubi_01213	GY17_00003803
mitochondrial pyruvate carrier protein 1							PF3D7_1340800
mitochondrial pyruvate carrier protein 2							PF3D7_1470400
acetyl-CoA transporter	cand_024500	Chro.60065	GY17_00000046	CMU_027760	cgd6_470	cubi_02174	CTYZ_00001220
citrate/oxoglutarate carrier protein							PF3D7_1223800
Oxoglutarate/malate translocator protein	cand_031240	Chro.10071	GY17_00001060	CMU_035290	cgd1_600		CTYZ_00003643
mitochondrial carrier protein	cand_013740		GY17_00001244	CMU_025080	cgd2_1030	cubi_00483	CTYZ_00002344
Adenine nucleotide translocator 1/ADP/ATP carrier	cand_021920	Chro.80141	GY17_00002864	CMU_025140	cgd8_1210	cubi_03345	CTYZ_00000130

* These protein annotations were used to predict the presence of the proteins. Bold shows the that the protein may be present (hypothetical)

Supplementary Table S 4: Showing the protein coding genes of the *Cryptosporidium* species present in the Ubiquinone synthesis.

Protein	<i>C.muris</i>	<i>C.andersoni</i>	<i>C.hominis</i>	<i>C.hominis</i>	<i>C.parvum</i>	<i>C.ubiquitum</i>	<i>C.tyrezzi</i>
	RN66	30847	30976	TU502	lowa II	39726	UGA55
UbiE/COQ5 methyltransferase			GY17_00001296		cgd1_2860		CTYZ_00003878
Coenzyme Q3/methyltransferase					cgd2_2830		CTYZ_00002533
ubiquinone biosynthesis protein COQ4 (Coenzyme Q biosynthesis protein 4)	CMU_035060	cand_031120	GY17_00001035	Chro.10049	cgd1_380		CTYZ_00003619
ubiquinone biosynthesis O-methyltransferase family protein	CMU_005250	cand_003800	GY17_00002238	Chro.20298	cgd2_2830		CTYZ_00002533
ubiquinone menaquinone biosynthesis methyltransferases family protein	CMU_029670	cand_026220					
UbiA prenyltransferase family	CMU_001010	cand_000970	GY17_00002470	Chro.30285	cgd3_2460		CTYZ_00002964

* These protein annotations were used to predict the presence of the proteins.

Supplementary Table S 5: Showing the protein coding genes of the *Cryptosporidium* species present in the pyruvate metabolism.

Protein	EC number	<i>C.andersoni</i> 30847	<i>C.muris</i> RN66	TU502	<i>C.hominis</i> 30976	<i>C.parvum</i> Iowa II	<i>C.ubiquitum</i> 39726	<i>C.tyzzeri</i> UGA55
Pyruvate kinase	2.7.1.40	cand_025370	CMU_028810	Chro.10234	GY17_00001209	cgd1_2040	cubi_00199	CTYZ_00003791
Phosphoenolpyruvate carboxylase	4.1.1.31	cand_027920	CMU_031720	Chro.50389	GY17_00002889	cgd5_70	cubi_01701	CTYZ_00003175
Fumarate hydratase	4.2.1.2	cand_023740	CMU_026970					
Acetyl-CoA carboxylase	6.4.1.2	cand_004520	CMU_005960	Chro.80425	GY17_00000811	cgd8_3680	cubi_03596	CTYZ_00000403
Acetate--CoA ligase	6.2.1.1	cand_017460	CMU_019880	Chro.10418	GY17_00001386	cgd1_3710	cubi_00366	CTYZ_00003969
Acetate--CoA ligase (ADP-forming)	6.2.1.13	cand_010920	CMU_013000					
L-lactate dehydrogenase	1.1.1.27	cand_004950	CMU_006390	Chro.70063	GY17_00003282	cgd7_480	cubi_02723	CTYZ_00000640
Malate dehydrogenase	1.1.1.37	cand_004960	CMU_006400	Chro.70062	GY17_00003281	cgd7_470	cubi_02722	CTYZ_00000639
Malate dehydrogenase (oxaloacetate-decarboxylating) (NADP(+))	1.1.1.40	cand_036890	CMU_041140	Chro.50314	GY17_00002956	cgd5_750	cubi_01766	CTYZ_00003239
Dihydrolipoyl dehydrogenase	1.8.1.4	cand_020200	CMU_023430					
Pyruvate synthase	1.2.7.1	cand_010750	CMU_012830	Chro.40087	GY17_00003157	cgd4_690	cubi_01315	CTYZ_00001835
Acyolphosphatase	3.6.1.7	cand_018710	CMU_021350		GY17_00000515	cgd6_4900	cubi_02620	CTYZ_00001696
Malate dehydrogenase (quinone)	1.1.5.4	cand_021080	CMU_024300	Chro.80050	GY17_00002782	cgd8_380	cubi_03261	CTYZ_00000042

* These protein annotations were used to predict the presence of the proteins. Kegg EC numbers are present for the complex name and function

References

References

- [1] Abrahamsen, M. (2004). Complete Genome Sequence of the Apicomplexan, *Cryptosporidium parvum*. *Science*, 304(5669), pp.441-445.
- [2] Alcock, F., Webb, C., Dolezal, P., Hewitt, V., Shingu-Vasquez, M., Likić, V., Traven, A. and Lithgow, T. (2011). A Small Tim Homohexamer in the Relict Mitochondrion of *Cryptosporidium*. *Molecular Biology and Evolution*, 29(1), pp.113-122.
- [3] Alvarez-Pellitero, P., and A. Sitja-Bobadilla. 2002. *Cryptosporidium molnari* n. sp. (Apicomplexa: Cryptosporidiidae) infecting two marine fish species, *Sparus aurata* L. and *Dicentrarchus labrax* L. *Int. J. Parasitol.* 32:1007–1021.
- [4] Alvarez-Pellitero, P., Quiroga, M., Sitja-Bobadilla, A., Redondo, M., Palenzuela, O., Padrós, F., Vázquez, S. and Nieto, J. (2004). *Cryptosporidium scophthalmi* n. sp. (Apicomplexa: Cryptosporidiidae) from cultured turbot *Scophthalmus maximus*. Light and electron microscope description and histopathological study. *Diseases of Aquatic Organisms*, 62, pp.133-145.
- [5] Artieda, J., Basterrechea, M., Arriola, L., Yagüe, M., Albisua, E., Arostegui, N., Astigarraga, U., Botello, R. and Manterola, J. (2012). Outbreak of cryptosporidiosis in a child day-care centre in Gipuzkoa, Spain, October to December 2011. *Eurosurveillance*, 17(5).
- [6] Ashbolt, R., Coleman, D., Misrachi, A., Conti, J. and Kirk, M. (2003). An outbreak of cryptosporidiosis associated with an animal nursery at a regional fair. *Communicable Diseases Intelligence*, 27(2).
- [7] Barker, I. and Carbonell, P. Z. *Parasitenkunde* (1974). *Cryptosporidium agni* sp.n. from lambs, and *Cryptosporidium bovis* sp.n. from a calf, with observations on the oocyst., 44(4), pp.289-298.
- [8] Beyer, T., Svezhova, N., Sidorenko, N. and Khokhlov, S. (2000). *Cryptosporidium parvum* (Coccidia, Apicomplexa): Some new ultrastructural observations on its endogenous development. *European Journal of Protistology*, 36(2), pp.151-159.
- [9] Bhat, N., Joe, A., PereiraPerrin, M. and Ward, H., 2020. *Cryptosporidium* P30, A Galactose/N-Acetylgalactosamine-Specific Lectin, Mediates Infection in Vitro.
- [10] Borowski, H., Clode, P. and Thompson, R. (2008). Active invasion and/or encapsulation? A reappraisal of host-cell parasitism by *Cryptosporidium*. *Trends in Parasitology*, 24(11), pp.509-516.
- [11] Bouzid, M., Hunter, P., Chalmers, R. and Tyler, K. (2013). *Cryptosporidium* Pathogenicity and Virulence. *Clinical Microbiology Reviews*, 26(1), pp.115-134.
- [12] Boxma, B., de Graaf, R., van der Staay, G., van Alen, T., Ricard, G., Gabaldón, T., van Hoek, A., Moon-van der Staay, S., Koopman, W., van Hellemond, J., Tielens, A., Friedrich, T., Veenhuis, M., Huynen, M. and Hackstein, J. (2005). An anaerobic mitochondrion that produces hydrogen. *Nature*, 434(7029), pp.74-79.
- [13] Brix, J., Rüdiger, S., Bukau, B., Schneider-Mergener, J. and Pfanner, N., 1999. Distribution of Binding Sequences for the Mitochondrial Import Receptors Tom20, Tom22, and Tom70 in a Presequence-carrying Preprotein and a Non-cleavable Preprotein. *Journal of Biological Chemistry*, 274(23), pp.16522-16530.

- [14] Budu-Amoako, E., Greenwood, S. J., Dixon, B. R., Barkema, H. W. and McClure, J. T. (2012). *Giardia* and *Cryptosporidium* on dairy farms and the role these farms may play in contaminating water sources in Prince Edward Island, Canada. *Journal of Veterinary Internal Medicine* 26, 668–73.
- [15] Burki, F. (2016). Mitochondrial Evolution: Going, Going, Gone. *Current Biology*, 26(10), pp.410-412.
- [16] Cacciò, S., Thompson, R., McLauchlin, J. and Smith, H. (2005). Unravelling *Cryptosporidium* and *Giardia* epidemiology. *Trends in Parasitology*, 21(9), pp.430-437.
- [17] Calvo, S. and Mootha, V. (2010). The Mitochondrial Proteome and Human Disease. *Annual Review of Genomics and Human Genetics*, 11(1), pp.25-44.
- [18] Chalmers, R., Elwin, K., Thomas, A., Guy, E. and Mason, B. (2009). Long-term *Cryptosporidium* typing reveals the aetiology and species-specific epidemiology of human cryptosporidiosis in England and Wales, 2000 to 2003. *Eurosurveillance*, 14(2).
- [19] Chalmers, R. and Davies, A. (2010). Minireview: Clinical cryptosporidiosis. *Experimental Parasitology*, 124(1), pp.138-146.
- [20] Current, W.L. and Reese, N.C. (1986). A comparison of endogenous development of three isolates of *Cryptosporidium* in suckling mice. *Journal of Protozoology* 33, 98–108.
- [21] Current, W. L., S. J. Upton, and T. B. Haynes. 1986. The life cycle of *Cryptosporidium baileyi* n. sp. (Apicomplexa, Cryptosporidiidae) infecting chickens. *J. Protozool.* 33:289–296.
- [22] Current, W. and Garcia, L. (1991). Cryptosporidiosis. *Clinical Microbiology Reviews*, 4(3), pp.325-358.
- [23] Ctrnacta, V., AULT, J., Stejskal, F. and Keithly, J. (2006). Localization of Pyruvate:NADP+ Oxidoreductase in Sporozoites of *Cryptosporidium parvum*. *The Journal of Eukaryotic Microbiology*, 53(4), pp.225-231.
- [24] D'Antonio, R. (1985). A Waterborne Outbreak of Cryptosporidiosis in Normal Hosts. *Annals of Internal Medicine*, 103(6_Part_1), p.886.
- [25] Deshpande, O. and Mohiuddin, S., 2020. *Biochemistry, Oxidative Phosphorylation*.
- [26] D. L. (David L. Nelson, M. M. Cox, and A. L. Lehninger, *Lehninger principles of biochemistry*.
- [27] Elwin, K., Hadfield, S., Robinson, G., Crouch, N. and Chalmers, R. (2012). *Cryptosporidium viatorum* n. sp. (Apicomplexa: Cryptosporidiidae) among travellers returning to Great Britain from the Indian subcontinent, 2007–2011. *International Journal for Parasitology*, 42(7), pp.675-682.
- [28] Essid, R., Mousli, M., Aoun, K., Mellouli, F., Kanoun, F., Abdelmalek, R., Derouin, F. and Bouratbine, A. (2008). Identification of *Cryptosporidium* Species Infecting Humans in Tunisia. *The American Journal of Tropical Medicine and Hygiene*, 79(5), pp.702-705.
- [29] Fayer, R., Morgan, U. and Upton, S. (2000). Epidemiology of *Cryptosporidium*: transmission, detection and identification. *International Journal for Parasitology*, 30(12-13), pp.1305-1322.
- [30] Fayer, R., J. M. Trout, L. Xiao, U. M. Morgan, A. A. Lai, and J. P. Dubey. 2001. *Cryptosporidium canis* n. sp. from domestic dogs. *J. Parasitol.* 87:1415–1422

- [31] Fayer, R., Santín, M. and Xiao, L. (2005). *Cryptosporidium bovis* n. sp. (Apicomplexa: Cryptosporidiidae) in cattle (*Bos Taurus*). *Journal of Parasitology*, 91(3), pp.624-629.
- [32] Fayer, R., Xiao, L., 2007. *Cryptosporidium and cryptosporidiosis*, 2nd edition. CRC Press Taylor & Francis Group, Boca Raton, London, New York, pp. 580.
- [33] Fayer, R., Santín, M. and Trout, J. (2008). *Cryptosporidium ryanae* n. sp. (Apicomplexa: Cryptosporidiidae) in cattle (*Bos taurus*). *Veterinary Parasitology*, 156(3-4), pp.191-198.
- [34] Fayer, R., Santín, M. and Macarisin, D. (2010). *Cryptosporidium ubiquitum* n. sp. in animals and humans. *Veterinary Parasitology*, 172(1-2), pp.23-32.
- [35] Feng, Y., Yang, W., Ryan, U., Zhang, L., Kváč, M., Koudela, B., Modry, D., Li, N., Fayer, R. and Xiao, L. (2011). Development of a multilocus sequence tool for typing *Cryptosporidium muris* and *Cryptosporidium andersoni*. *Journal of Clinical Microbiology* 49, 34–41
- [36] Gentile, G., Venditti, M., Micozzi, A., Caprioli, A., Donelli, G., Caprioli, A., Donelli, G., Tirindelli, C., Meloni, G., Arcese, W. and Martino, P. (1991). Cryptosporidiosis in Patients with Hematologic Malignancies. *Clinical Infectious Diseases*, 13(5), pp.842-846.
- [37] Gentle, I., Perry, A., Alcock, F., Likic, V., Dolezal, P., Ng, E., Purcell, A., McConville, M., Naderer, T., Chanez, A., Charriere, F., Aschinger, C., Schneider, A., Tokatlidis, K. and Lithgow, T. (2007). Conserved Motifs Reveal Details of Ancestry and Structure in the Small TIM Chaperones of the Mitochondrial Intermembrane Space. *Molecular Biology and Evolution*, 24(5), pp.1149-1160.
- [38] Germot, A., Philippe, H. and Le Guyader, H. (1996). Presence of a mitochondrial-type 70-kDa heat shock protein in *Trichomonas vaginalis* suggests a very early mitochondrial endosymbiosis in eukaryotes. *Proceedings of the National Academy of Sciences*, 93(25), pp.14614-14617.
- [39] Goldberg, A., Molik, S., Tsaousis, A., Neumann, K., Kuhnke, G., Delbac, F., Vivares, C., Hirt, R., Lill, R. and Embley, T. (2008). Localization and functionality of microsporidian iron–sulphur cluster assembly proteins. *Nature*, 452(7187), pp.624-628.
- [40] Gross J, Bhattacharya D. Mitochondrial and plastid evolution in eukaryotes: an outsiders' perspective. *Nat Rev Genet*. 2009;10(7): 495-505
- [41] Henriquez, F., Richards, T., Roberts, F., McLeod, R. and Roberts, C. (2005). The unusual mitochondrial compartment of *Cryptosporidium parvum*. *Trends in Parasitology*, 21(2), pp.68-74.
- [42] Hijjawi, N., Meloni, B., Morgan, U. and Thompson, R. (2001). Complete development and long-term maintenance of *Cryptosporidium parvum* human and cattle genotypes in cell culture. *International Journal for Parasitology*, 31(10), pp.1048-1055.
- [43] Hijjawi, N., Meloni, B., Ryan, U., Olson, M. and Thompson, R. (2002). Successful in vitro cultivation of *Cryptosporidium andersoni*: evidence for the existence of novel extracellular stages in the life cycle and implications for the classification of *Cryptosporidium*. *International Journal for Parasitology*, 32(14), pp.1719-1726.
- [44] Hong, D., Wong, C. and Gutierrez, K. (2007). Severe cryptosporidiosis in a seven-year-old renal transplant recipient - Case report and review of the literature. *Paediatric Transplantation*, 11(1), pp.94-100.
- [45] Hunt, D., Shannon, R., Palmer, S. and Jephcott, A. (1984). Cryptosporidiosis in an urban community. *BMJ*, 289(6448), pp.814-816.

- [46] Hunter, P.R., Chalmers, R.M., Syed, Q., Hughes, L.S., Woodhouse, S. and Swift, L. (2003). Foot and mouth disease and cryptosporidiosis: possible interaction between two emerging infectious diseases. *Emerging Infectious Diseases* 9, 109–112.
- [47] Insulander, M., Lebbad, M., Stenström, T. and Svenungsson, B. (2005). An outbreak of cryptosporidiosis associated with exposure to swimming pool water. *Scandinavian Journal of Infectious Diseases*, 37(5), pp.354-360.
- [48] Insulander, M., Silverlas, C., Lebbad, M., Karlsson, L., Mattsson, J. G. and Svenungsson, B. (2013). Molecular epidemiology and clinical manifestations of human cryptosporidiosis in Sweden. *Epidemiology and Infection* 141, 1009–1020.
- [49] Iseki, M. 1979. *Cryptosporidium felis* sp. n. (Protozoa: Eimeriorina) from the domestic cat. *Jpn. J. Parasitology*. 28:285–307
- [46] Jaggi, N., Rajeshwari, S., Mittal, S., Mathur, M. and Baveja, U. (1994). Assessment of the immune and nutritional status of the host in childhood diarrhoea due to cryptosporidium. *J Commun Dis*, 26(4), pp.181-5.
- [50] Jenkins, M., Anguish, L., Bowman, D., Walker, M. and Ghiorse, W. (1997). Assessment of a dye permeability assay for determination of inactivation rates of *Cryptosporidium parvum* oocysts. *Applied and Environmental Microbiology*, 63(10), pp.3844–3850.
- [51] Jenkins, M., Liotta, J., Lucio-Forster, A. and Bowman, D. (2010). Concentrations, Viability, and Distribution of *Cryptosporidium* Genotypes in Lagoons of Swine Facilities in the Southern Piedmont and in Coastal Plain Watersheds of Georgia. *Applied and Environmental Microbiology*, 76(17), pp.5757-5763.
- [52] Jirku, M., Valigurova, A., Koudela, B., Krizek, J., Modry, D. and Slapeta, J. (2008). New species of *Cryptosporidium* Tyzzer, 1907 (Apicomplexa) from amphibian host: morphology, biology and phylogeny. *Folia Parasitologica*, 55(2), pp.81-94.
- [53] Jokipii, L., Pohjola, S. and Jokipii, A. (1983). *Cryptosporidium*: A Frequent finding in patients with gastrointestinal symptoms. *The Lancet*, 322(8346), pp.358-361.
- [54] Keithly, J., Langreth, S., Buttle, K. and Mannella, C. (2005). Electron Tomographic and Ultrastructural Analysis of the *Cryptosporidium parvum* Relict Mitochondrion, its Associated Membranes, and Organelles. *The Journal of Eukaryotic Microbiology*, 52(2), pp.132-140.
- [55] Khan, S., Debnath, C., Pramanik, A., Xiao, L., Nozaki, T. and Ganguly, S. (2010). Molecular characterization and assessment of zoonotic transmission of *Cryptosporidium* from dairy cattle in West Bengal, India. *Veterinary Parasitology*, 171(1-2), pp.41-47.
- [56] Kobayashi, M., Matsuo, Y., Takimoto, A., Suzuki, S., Maruo, F. and Shoun, H. (1996). Denitrification, a Novel Type of Respiratory Metabolism in Fungal Mitochondrion. *Journal of Biological Chemistry*, 271(27), pp.16263-16267.
- [57] Koudela, B., and D. Modry. 1998. New species of *Cryptosporidium* (Apicomplexa, Cryptosporidiidae) from lizards. *Folia Parasitol.* 45:93–100
- [58] Kuznar, Z. and Elimelech, M. (2005). Role of surface proteins in the deposition kinetics of *Cryptosporidium parvum* oocysts. *Langmuir*, 21(2), pp.710-716.

- [59] Kulawiak, B., Höpker, J., Gebert, M., Guiard, B., Wiedemann, N. and Gebert, N. (2013). The mitochondrial protein import machinery has multiple connections to the respiratory chain. *Biochimica et Biophysica Acta (BBA) - Bioenergetics*, 1827(5), pp.612-626.
- [60] Kváč, M., Hanzlíková, D., Sak, B. and Květoňová, D. (2009). Prevalence and age-related infection of *Cryptosporidium suis*, *C. muris* and *Cryptosporidium pig* genotype II in pigs on a farm complex in the Czech Republic. *Veterinary Parasitology*, 160(3-4), pp.319-322.
- [61] Kváč, M., Kestřánová, M., Pinková, M., Květoňová, D., Kalinová, J., Wagnerová, P., Kotková, M., Vítovec, J., Ditrich, O., McEvoy, J., Stenger, B. and Sak, B. (2013). *Cryptosporidium scrofarum* n. sp. (Apicomplexa: Cryptosporidiidae) in domestic pigs (*Sus scrofa*). *Veterinary Parasitology*, 191(3-4), pp.218-227.
- [62] Kváč, M., Saková, K., Květoňová, D., Kicia, M., Wesołowska, M., McEvoy, J. and Sak, B. (2014). Gastroenteritis caused by the *Cryptosporidium hedgehog* genotype in an immunocompetent man. *Journal of Clinical Microbiology* 52, 347–349.
- [63] Leitch, G. and He, Q. (2012). Cryptosporidiosis-an overview. *Journal of Biomedical Research*, 25(1), pp.1-16.
- [64] Leoni, F. (2006). Genetic analysis of *Cryptosporidium* from 2414 humans with diarrhoea in England between 1985 and 2000. *Journal of Medical Microbiology*, 55(6), pp.703-707.
- [65] Levine, N. D. 1980. Some corrections of coccidian (Apicomplexa: Protozoa) nomenclature. *J. Parasitol.* 66:830–834.
- [66] Lill, R. (2009). Function and biogenesis of iron–sulphur proteins. *Nature*, 460(7257), pp.831-838.
- [67] Lindmark, D. and Muller, M. (1973). Hydrogenosome, a Cytoplasmic Organelle of the Anaerobic Flagellate *Tritrichomonas foetus*, and Its Role in Puvrate Metabolism*. *The Journal of Biological Chemistry*, 248(22), pp.7724-7728.
- [68] Lindsay, D., Upton, S., Owens, D., Morgan, U., Mead, J. and Blagburn, B. (2000). *Cryptosporidium andersoni* n. sp. (Apicomplexa: Cryptosporiidae) from Cattle, *Bos taurus*. *The Journal of Eukaryotic Microbiology*, 47(1), pp.91-95.
- [69] Liu, S., Roellig, D., Guo, Y., Li, N., Frace, M., Tang, K., Zhang, L., Feng, Y. and Xiao, L. (2016). Evolution of mitosome metabolism and invasion-related proteins in *Cryptosporidium*. *BMC Genomics*, 17(1).
- [70] Llorente, M. T., Clavel, A., Goni, M. P., Varea, M., Seral, C., Becerril, R., Suarez, L. and Gomez-Lus, R. (2007). Genetic characterization of *Cryptosporidium* species from humans in Spain. *Parasitology International* 51, 201–205.
- [71] Mac Kenzie, W., Hoxie, N., Proctor, M., Gradus, M., Blair, K., Peterson, D., Kazmierczak, J., Addiss, D., Fox, K., Rose, J. and Davis, J. (1994). A Massive Outbreak in Milwaukee of *Cryptosporidium* Infection Transmitted through the Public Water Supply. *New England Journal of Medicine*, 331(15), pp.1035-1035.
- [72] Makiuchi, T. and Nozaki, T. (2014). Highly divergent mitochondrion-related organelles in anaerobic parasitic protozoa. *Biochimie*, 100, pp.3-17.
- [73] Martínez-Reyes, I. and Chandel, N., 2020. Mitochondrial TCA cycle metabolites control physiology and disease. *Nature Communications*, 11(1).

- [74] McKerr, C., Adak, G., Nichols, G., Gorton, R., Chalmers, R., Kafatos, G., Cosford, P., Charlett, A., Reacher, M., Pollock, K., Alexander, C. and Morton, S. (2015). An Outbreak of *Cryptosporidium parvum* across England & Scotland Associated with Consumption of Fresh Pre-Cut Salad Leaves, May 2012. *PLOS ONE*, 10(5), p.e0125955.
- [75] Millard, P. (1994). An Outbreak of Cryptosporidiosis From Fresh-Pressed Apple Cider. *JAMA: The Journal of the American Medical Association*, 272(20), p.1592.
- [76] Miller, C., Jossé, L. and Tsaousis, A. (2018). Localization of Fe-S Biosynthesis Machinery in *Cryptosporidium parvum* Mitosome. *Journal of Eukaryotic Microbiology*, 65(6), pp.913-922.
- [77] Mogi, T. and Kita, K. (2010). Diversity in mitochondrial metabolic pathways in parasitic protists *Plasmodium* and *Cryptosporidium*. *Parasitology International*, 59(3), pp.305-312.
- [78] Mokranjac, D., Popov-[Cbreve]eleketić, D., Hell, K. and Neupert, W. (2005). Role of Tim21 in Mitochondrial Translocation Contact Sites. *Journal of Biological Chemistry*, 280(25), pp.23437-23440.
- [79] Morgan-Ryan, U. M., A. Fall, L. A. Ward, N. Hijjawi, I. Sulaiman, R. Fayer, R. C. Thompson, M. Olson, A. Lal, and L. Xiao. 2002. *Cryptosporidium hominis* n. sp. (Apicomplexa: Cryptosporidiidae) from *Homo sapiens*. *J. Eukaryot. Microbiol.* 49:433–440.
- [80] Muller, M., Mentel, M., van Hellemond, J., Henze, K., Woehle, C., Gould, S., Yu, R., van der Giezen, M., Tielens, A. and Martin, W. (2012). Biochemistry and Evolution of Anaerobic Energy Metabolism in Eukaryotes. *Microbiology and Molecular Biology Reviews*, 76(2), pp.444-495.
- [81] O'Donoghue, P. (1995). *Cryptosporidium* and cryptosporidiosis in man and animals. *International Journal for Parasitology*, 25(2), pp.139-195.
- [82] Osellame, L., Blacker, T. and Duchon, M. (2012). Cellular and molecular mechanisms of mitochondrial function. *Best Practice & Research Clinical Endocrinology & Metabolism*, 26(6), pp.711-723.
- [83] Pedraza-Díaz, S., Amar, C., McLauchlin, J., Nichols, G., Cotton, K., Godwin, P., Iversen, A., Milne, L., Mulla, J., Nye, K., Panigrahl, H., Venn, S., Wiggins, R., Williams, M. and Youngs, E. (2001). *Cryptosporidium meleagridis* from Humans: Molecular Analysis and Description of Affected Patients. *Journal of Infection*, 42(4), pp.243-250.
- [84] Power, M. and Ryan, U. (2008). A New Species of *Cryptosporidium* (Apicomplexa: Cryptosporidiidae) from Eastern Grey Kangaroos (*Macropus giganteus*). *Journal of Parasitology*, 94(5), pp.1114-1117.
- [85] Preiser, G., Preiser, L. and Madeo, L. (2003). An Outbreak of Cryptosporidiosis Among Veterinary Science Students Who Work With Calves. *Journal of American College Health*, 51(5), pp.213-215.
- [86] Putignani, L., Tait, A., Smith, H., Horner, D., Tovar, J., Tetley, L. and Wastling, J. (2004). Characterization of a mitochondrion-like organelle in *Cryptosporidium parvum*. *Parasitology*, 129(1), pp.1-18.
- [87] Raskova, V., Kvetonova, D., Sak, B., McEvoy, J., Edwinson, A., Stenger, B. and Kvac, M. (2013). Human cryptosporidiosis caused by *Cryptosporidium tyzzeri* and *C. parvum* isolates presumably transmitted from wild mice. *Journal of Clinical Microbiology* 51, 360–362.

- [88] Reinoso, R., Becares, E. and Smith, H. (2008). Effect of various environmental factors on the viability of *Cryptosporidium parvum* oocysts. *Journal of Applied Microbiology*, 104(4), pp.980-986.
- [89] Ren, X., Zhao, J., Zhang, L., Ning, C., Jian, F., Wang, R., Lv, C., Wang, Q., Arrowood, M. and Xiao, L. (2012). *Cryptosporidium tyzzeri* n. sp. (Apicomplexa: Cryptosporidiidae) in domestic mice (*Mus musculus*). *Experimental Parasitology*, 130(3), pp.274-281.
- [90] Riordan, C., Langreth, S., Sanchez, L., Kayser, O. and Keithly, J. (1999). Preliminary evidence for a mitochondrion in *Cryptosporidium parvum*: phylogenetic and therapeutic implications. *Journal of Eukaryotic Microbiology*, 46, pp.52S–55S.
- [91] Robinson, G., Wright, S., Elwin, K., Hadfield, S., Katzer, F., Bartley, P., Hunter, P., Nath, M., Innes, E. and Chalmers, R. (2010). Re-description of *Cryptosporidium cuniculus* In man and Takeuchi, 1979 (Apicomplexa: Cryptosporidiidae): Morphology, biology and phylogeny. *International Journal for Parasitology*, 40(13), pp.1539-1548.
- [92] Rotte, C., Stejskal, F., Zhu, G., Keithly, J. and Martin, W. (2001). Pyruvate:NADP Oxidoreductase from the Mitochondrion of *Euglena gracilis* and from the Apicomplexan *Cryptosporidium parvum*: A Biochemical Relic Linking Pyruvate Metabolism in Mitochondriate and Amitochondriate Protists. *Molecular Biology and Evolution*, 18(5), pp.710-720.
- [93] Ryan, U. M., L. Xiao, C. Read, I. M. Sulaiman, P. Monis, A. A. Lal, R. Fayer, and I. Pavlašek. 2003. A redescription of *Cryptosporidium galli* Pavlašek, 1999 (Apicomplexa: Cryptosporidiidae) from birds. *J. Parasitol.* 89: 809–813.
- [94] Ryan, U., Monis, P., Enemark, H., Sulaiman, I., Samarasinghe, B., Read, C., Buddle, R., Robertson, I., Zhou, L., Thompson, R. and Xiao, L. (2004). *Cryptosporidium suis* n. sp. (Apicomplexa: Cryptosporidiidae) in pigs (*sus scrofa*). *Journal of Parasitology*, 90(4), pp.769-773.
- [95] RYAN, U., POWER, M. and XIAO, L. (2008). *Cryptosporidium fayerin*. sp. (Apicomplexa: Cryptosporidiidae) from the Red Kangaroo (*Macropus rufus*). *Journal of Eukaryotic Microbiology*, 55(1), pp.22-26.
- [96] Ryan, U., Fayer, R. and Xiao, L. (2014). *Cryptosporidium* species in humans and animals: current understanding and research needs. *Parasitology*, 141(13), pp.1667-1685.
- [97] Sischo, W., Atwill, E., Lanyon, L. and George, J. (2000). *Cryptosporidia* on dairy farms and the role these farms may have in contaminating surface water supplies in the northeastern United States. *Preventive Veterinary Medicine*, 43(4), pp.253-267.
- [98] Slapeta, J. (2006). *Cryptosporidium* species found in cattle: a proposal for a new species. *Trends in Parasitology* 22, 469–474.
- [99] Slavin, D. 1955. *Cryptosporidium meleagridis* (sp. nov.). *J. Comp. Pathol.* 65:262–270.
- [100] Sunnotel, O., Lowery, C., Moore, J., Dooley, J., Xiao, L., Millar, B., Rooney, P. and Snelling, W. (2006). *Cryptosporidium*. *Letters in Applied Microbiology*, 43, pp.7-16.

- [101] Stairs, C., Eme, L., Brown, M., Mutsaers, C., Susko, E., Dellaire, G., Soanes, D., van der Giezen, M. and Roger, A. (2014). A SUF Fe-S Cluster Biogenesis System in the Mitochondrion-Related Organelles of the Anaerobic Protist *Pygsuia*. *Current Biology*, 24(11), pp.1176-1186.
- [102] Thompson, R. C. A., Olson, M. E., Zhu, G., Enomoto, S., Abrahamsen, M. S., & Hijjawi, N. S. (2005). *Cryptosporidium* and *Cryptosporidiosis*. *Advances in Parasitology*, 77–158.
- [103] Tovar, J., Fischer, A. and Clark, C. (1999). The mitosome, a novel organelle related to mitochondria in the mitochondrial parasite *Entamoeba histolytica*. *Molecular Microbiology*, 32(5), pp.1013-1021.
- [104] Tovar, J., León-Avila, G., Sánchez, L., Sutak, R., Tachezy, J., van der Giezen, M., Hernández, M., Müller, M. and Lucocq, J. (2003). Mitochondrial remnant organelles of *Giardia* function in iron-sulphur protein maturation. *Nature*, 426(6963), pp.172-176.
- [105] Traversa, D. (2010). Evidence for a new species of *Cryptosporidium* infecting tortoises: *Cryptosporidium ducismarci*. *Parasites & Vectors*, 3(1), p.21.
- [106] Tsaousis A.D., Keithly J.S. (2019) The Mitochondrion-Related Organelles of *Cryptosporidium* Species. In: Tachezy J. (eds) *Hydrogenosomes and Mitosomes: Mitochondria of Anaerobic Eukaryotes*. *Microbiology Monographs*, vol 9. Springer, Cham
- [107] Tyzzer, E. (1907). A sporozoan found in the peptic glands of the common mouse. *Experimental Biology and Medicine*, 5(1), pp.12-13.
- [108] Tyzzer, E. (1910). An extracellular Coccidium, *Cryptosporidium Muris* (Gen. Et Sp. Nov.), of the gastric Glands of the Common Mouse. *J Med Res.*, 23(3), pp.487–510.3.
- [109] Tyzzer, E. (1912). *Cryptosporidium parvum* (sp. nov.), a coccidium found in the small intestine of the common mouse. *Arch. Protisenkd.* 26:394–412.
- [110] Tumwine, J., Tzipori, S., Akiyoshi, D., Kekitiinwa, A., Rich, S., Feng, X., Widmer, G. and Nabukeera, N. (2003). *Cryptosporidium parvum* in children with diarrhea in Mulago Hospital , Kampala, Uganda. *The American Journal of Tropical Medicine and Hygiene*, 68(6), pp.710-715.
- [111] Tzipori, S., Angus, K., Gray, E. and Campbell, I. (1980). Vomiting and Diarrhea Associated with *Cryptosporidial* Infection. *New England Journal of Medicine*, 303(14), pp.818-818.
- [112] Uni, S., Iseki, M., Maekawa, T., Moriya, K. and Takada, S. (1987). Ultrastructure of *Cryptosporidium muris* (strain RN 66) parasitizing the murine stomach. *Parasitology Research*, 74(2), pp.123-132.
- [113] Vetterling, J. M., H. R. Jervis, T. G. Merrill, and H. Sprinz. 1971. *Cryptosporidium wrairi* sp. n. from the guinea pig *Cavia porcellus*, with an emendation of the genus. *J. Protozool.* 18:243–247.
- [114] Waldron, L. S., Cheung-Kwok-Sang, C. and Power, M. L. (2010). Wildlife-associated *Cryptosporidium fayeri* in humans, Australia. *Emerging Infectious Disease* 16, 2006–2007.
- [115] Wang, Z. and Wu, M. (2014). Phylogenomic Reconstruction Indicates Mitochondrial Ancestor Was an Energy Parasite. *PLoS ONE*, 9(10), p.e110685.
- [116] Wachnowsky, C., Fidai, I. and Cowan, J., 2018. Iron–sulfur cluster biosynthesis and trafficking – impact on human disease conditions. *Metallomics*, 10(1), pp.9-29.

- [117] Wiedemann, N. and Pfanner, N. (2017). Mitochondrial Machineries for Protein Import and Assembly. *Annual Review of Biochemistry*, 86(1), pp.685-714.
- [118] Wielinga, P. R., de Vries, A., van der Goot, T. H., Mank, T., Mars, M. H., Kortbeek, L. M. and van der Giessen, J. W. (2008). Molecular epidemiology of *Cryptosporidium* in humans and cattle in the Netherlands. *International Journal for Parasitology* 38, 809–817.
- [119] Neupert, W. and Herrmann, J., 2007. Translocation of Proteins into Mitochondria. *Annual Review of Biochemistry*, 76(1), pp.723-749.
- [120] Williams, B., Elliot, C., Burri, L., Kido, Y., Kita, K., Moore, A. and Keeling, P. (2010). A Broad Distribution of the Alternative Oxidase in Microsporidian Parasites. *PLoS Pathogens*, 6(2), p.e1000761.
- [121] Xiao, L. and Feng, Y. (2008). Zoonotic cryptosporidiosis. *FEMS Immunology and Medical Microbiology* 52, 309–323.
- [122] Zintl, A., Proctor, A. F., Read, C., Dewaal, T., Shanaghy, N., Fanning, S. and Mulcahy, G. (2009). The prevalence of *Cryptosporidium* species and subtypes in human faecal samples in Ireland. *Epidemiology and Infection* 137, 270–277.